Risk Assessment – with Apllication for Bridges and Wind Turbines

Rastayesh, Sima

Publication date:
2020

Document Version
Publisher's PDF, also known as Version of record

RISK ASSESSMENT – WITH APPLICATION FOR BRIDGES AND WIND TURBINES

BY
SIMA RASTAYESH

DISSERTATION SUBMITTED 2020

AALBORG UNIVERSITY
DENMARK

RISK ASSESSMENT – WITH APPLICATION FOR BRIDGES AND WIND TURBINES

PH.D. DISSERTATION

by

Sima Rastayesh

AALBORG UNIVERSITY
DENMARK

Dissertation submitted

Dissertation submitted: December 2020

PhD supervisor: Prof. John Dalsgaard Sørensen,
Aalborg University

PhD committee: Associate Professor Peter Frigaard (chairman)
Aalborg University

Professor Poul Henning Kirkegård
Aarhus University

Professor Dimitri Val
Heriot-Watt University

PhD Series: Faculty of Engineering and Science, Aalborg University

Department: Department of the Build Environment

ISSN (online): 2446-1636
ISBN (online): 978-87-7210-867-4

Published by:
Aalborg University Press
Kroghstræde 3
DK – 9220 Aalborg Ø
Phone: +45 99407140
aauf@forlag.aau.dk
forlag.aau.dk

Printed in Denmark by Rosendahls, 2021

SIMA RASTAYESH'S CV

LinkedIn: https://www.linkedin.com/in/sima-rastayesh/

Email Address: sima_ras67@yahoo.com

SUMMARY

My strong theoretical skills in risk and reliability engineering calculations coupled with powerful analytical mind have now blended with 5 years of practical experience with multidisciplinary projects in extensive fields with wind turbines, bridges as well as electrical and mechanical components; made me a high-qualified engineer in different aspects of risk and reliability engineering such as sensitivity and uncertainty analysis, Reliability, Availability, Maintainability and Safety (RAMS), risk-based decision making and qualitative and quantitative risk assessment.

EXPERIENCE

- **Risk Specialist** **(2020-Present)**

Ørsted, Gentofte, Denmark

- **Ph.D. Fellow** **(2017-2019)**

Aalborg University (AAU), Aalborg, Denmark

- **Visiting Research Fellow**
  - **COWI**, Kongens Lyngby, Denmark: 3 months
  - **PHIMECA Engineering**, Cournon d'auvergne, France: 1 month
  - **IFSTTAR**, Champs sur Marne, France: 2 months

- **RAMS Specialist** **(2014-2016)**

Petro-Tirazis Energy Development (PTED), Tehran, Iran

EDUCATION

- M.Sc. Degree in **Energy Engineering** **(2011-2013)**

Science and Research Branch, Islamic Azad University (SRBIAU), Tehran, Iran

- B.Sc. Degree in **Energy Engineering** **(2007-2011)**

Science and Research Branch, Islamic Azad University (SRBIAU), Tehran, Iran

AFFILIATION

Board member of the Society for Risk Analysis (**SRA**) Nordic chapter as a student representative.

ENGLISH SUMMARY

Risk analysis and risk assessment are becoming more and more relevant for practical applications and have received an increasing importance in research and development. The application of risk analysis and risk assessment has been more highlighted in recent years and is considered at different levels in the industries. Nowadays, new technologies are rapidly growing, and new risks must be considered in the risk assessment. Bridges and wind turbines are two types of infrastructures where their failures can lead to severe damages, and thereby a high risk. Hence, rational decisions are needed to reduce their risk.

This Ph.D. project is part of the EU Marie Sklodowska-Curie project INFRASTAR. The aim of INFRASTAR (Innovative and Networking for Fatigue and Reliability Analysis of Structures Training for Assessment of Risk) project is to develop knowledge, expertise, and skill for optimal and reliable management of structures. Along with that, the objective of this Ph.D. project is to develop methods for risk assessment for wind turbines and bridges. This Ph.D. study includes a case study on a composite bridge and several case studies considering different risk assessment scenarios on wind turbines (wind turbines near a highway throwing off ice and blades and power stage utilized in wind-fuel cell hybrid energy systems).

Methods that are already available and used in bridges and wind turbines, such as risk-based decision-making, are modified and adapted to make it possible to use them as decision support tools for Operation and Maintenance (O&M) activities for the case study of the bridge. In addition to risk-based O&M methodologies, available methodologies to model the consequences of adverse events are modified based on existing risk assessment methodologies for wind turbines, such as Failure Mode and Effect Analysis (FMEA), Fault Tree Analysis (FTA), Decision Tree, and finally Bayesian Network (BN). These methods are demonstrated in different case studies presented in the Ph.D. thesis.

DANSK RESUME

Risikoanalyse og risikovurdering er i stigende grad relevant for den praktiske implementering og er ligeledes af større betydning inden for forskning og udvikling. I de seneste år er anvendelsen kommet i større fokus og tages i betragtning på forskellige niveauer inden for forskellige industrigrene. Nye teknologier udvikles med større hastighed, og nye risici skal tages i betragtning ved en risikovurdering. Broer og vindturbiner er to kategorier af infrastruktur, hvor nedbrud kan forårsage voldsomme skader, og de udgør dermed en stor risiko. Vi har derfor behov for rationelle beslutninger for at kunne vurdere disse risici.

Dette ph.d.-projekt er en del af et større EU-finansieret projekt INFRASTAR under Marie Sklodowska-Curie programmet. Formålet med INFRASTAR (Innovative and Networking for Fatigue and Reliability Analysis of Structures Training for Assessment of Risk) er at udvikle viden, ekspertise og færdigheder for optimal og pålidelig styring af strukturer. I forlængelse af dette er det ph.d.-projektets formål at udvikle metoder for risikovurdering for vindturbiner og broer. I denne afhandling anvendes flere casestudier vedrørende en kompositbro samt studier af forskellige risikovurderingsscenarier: isbelægning samt vinger, der falder af i nærheden af motorvej, drivkraftsstadiet udnyttet i vind–brændselscelle hybrid energisystemer.

Eksisterende metoder som i dag anvendes ved broer og vindturbiner, som for eksempel risikobaserede beslutningsprocesser, er viderebearbejdet og tilpasset, så det er muligt at anvende disse i beslutningsgrundlaget for drifts- og vedligeholdelsesaktiviteter i casestudiet af broen. Udover de risikobaserede drifts- og vedligeholdelsesteknologier, videreudvikles nuværende metodologier til modellering af konsekvenser af kritiske hændelser, baseret på eksisterende risikovurderings metodologier for vindturbiner, som fx. Failure Mode and Effect Analysis (FMEA), Fault Tree Analysis (FTA), Decision Tree og sluttelig Bayesian Network (BN).

PREFACE

This Ph.D. project was carried out at the Department of Civil Engineering, Aalborg University. The work was performed within the European project INFRASTAR, which has received funding from the European Union's Horizon 2020 research and innovation programme under the Marie Skłodowska-Curie grant agreement No. 676139. The financial support is gratefully acknowledged.

My entire Ph.D. I was based at Aalborg University. As part of the agreement with INFRASTAR, for a total duration of six months, I was hosted by IFSTTAR, PHIMECA, and COWI. Their support is acknowl

ACKNOWLEDGEMENTS

Firstly, I would like to express my sincere gratitude to my supervisor John Dalsgaard Sørensen for the guidance, continuous support, and invaluable advice throughout the project. I appreciate his dedication to the project, the time spent for fruitful discussions, and the given freedom to explore and apply different approaches for achieving the set goals; and for the enthusiasm to bring all INFRASTAR work packages and ESRs closer throughout the project. Thanks for always being available even out of working hours and understanding my personal life issues during my study.

I am very thankful to my co-authors, especially, Sajjad Bahrebar; Amol Mankar who was not only my best colleague also one of the best friends which I gained a lot from this friendship, He was supporting me anytime in any occasion; Professor Frede Blaabjerg for his support; Associate Professor Jannie Sønderkær Nielsen for her invaluable support; Amir Sajjad Bahman and others for their contribution to the present research.

Many thanks also go to all the staff at the Aalborg University and INFRASTAR project for their support and advice during my research. I would also like to thank the administration of the Department of civil engineering of Aalborg University for their kind help and generous support during the period of this research, especially Vivi Søndergaard, Linda Vabbersgaard Andersen, and Maria Friis.

The INFRASTAR consortium has been a great support for the duration of the project. I wish to thank all the people behind INFRASTAR, especially Dr. Hakim Ferria and Dr. Odile Abraham, for their support and encouragement. I had the great pleasure of meeting and working with all the INFRASTAR fellows.

During my secondment at COWI, I would like to acknowledge guidance from Katrina Konakli and Hyun-Joong Kim's support.

Privately, I am grateful and blessed to be surrounded by amazing people, many of whom I can call my close friends. You kept me sane and going throughout all these years. Thank you for all the knowledge, love, and fun you enrich my life. I am indebted to all of my friends, colleagues, and relatives for making it possible for me to reach here.

My deepest love and gratitude goes to my patient husband Sajjad Bahrebar, for his boundless emotional support and enormous scientific insight, and motivation, and for standing by my side with unconditional endless love, giving me the power and

confidence to bear the rough times and reminding me to never give up on things I truly believe during this academic endeavor.

Last but not least, I wish to express my love and sincerest appreciation to my mother for her unconditional love, continuous support, and encouragement in any way possible, and I am also very much thankful to my father for his invaluable never-ending support and his wishes and inspiration and love. I am also thankful to my brother for his friendship, trust, and backing me up throughout my life.

LIST OF PAPERS

This Ph.D. thesis follows an article-based format. The first part presents an extended summary of the study. The second part consists of the appended papers.

List of published papers included in the thesis:

1. Rastayesh, S., Mankar, A., Dalsgaard Sørensen, J., & Bahrebar, S. (2020). Development of stochastic fatigue model of reinforcement for reliability of concrete structures. *Applied Sciences*, *10*(604). https://doi.org/10.3390/app10020604

2. Mankar, A., Rastayesh, S., & Dalsgaard Sørensen, J. (2019). Fatigue reliability analysis of crêt de l'Anneau viaduct: a case study. *Structure and Infrastructure Engineering*. https://doi.org/10.1080/15732479.2019.1633361

3. Rastayesh, S., Long, L., Dalsgaard Sørensen, J., & Thöns, S. (2019). Risk assessment and value of action analysis for icing conditions of wind turbines close to highways. *Energies*, *12*(14), 2653. https://doi.org/10.3390/en12142653

4. Rastayesh, S., Bahrebar, S., Bahman, A. S., Dalsgaard Sørensen, J., & Blaabjerg, F. (2019). Lifetime estimation and failure risk analysis in a power stage used in wind-fuel cell hybrid energy systems. *Electronics*, *8*(12), 1412. https://doi.org/10.3390/electronics8121412

5. Rastayesh, S., Bahrebar, S., Blaabjerg, F., Zhou, D., & Wang, H. (2020). A system engineering approach using FMEA and Bayesian network for risk analysis — A case study. *Sustainability*, *12*(77). https://doi.org/10.3390/su12010077

6. Bahrebar, S., Zhou, D., Rastayesh, S., Wang, H., & Blaabjerg, F. (2018). Reliability assessment of power conditioner considering maintenance in a PEM fuel cell system. *Microelectronics Reliability*, *88–90*, 1177–1182. https://doi.org/10.1016/j.microrel.2018.07.085

Other publications:

7. Bahrebar, S., Blaabjerg, F., Wang, H., Vafamand, N., Khooban, M.-H., Rastayesh, S., & Zhou, D. (2018). A novel type-2 fuzzy logic for improved risk analysis of proton exchange membrane fuel cells in marine power systems application. *Energies*, *11*(4), 721. https://doi.org/10.3390/en11040721

8. Rastayesh, S., Sønderkær Nielsen, J., & Dalsgaard Sørensen, J. (2018). Bayesian network methods for risk-based decision making for wind turbines. 14th EAWE PhD

Seminar on Wind Energy 18-20 September 2018 Vrije Universiteit Brussel, Belgium: European Academy of Wind Energy.

9. Rastayesh, S., Mankar, A., & Dalsgaard Sørensen, J. (2018). Comparative investigation of uncertainty analysis with different methodologies on the fatigue data of rebars. In *5th International Reliability and Safety Engineering Conference*. Shiraz: Arzhang Printing.

10. Bahrebar, S., Blaabjerg, F., Wang, H., Zhou, D., & Rastayesh, S. (2018). System-level risk analysis of PEM fuel cell using failure mode and effect analysis. In *5th International Reliability and Safety Engineering Conference*. Shiraz: Arzhang Printing.

11. Mankar, A., Rastayesh, S., & Dalsgaard Sørensen, J. (2018). Sensitivity and identifiability study for uncertainty analysis of material model for concrete fatigue. In *5th International Reliability and Safety Engineering Conference*. Shiraz: Arzhang Printing.

12. Mankar, A., Rastayesh, S., & Dalsgaard Sørensen, J. (2018a). Fatigue reliability analysis of Cret De l'anneau viaduct: A case study. In *6th International Symposium on Life-Cycle Civil Engineering, IALCCE 2018*. Ghent.

13. Bahrebar, S., Blaabjerg, F., Wang, H., Rastayesh, S., & Zhou, D. (2018). Failure modes and effect analysis for risk minimizing in critical components of proton exchange membrane fuel cell system. In *7th Conference on Safety Engineering and HSE Management*.

14. Rastayesh, S. (2019). Bayesian network for risk-based decision making. In *38th International Conference on Ocean, Offshore and Arctic Engineering*. Glasgow: OMAE 2019.

15. Rastayesh, S., & Dalsgaard Sørensen, J. (2019). Dynamic influence diagrams for risk-based decision making for rebars. In *5th Society for Risk Analysis (SRA) Nordic Conference 2019: Risk Management for Innovation* (p. 31). Copenhagen: DTU.

16. Rastayesh, S., Zorzi, G., Miraglia, S., & Dalsgaard Sørensen, J. (2019). Risk assessment of adverse events for wind turbines caused by strong winds. In *Wind Energy Science Conference 2019*. Cork: University College Cork.

17. Rastayesh, S., & Dalsgaard Sørensen, J. (2018). Risk analysis for wind turbines near highways. In *The 4th Society for Risk Analysis (SRA) Nordic Conference*. Stavanger: University of Stavanger.

TABLE OF CONTENTS

LIST OF FIGURES

LIST OF TABLES

CHAPTER 1. INTRODUCTION

1.1. THESIS OBJECTIVE

For both new and existing structures, it is vital to be able to make rational decisions on design, inspections, operation, maintenance, and repairs and to account for both uncertainties and consequences. The decisions can be related to both the design stage and throughout the service life of the structure; the decisions can be made using methods for risk analysis and assessment (Dalsgaard Sørensen, 2011; Havbro Faber, 2007, 2008; Havbro Faber & Stewart, 2003; Havbro Faber, Straub, & A. Maes, 2006; Rastayesh, 2018; Rastayesh & Dalsgaard Sørensen, 2017; Vrouwenvelder & Holicky, 2001).

The objective of this thesis is to develop and illustrate by case studies, methods for risk-based assessment for bridges and wind turbines, employing information from inspections, sensors, and condition monitoring, i.e. to apply measurement data to rational decision-making.

To assess the risk, the adverse events are first modeled, the methods and tools for estimation of the probability of the adverse events identified, and then the consequences are modeled and combined with the probabilities.

Additionally, the goal is to identify and develop illustrative tools for decision-making using the applied methodologies for risk assessment for each case study.

For the case studies, the objective is to use existing methodologies for risk assessment of wind turbines and bridges; these methodologies are developed for specific applications. Another aim is to employ different methodologies and compare them to find the ones most suitable in each case study. Especially different methodologies such as FMEA, FTA, and BN are to be considered.

1.2. OUTLINE AND KEY METHODS

This project uses the framework described in the JCSS (Joint Committee for Structural Safety) guideline for risk assessment (JCSS, 2008) as the basis for advanced methods for risk-based decision-making and assessment for bridges and wind turbines, utilizing information from inspections, sensors, and condition monitoring, i.e., applying measurement data in rational decision-making (Rastayesh & Dalsgaard Sørensen, 2017).

The goals of the Ph.D. project are achieved using structural reliability theory, which includes statistical methods dealing with modeling of uncertainties related to loads, strengths, and modeling/calculation methods (Dalsgaard Sørensen, 2017).

As mentioned previously, the approaches already available and used for bridges and wind turbines have modified and adapted, such as risk-based decision-making, in order to make it possible to use them as decision support tools for O&M activities for the case study of the bridge. In addition to risk-based O&M Approaches, available methods to model the impacts of adverse events are modified based on available risk analysis methods for wind turbines, such as FMEA, FTA, Decision Tree, and finally BN. These approaches are established in different case studies presented in the Ph.D. thesis.

Chapter 2 presents a state of the art of the methodologies used for risk assessment in this thesis. Chapter 3 presents the case studies related to bridges, and Chapter 4 presents the wind turbine applications. Finally, the conclusion and future works are discussed in Chapter 5 and 6.

CHAPTER 2. RISK ASSESSMENT METHODOLOGIES

2.1. RISK ASSESSMENT BACKGROUND

In recent years, attention is more focused on sustainable economic growth being about saving nature and the well-being and safety of the individuals. Simultaneously, optimal allocations of existing resources should particularly be taken into account. The importance of risk and reliability engineering has been highlighted increasingly as a decision support tool. As an example of civil engineering, the different types of failure are load, mechanical, operational, installation, and structural failures. These failures could cause risk in different forms: environmental, fatality, and economical (Dalsgaard Sørensen, 2011; Velarde, Kramhøft, Sørensen, & Zorzi, 2020), see Figure 2-1: Elements of decision making. The figure shows that different kinds of failure leading to different kinds of risk as the elements aiding the decision-making. These failures could be related to different life-cycles: design, manufacturing, commissioning, installation, operation, and decommissioning. Moreover, they could relate to different areas such as mechanical, electrical, structural, chemical, human, control systems, and cybersecurity issues.

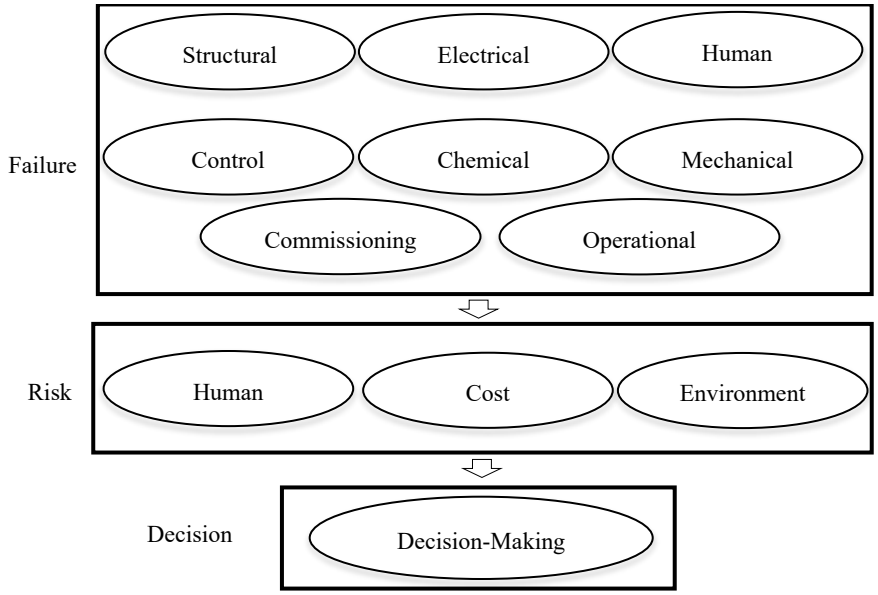

Figure 2-1: Elements of decision making

Wind turbines and bridges are exposed to climatic conditions as well as environmental impacts, which decrease their life-cycle performance and further increase the risk of failure of these structures. For example, to guarantee acceptable risk levels of wind turbines during the entire lifetime, diverse O&M plans are used in the offshore wind industry contributing to 20-30% of the cost of energy (Jessen Nielsen & Dalsgaard Sørensen, 2011).

When looking into the main difference between wind turbines and bridges, a wind turbine is a mixture between a building and a machine with a control system. This means that besides the structural point of view, electrical and mechanical components are required for their assessment. On the other hand, a bridge is more like a building, although some very large bridges can have some active control / demanding devices. Hence, in most of the bridges, a structural analysis is needed for the assessment. Moreover, wind turbines are mass-produced i.e. a large number of almost identical wind turbines. Further prototypes and zero-series wind turbines are typically made before mass production is started; although, bridges are typically a one-of-a-kind structure.

A rational and comprehensive technique is needed to assess the risk exposure to the structures and to account for the consequences in order to prevent bridge failures, such as the Genova bridge collapse in 2018 or the collapsed 35W bridge in Minneapolis in 2007 (Gash, 2007), or even wind turbine collapses (Miceli, 2013).

Both bridges and wind turbines need to be maintained during their design lifetime to ensure a satisfactory reliability level.

Bridges and wind turbines are generally designed to quite different reliability levels. Failure of a bridge can result in considerable economic consequences and loss of human lives whereas failure of a wind turbine typically does not expose people to risk and the economic consequences are low although there is a very high focus on minimizing the levelized cost of energy for wind turbines.

Typical reliability levels for bridges and wind turbines are as follows (Dalsgaard Sørensen & Stensgaard Toft, 2014; DNV.GL, 2018; EN, 2019):

- Bridges: the annual probability of failure of the order $10^{-7} - 10^{-6}$
- Wind turbines: the annual probability of failure of the order $10^{-4} - 10^{-3}$

2.1.1. BASIC DEFINITIONS

2.1.1.1 Risk

Risk is introduced as a measure of the expected potential loss occurring because of natural or human activities (Modarres, 2006). Risk is described as the expected

consequences consort with a specified activity (Dalsgaard Sørensen, 2011; Havbro Faber, 2007, 2008; Havbro Faber & Stewart, 2003; Modarres, Kaminskiy, & Krivtsov, 2016). Bearing in mind an activity with only one event with probability P of this event occurring and with potential consequences C, then the risk R is expressed as the product of the probability and the consequences (Dalsgaard Sørensen, 2011; Havbro Faber, 2007, 2008):

$$R = P \cdot C \qquad Eq.\ 1$$

In the situation of multiple events, risk is calculated by

$$R = \sum_{i=1}^{N} P_i\, C_i \qquad Eq.\ 2$$

where N is the number of events and index i designates event number i (Dalsgaard Sørensen, 2011; Havbro Faber, 2007).

2.1.1.2 Risk Analysis

Risk analysis consists of three main constituents: risk assessment, risk management, and risk communication (National Academy Press, 1983; Spitzer, Schmocker, & Dang, 2004). Firstly, risk assessment, in this process, the probability or frequency of a loss by or to an engineering system is estimated, as well as the magnitude of the loss (consequence) is calculated or approximated (Modarres, 2006). Secondly, in the risk management procedure, the potential magnitude and contributors to risk are estimated, evaluated, minimized, and controlled (Modarres, 2006). Thirdly, in risk communication, the decision-makers and other stakeholders swapped, shared, and deliberated the information regarding the kind of risk (expected loss) and consequences, risk assessment method, and risk management decisions (Modarres, 2006; Modarres et al., 2016; Vrouwenvelder & Holicky, 2001).

Risk analysis is an estimation of the potential and magnitude of any loss and approaches to control it from or to a system (Modarres, 2006). Commonly, risk analyses are divided into three kinds: quantitative, qualitative, and their combination.

Quantitative Risk Analysis

Quantitative risk analysis calculates the risk in the form of the probability (or frequency) of a loss and evaluates such probabilities to make decisions and communicate the outcome (Modarres, Kaminskiy, & Krivtsov, 1999). When sufficient relevant data is available for risk analysis, this approach is preferable; although, collecting this kind of data is usually time-consuming, challenging, and expensive. This approach became recommended especially when costs are considered

as the consequence. (Vinnem, 2014) recommends in his book this approach rather than the other two for risk assessment of offshore structures such as wind turbines. Papers 1–6 in the annexes of this thesis used this methodology or (Bahrebar, Blaabjerg, Wang, Vafamand, et al., 2018; Bahrebar, Blaabjerg, Wang, Zhou, & Rastayesh, 2018; Bahrebar, Rastayesh, & Sepanloo, 2014; Bahrebar, Zhou, Rastayesh, Wang, & Blaabjerg, 2018; Mankar, Rastayesh, & Dalsgaard Sørensen, 2019; Rastayesh & Bahrebar, 2014; Rastayesh, Bahrebar, Bahman, Dalsgaard Sørensen, & Blaabjerg, 2019; Rastayesh, Bahrebar, Blaabjerg, Zhou, & Wang, 2020; Rastayesh, Bahrebar, & Sepanloo, 2014; Rastayesh, Long, Dalsgaard Sørensen, & Thöns, 2019; Rastayesh, Mankar, Dalsgaard Sørensen, & Bahrebar, 2020).

Qualitative Risk Analysis

Due to the simplicity and quick way of utilizing the qualitative approach, it is more common for risk analysis. In this category, the potential loss is qualitatively estimated by linguistic scales. In this kind, a matrix is created which specifies the risk in the form of the frequency (or likelihood/probability) of the loss versus the potential magnitudes (amount) of the loss or impact in qualitative scales. Later, this matrix is utilized to make policy and risk management decisions (Modarres, 2006). Since data is not needed here from tests or other sources, it is easy to use; however, it is subjective and could influence the uncertainty of the risk analysis.

A Mixture of Qualitative and Quantitative Analysis or Semi-quantitative Risk Analysis

A mixture of both approaches mentioned earlier could be used for risk analysis in two different forms: the frequency or potential for loss is measured qualitatively, but the magnitude of the loss (consequence) is measured quantitatively or the other way around. Moreover, it is feasible that both the frequency and magnitude of the loss are calculated quantitatively; however, the policy setting and decision making part of the analysis depend on qualitative approaches (Modarres, 2006).

2.1.1.3 Risk Assessment

Risk assessment is an organized and efficient process for recognition and quantification of events, frequencies, or probabilities and the magnitude of consequences or losses to recipients as a reason of exposure to hazards from failures (Modarres, 2006; Modarres et al., 2016).

Risk assessment is a process to answer three basic questions (Kaplan & Garrick, 1981; Misra, 2008; Modarres et al., 1999):

- What can happen or become wrong, that could lead to a hazard exposure outcome?

- How likely is it that it will fail, i.e. the probability of failure?
- What consequences are expected if it happens?

The procedure of decision-making based on risks is understood as risk assessment. Risk assessments should start from the initial stage of a system means from design, and it should continue until the last phase of service life (decommissioning). In the process of risk assessment, a clear explanation is needed for the assumptions considered for identifying the system as well as the consequences and frequencies. There are always uncertainties associated with risk assessment; using a sensitivity analysis, these uncertainties could be adjusted. Uncertainties associated with data or expert judgments should be identified. It is worthwhile to make sure that common uncertain factors for risk assessment should be identified (Havbro Faber, 2008; Havbro Faber & Stewart, 2003).

The fundamentals of risk assessment start with identifying uncertainty and modeling of events in a probabilistic approach and finding the consequences and the acceptable risk. Meanwhile, risk reduction and/or risk mitigation and updating knowledge in all previous steps could be defined as the principal elements for risk assessment (Dalsgaard Sørensen, 2011).

The key elements of risk assessment can be listed as identifying hazards and barriers, assessment of the likelihood of loss of barriers, estimation of the consequences of exposure to hazards, and finally, risk evaluation.

Figure 2-2 shows a general and straightforward illustration for system risk assessment (Havbro Faber, 2008).

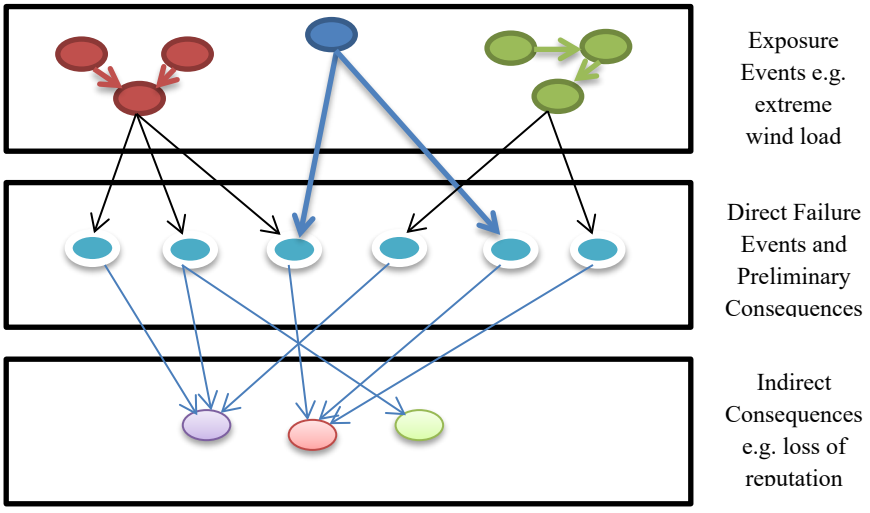

Figure 2-2: Generic system representation in risk assessments (Havbro Faber, 2008).

Utilizing the simplified process in Figure 2-2, the following shows the risk assessment of a wind turbine near a high way. In this example, the weather conditions are icy and snowy, and additionally the blade of the wind turbine may have a failure. The direct and indirect consequences are identified in the following tables.

Figure 2-3: Exposure

Table 2-1: Exposure

Physical Features	**Indicator**	**Potential Consequences**
Ice Wind loads Design and fabrication errors	Unbalanced blades[1] Environment Location Societal importance	Road accidents Failures of blade Reduced/Loss of Production

[1] The reason for this is that the ice is not equally distributed on the blades.

Figure 2-4: Vulnerability

Table 2-2: Vulnerability

Physical Features	Indicator	Direct Consequences
Fatigue Cracking Wear Corrosion	Cracks Corrosion on surface Increased vibrations Large deflection of blades Design target reliability Age Materials Quality of workmanship	Blade failure Part / whole blade thrown off Lost production Repair cost Material losses Injuries and fatalities Damage to environment

Figure 2-5: Robustness

Table 2-3: Robustness

Physical Features	Indicator	Indirect Consequences
Partial collapse	Visible larger damages Increased stresses and vibration on the other parts of the wind turbine Design codes Ductility Joint characteristics Condition control/monitoring Emergency preparedness	Reconstruction cost Clean up costs Rescue costs Loss of functionality Injuries and fatalities Socio-economic losses Damage to environment Loss of reputation

Figure 2-6 illustrates the decision theory, which provides a theoretical framework for risk assessment.

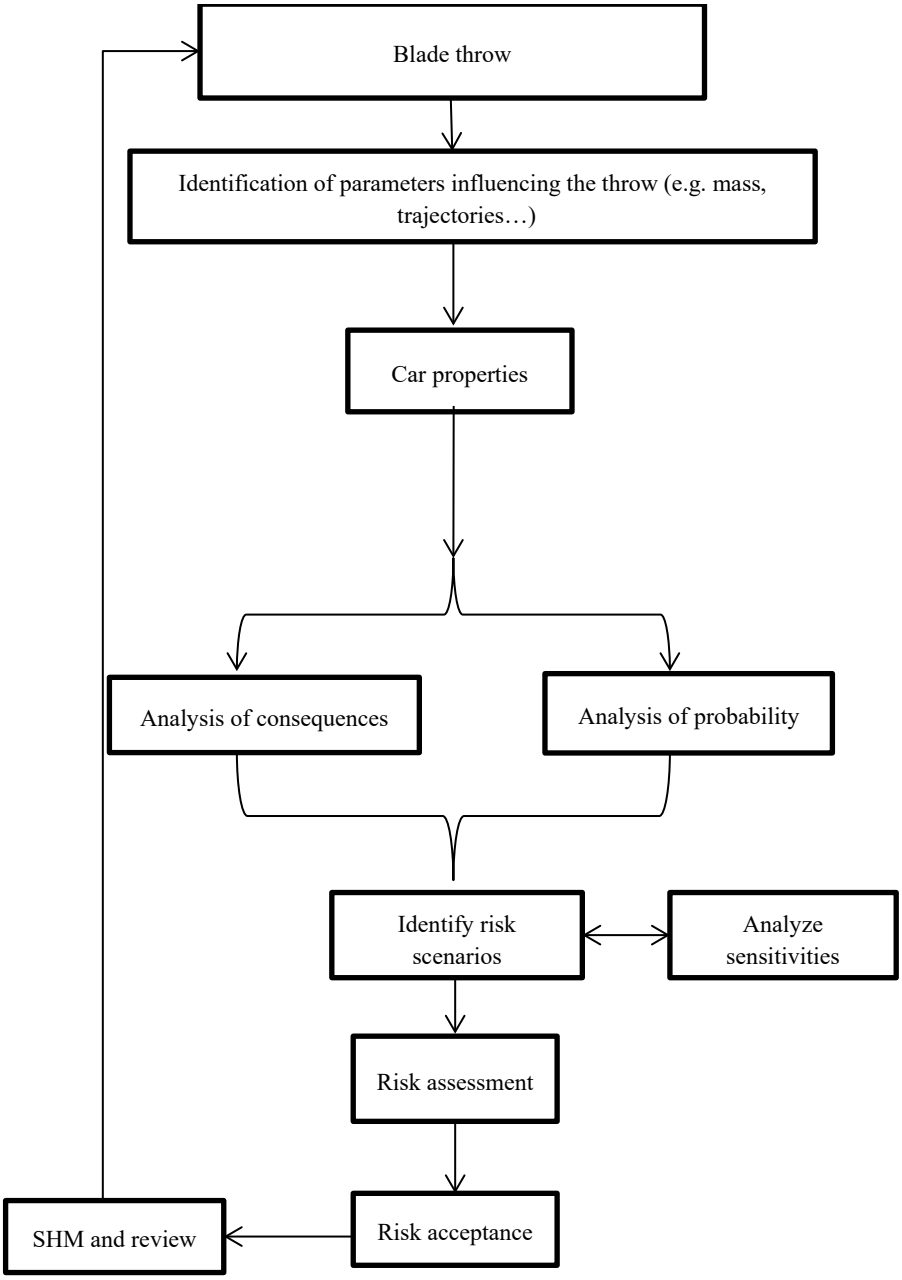

Figure 2-6: General scheme for risk-based decision analysis for risk assessment of ice or blades thrown off a wind turbine and hitting a car (Rastayesh, Long, et al., 2019).

However, with bridges hazards can be categorized as bellow (Imhof, 2004; Nowak, 2007; Nowak, Kozikowski, & Lutomirska, 2009):

Natural Hazards

- Earthquakes
- Material degradation
- Wind (hurricanes, tornadoes)
- Floods (tsunami)
- Snow and ice
- Temperature effects

Man-Made Hazards

- Terrorist attacks, explosions, fires
- Overloads (weight, height)
- Inadequate maintenance (corrosion, cracking)
- Acts on vandalism, intentional damage
- Collisions –vehicles and vessels

Various techniques for Hazard Identification (HAZID) are available such as Risk Screening (HAZID sessions), FMEA, Preliminary Hazard Analysis (PHA), Hazard and Operability Studies (HAZOP), Failure Mode Effect and Criticality Analysis (FMECA), see e.g. (Dalsgaard Sørensen, 2011; Havbro Faber & Stewart, 2003; Stewart & Melchers, 1997) for a comprehensive review. In this thesis, methodologies such as fault tree, BN, decision tree, and FMEA will be discussed in the following sections.

2.2. FAILURE MODES AND EFFECT ANALYSIS (FMEA)

One of the most efficient methods which can be used for system recognition and identification for risk assessment is FMEA. FMEA is a methodology that focuses on prevention by facilitating process improvement as well as identifying and eliminating concerns early in the development of a process or design (Narayanagounder & Gurusami, 2009; Rastayesh, Bahrebar, et al., 2019). FMEA is a systematic and structured approach to identify, analyze, and rank estimated risk with various potential failure modes (Rastayesh, Bahrebar, et al., 2020). FMEA can assist engineers by preventing failures or reducing their effects by altering the design or control tests (Modarres, 2006; Modarres et al., 1999, 2016; Rastayesh, Bahrebar, et al., 2020). FMEA is an important risk tool to identify critical failure modes, causes, and mechanisms (Rastayesh, Bahrebar, et al., 2020). The aim is to reduce the risks before they happen. Therefore, with using FMEA, diagnosing probable failure and dissatisfactions of functions for any component in a system would be feasible (Modarres, 2006; Modarres et al., 1999, 2016; Rastayesh, Bahrebar, et al., 2020).

The FMEA method has been used in different industries and it holds the three risk factors Occurrence (O), Detectability (D), and Severity (S). 'O' designates the rate of the risks, 'D' indicates the likelihood of predicting risks before they happen, and 'S' is the significance of the risk in the system (Rastayesh, Bahrebar, et al., 2020). The yield factor represented as the Risk Priority Number (RPN) is the multiplication of these three input parameters graded as the failure state (Rastayesh, Bahrebar, et al., 2020). There are different standards that have been used to classify different faults that occur in every system. Afterward, by multiplying these input factors, the highest RPN is recognized (Jensen et al., 2012; Rastayesh, Bahrebar, et al., 2019; Sutrisno, Gunawan, & Tangkuman, 2015). These results make it easier for specialists to identify failures and their causes, while analysts allocate an edge rate to classify failures (Collong & Kouta, 2015; Rastayesh, Bahrebar, et al., 2019; Whiteley, Dunnett, & Jackson, 2016).

All failure causes and effects of the systems can be addressed by using FMEA; moreover, the RPNs will help classify the critical system. The aim is enhancement of reliability and reduction of risk to avoid the risk event happening (Adar, İnce, Karatop, & Bilgili, 2017). Figure 2-7 shows the process of the FMEA used in this thesis for the PEMFC system.

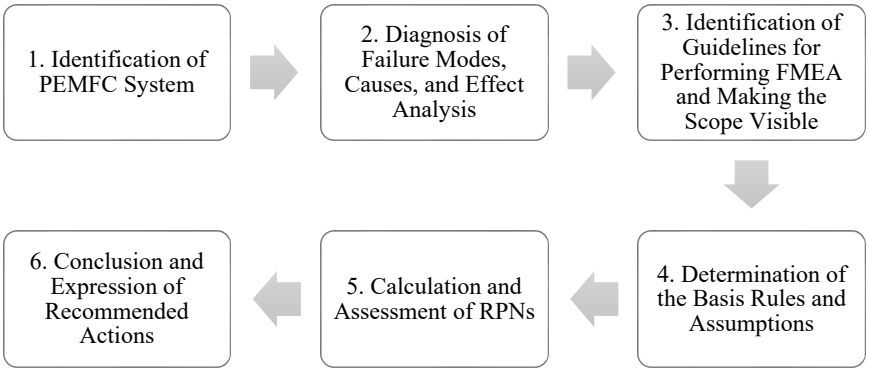

Figure 2-1: FMEA Process (Rastayesh, Bahrebar, et al., 2019)

2.2.1. FMEA OBJECTIVE

Design improvement is the principal aim of FMEA. The objectives in System FMEA and Design FMEA are design improvement of the system), sub-system or component as well as improving test and verification plans. For Process FMEAs, the objective is the improvement of the manufacturing process design and the improvement of Process Control Plans (Carlson, n.d.; Pawar & Chikalthankar, 2017).

FMEA identifies failure modes, causes, and their effects on the system, and subsequently, uses these identifications in the risk assessment for prioritization. In this way, the most necessary corrective actions could be found.

2.2.2. FMEA PROCEDURE

A logical sequence of steps using FMEA could be as follows (Bech Andersen, 2012; Jensen et al., 2012):

- System definition.
- Building system block diagram: structural (hardware)/ functional/ combined/ master logic diagram.
- Identification of failure modes, effects, and causes.
- Assigning severity for the causes by defining classification categories.
- Find the occurrence rate of each failure mode.
- Investigate if the failure is detectable, if yes it can be controlled.
- Documentation and identification of the problem solutions in the design.

For the presentation of the data of FMEA, Table 2-4 is used (Rastayesh, Bahrebar, et al., 2020).

Table 2-1: Generic FMEA worksheet

ID	Item Function	Failure Mode	Failure Causes	Failure Effects	S	O	D	RPN

For estimation of Risk Priority Number (RPN), a successful approach is focusing on the severity, occurrence, and detection rankings within the context of a three–dimensional risk matrix.

For the goals mentioned above, FMEA is a powerful tool; however, when it comes to interactions between failure modes or, in other words, common cause failures, FMEA cannot meet this target. In this case, FTA could be the solution that is mentioned in the next sub-section.

2.3. FAULT TREE ANALYSIS (FTA)

System modeling in any system has a direct relation with the type of components, interactions, failure distributions, different assumptions, and various condition

characterizations. These are needed to have a perfect understanding of the system, which can be characterized to two main parts: Failure Modeling (using e.g. fault tree) and Event Modeling (by e.g. event tree) (Rastayesh & Bahrebar, 2014; Rastayesh et al., 2014).

In the FTA methodology, the undesirable event is also known as the top event. Afterward, the procedure is to use a systematic and logical approach in order find the probable paths that could cause the top event. As a result, all component failures, or in other words their failure modes, are included in the fault tree, causing the top event to happen. Consequently, this methodology can be considered as a deductive approach. A fault tree can be introduced as a graphical tool that can represent the failure interactions leading to the top event (Modarres, 1993; Whiteley et al., 2016).

It is hard to assume all fault events on the fault tree. Typically, important ones are selected although, the decision-making for this selection is not a random process. The selection of fault events is based on the fault tree construction process, design of the system and operation, operating history, existing failure data, and the expert's judgments and their experience (Modarres et al., 1999; Placca & Kouta, 2011).

Although the fault tree looks like an illustration of qualitative assessment, it can also be classified as a quantitative assessment. The most common quantitative approach is the cut sets using Boolean algebra.

As a very simple example, Figure 2-8 is the fault tree of the Printed Circuit Board (PCB) failure where the top event is PCB fail. Top event fails if the connector or board fails. In Figure 2-8, events shown by a circle are basic events.

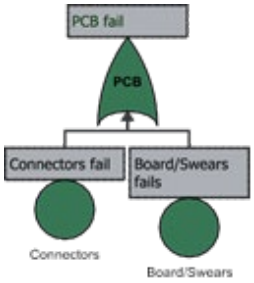

Figure 2-1: Fault tree of PCB failure (Bahrebar, Zhou, et al., 2018)

2.4. EVENT TREE METHOD

The event tree method is suitable when successful operation of a system is dependent on an approximately chronological but separate operation of its sub-systems or units (Modarres, 1993). The event tree method may not be very important in simple systems; while it is a crucial factor in complex systems which require the sub-systems

to perform according to a planned sequence of events to reach a desirable outcome (Modarres et al., 2016).

Event trees are constructed horizontally, where the initiating event is modeled from the left side (Modarres et al., 1999). The initiating event describes a condition when the operation of a system(s) occurs based on a valid demand. The development of the tree chronologically proceeds with the postulation of demand on each unit (or sub-system). The top branch at each branch point represents event success, while the lower branch represents the failure of the event (Modarres, 2006). Figure 2-9 shows the concept of how to make an event tree.

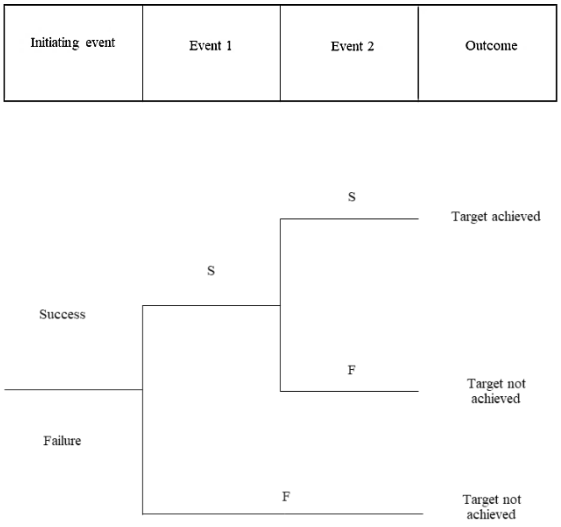

Figure 2-1: Illustration of the event tree concept

2.5. DECISION TREE

For risk assessment, another assisting tool that could help decision-makers is the decision tree. This methodology looks like a tree. Each scenario is modeled in a branch or route. The tree illustrates possible outcomes and costs, and it utilities that all outcomes and costs are the consequences of each scenario ("Decision Tree," n.d.; Magee, 1964). Figure 2-10 illustrates the decision tree for risk analysis of the Value of Action (VoA) of wind turbines close to highways as an example of a decision tree.

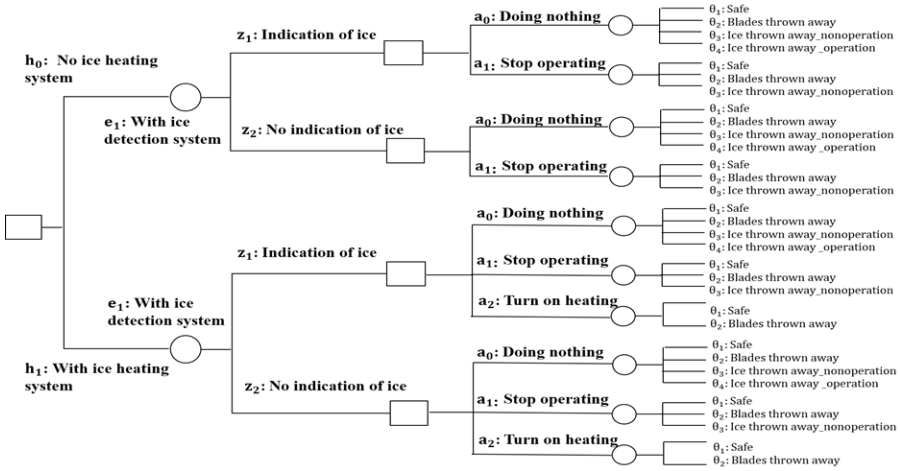

Figure 2-1: Illustration of the decision tree for risk assessment of the VoA of wind turbines close to highways (Rastayesh, Long, et al., 2019).

The aim of a decision-maker is to optimize the utility cost. There are two different forms of analysis: the so-called normal form and extensive form. In the end, the results of these two methods are the same, but each having some advantages for problem solving. In a few words, the extensive form works as a backward induction, while the normal form is the other way around (Raiffa & Schlaifer, 2013). The decision analysis approach in (Raiffa & Schlaifer, 2013) is also closely linked to Bayesian decision analysis including prior analysis, posterior analysis and pre posterior analysis (Havbro Faber, 2007, 2008). The assumptions and maximization of the utility for Figure 2-10 are explained in paper (3) (Rastayesh, Long, et al., 2019).

2.6. RISK-BASED APPROACHES

2.6.1. RISK-BASED INSPECTIONS

Risk-based inspection (RBI) plans have been advanced to optimize the cost of inspection planning as well as the design of the structures, for instance, concerning fatigue loads (Márquez-Domínguez, 2013). A chronological state of the art can be found in the following references: (Dalsgaard Sørensen, 2009; Havbro Faber, Dalsgaard Sørensen, Tychsen, & Straub, 2005; T Moan, 2005; Rangel-Ramírez & J.D., 2010; Sønderkær Nielsen, 2013; Thoft-Christensen & Dalsgaard Sørensen, 1987). In (Straub & Havbro Faber, 2006), for cost benefit purposes, RBI is introduced as an appropriate strategy for inspecting, monitoring, as well as controlling the deterioration damage in offshore substructures.

Fundamentals of RBI are the Bayesian decision theory, see section 2.5 as well as structural reliability approaches. With the aim of RBI planning, it is necessary to do some computations. (Havbro Faber et al., 2005; Márquez-Domínguez, 2013; Straub & Havbro Faber, 2006) both suggest the computational process for offshore structures for RBI planning.

With the purpose of finding the best maintenance plan, RBI can be used as a proper methodology for deteriorating structures using a tool for decision-making. In a nutshell, RBI is a method that uses any prior information such as data collected by inspection previously and tries to find the most cost-effective plan. For more information and understanding about RBI usage in e.g. steel structures (Márquez-Domínguez, 2013; Rouhan, Goyet, & Havbro Faber, 2004) can be studied. In summary for risk and reliability updating, the key elements of information that can be obtained to help in this regard are the survival of structures, inspection data, and condition monitoring. As an example, the inspection outcome could be detection or no-detection of the cracks or of the crack length (Márquez-Domínguez & Dalsgaard Sørensen, 2012). In these situations, it is important to account for the uncertainty of the inspection, which can be done by Probability of Detection (PoD) curves (Márquez-Domínguez, 2013).

2.6.2. RISK-BASED O&M

2.6.2.1 O&M planning

Operators or owners of structures decide on O&M planning strategies during the lifetime of the structures (Chemweno, Pintelon, Nganga Muchiri, & Van Horenbeek, 2018; Eduard Kostandyan, 2013). There are two different categories for O&M: preventive and corrective. The first one, preventive, means performing maintenance/repair before failure using information from inspections or condition monitoring. The second one, corrective, means no inspections/monitoring, but waiting until failure and then repairing or replacing the failed components. With the purpose of finding the optimum O&M, the goal is to minimize the cost and maximize the benefit during service life, considering downtimes as a significant factor. For example, in offshore structures, weather conditions during O&M greatly influence this decision-making as they have a direct impact on reliability (Eduard Kostandyan, 2013).

2.6.2.2 Risk-based O&M

This thesis will implement the Bayesian decision theory, see section 2.5 as the theoretical basis for risk-based O&M planning of inspections and maintenance, which allows for updating of stochastic deterioration models of wind turbines support structures and bridges when new information becomes available from inspections and sensors/condition monitoring. Figure 2-11 shows this process. In the service life of a

structure, the aim is to maximize the total expected benefits minus costs. (Dalsgaard Sørensen, 2009) is explained the computational procedure. As a brief explanation, at the design stage, there are already some decisions planned, including the inspection and monitoring plans; however, these decisions will be updated based on the outcome of inspection/monitoring during the lifetime. As a result, new decisions can be made during service life. This process is ongoing until the end of the service life (Havbro Faber & Stewart, 2003).

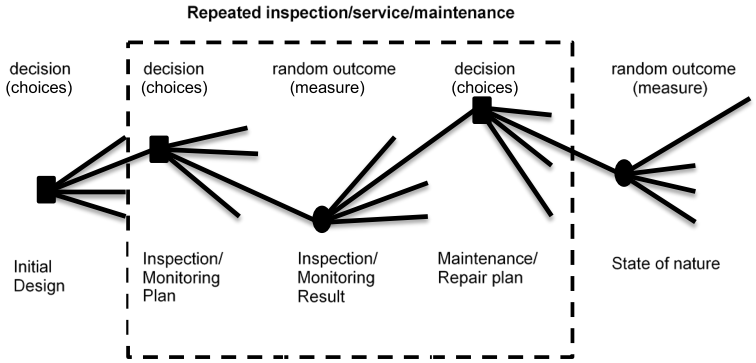

Figure 2-1: Decision tree for optimal O&M planning (Dalsgaard Sørensen, 2009; Sønderkær Nielsen, 2013)

For this updating process, conditional probabilities can help with new available information collected for instance by inspection or monitoring (Havbro Faber, 2012). The Bayes rule, which is correspondingly the basis for the BN, is formulated in Eq. 3. Given the event '*B*', the probability of event '*A*' is *P(A|B)* (Kjaerulff & Madsen, 2008):

$$P(A|B) = \frac{1}{P(B)} P(B|A)P(A) \qquad \textit{Eq. 3}$$

where *P(A)* is the prior estimate, the marginal probability of *B, is P(B),* the likelihood of *A* given *B* is *P(B|A)* the posterior estimate (Sønderkær Nielsen & Dalsgaard Sørensen, 2010).

Figure 2-10 was an example of Figure 2-11 in a case study solved in the paper (3) (Rastayesh, Long, et al., 2019).

2.6.2.3 Bayesian Networks

By means of nodes, a BN represents variables in a graphical manner using links between the variable to show their interdependencies. (Ashrafi, Davoudpour, &

Khodakarami, 2015, 2016) used BNs for reliability assessment of wind turbines. BN allows for the development of the damage over time. Fundamentals of BNs is discussed in (Fenton & Neil, 2013; Kjaerulff & Madsen, 2008). Moreover, (Sønderkær Nielsen & Dalsgaard Sørensen, 2010) used BN as a tool for O&M planning for wind turbines using fracture mechanics approach and S-N curves to predict the damage size over time (Sønderkær Nielsen & Dalsgaard Sørensen, 2010). (Luque & Straub, 2019; Rafiq, Chryssanthopoulos, & Sathananthan, 2014; Sønderkær Nielsen & Dalsgaard Sørensen, 2017) used the dynamic Bayesian network (DBN) as a framework for risk-based planning. Figure 2-12 illustrates the BN for the Metal Oxide Semiconductor Field Transistor (MOSFET) as an example of a BN.

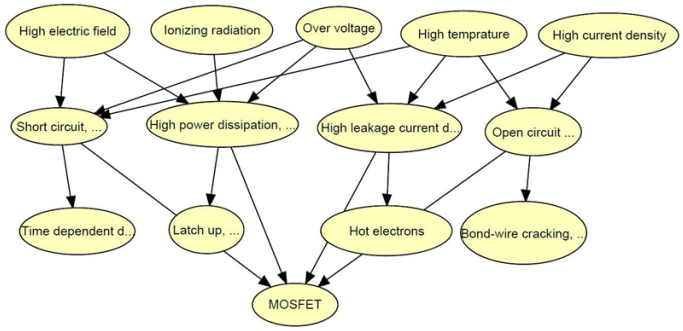

Figure 2-2: Bayesian Network for the MOSFET (Rastayesh, Bahrebar, et al., 2020).

CHAPTER 3. BRIDGES

3.1. INTRODUCTION

This chapter investigates aspects of the objectives of the Ph.D. study through case studies presented in paper (1) and paper (2), applied to a bridge infrastructure.

There are different approaches in literatures for risk assessment of bridges (Honfi, Leander, & Björnsson, 2017; Krogness Forsnes, 2015; Leander, Honfi, & Björnsson, 2017; Liu, Xiao, Lu, & Deng, 2016; Zhou et al., 2015). Conventionally, fatigue problem is faced with two approaches: Wohler Curves or S-N curve and fracture mechanics (Ambühl, 2015). In this section, respectively, paper (1) uses the S-N approach, and paper (2) tries to establish compatibility between crack growth and S-N Model in the Crêt De l'Anneau viaduct in Switzerland.

3.1.1. S-N APPROACH FOR RELIABILITY ASSESSMENT

The S-N (Wöhler) curve, in combination with Miner's rule, is the recommended approach for fatigue life calculations in all international codes and standards (Márquez-Domínguez, 2013). A broad state of the art review on fatigue life assessment for steel bridges is reviewed in (Ye, Su, & Han, 2014). A probabilistic S-N fatigue model is used to determine the reliability level.

3.1.2. FRACTURE MECHANICS APPROACH

Fracture mechanics is used to model crack growth or, in other words, the damage evolution. Paris's propagation law is a common approach to be used (Ayala-Uraga & Moan, 2007; Beržonskis & Dalsgaard Sørensen, 2016; Leander et al., 2017; Lotsberg & Sigurdsson, 2005; Madsen, Krenk, & Lind, 2006; Torgeir Moan., Hovde, & Blanker, 1993; Shabakhty, Haselibozchaloee, & Correia, 2020).

Reliability assessment based on the fracture mechanics approach is highly sensitive to estimated initial cracks (Leander et al., 2017; T Moan, 2005) as well as crack growth parameters and stress intensity factors (Kaminski & Rigo, 2018; Lotsberg, Sigurdsson, Fjeldstad, & Moan., 2016).

3.1.3. RELIABILITY UPDATING BACKGROUND

The reliability of the inspection method and procedure is of crucial importance for inspection planning. The more accurately the inspections are carried out, the more information can be revealed about the state of deterioration. However, more accuracy

implies more expensive methods, and it is essential to include this aspect into inspection planning.

PoD curve is required for each of the relevant techniques modelling the reliability of the inspection technique (Márquez-Domínguez, 2013). For example, (Márquez-Domínguez & Dalsgaard Sørensen, 2012) used it for reliability updating.

In a nutshell, reliability can be updated based on new information obtained from the inspection. This information is beneficial both for the current state of the structure and planning as well as for the future (Márquez-Domínguez, 2013).

3.1.4. CALIBRATION OF FRACTURE MECHANICS MODELS TO S-N APPROACH

From inspections and measurements, the obtained information is about the crack. While in the S-N curve based fatigue approach, there is nothing concerning cracks, it is just damage accumulation, which is obtained by the S-N approach. Thus, calibration is needed to relate cracks in the fracture mechanics approach and damage accumulation in the fatigue approach (Torgeir Moan. et al., 1993). Therefore, a calibration of the S-N fatigue approach to the fracture fatigue approach is often performed in order to derive the same level of reliability as S-N fatigue (Lotsberg et al., 2016; Mankar, Rastayesh, & Dalsgaard Sørensen, 2018a). There is a high correlation between the resulting amount of required in-service inspection and this calibration (Mankar et al., 2019).

3.1.5. BAYESIAN NETWORKS

The crack propagation model obtained from the fracture mechanics model and the initial crack found from the calibration would be the input to a model using a BN, which is a methodology which can be used for decision-making for O&M planning (Rastayesh & Dalsgaard Sørensen, 2019). There is more detailed discussion and detailed process in the following sections.

3.1.6. UNCERTAINTY ANALYSIS

Each decision-making process requires an uncertainty analysis as there are always uncertainties to be accounted for in the recorded data and/or the model. The data can come from the outcome of inspections from different kinds of sensors (Urban, Strauss, Schütz, Bergmeister, & Dehlinger, 2014), inspections, and condition monitoring, or it could come from laboratory test results.

3.2. COMPARATIVE INVESTIGATION ON REBAR DATA SET (PAPER 1)

Uncertainty analysis is an important step in risk assessment (Mankar, Rastayesh, & Dalsgaard Sørensen, 2018b). For consideration of the uncertainty, there are different methodologies available. Taking into account the uncertainty in the probabilistic approaches is a key element. In this section, the aim is to investigate one of these methods suitable for the case study presented in paper (1). A comparative investigation is carried out in this paper on the available fatigue data set tested at Aalborg University by (Hansen & Heshe, 2001). Three different uncertainty approaches for this data set are used to investigate their impact in the reliability analysis of the Swiss bridge, Crêt De l'Anneau viaduct (Rastayesh, Mankar, & Dalsgaard Sørensen, 2018). Firstly, the Maximum Likelihood Method (MLM) is used to fit the statistical parameters in a regression model for the fatigue strength of rebars (Rastayesh, Mankar, et al., 2020). Moreover, the bootstrap methodology is analyzed for uncertainty analysis; however, it did not pass its test to be used for further investigation because of run-out data. Finally, the use of the Bayesian inference with the Markov Chain Monto Carlo approach is investigated (Rastayesh, Mankar, et al., 2020). The usage of this approach showed that the reliability analysis could be more precise rather than using the MLM by Bayesian inference. For more details, please go through paper (1) in Annex 1.

3.3. BAYESIAN NETWORK FOR RISK-BASED DECISION-MAKING OF A COMPOSITE BRIDGE

Nowadays, one of the challenges in the industries is to minimize the cost of O&M. Two related topics to find the best solution are: risk-based inspection and risk-based operation and maintenance. They could be considered to be a subset of risk-based decision-making. Offshore structures such as wind turbines are continuously exposed to loads that have a direct influence on the structure lifetime. This is the same situation with the loads on bridges, for example by vehicles. Thus, different strategies are applied to prolong their life cycle performance using risk-based inspection and risk-based operation and maintenance. This section will investigate the use of BNs for risk-based inspection and O&M planning. A framework utilizing BNs is suggested and a decision tool is proposed to manage structures subjected to deterioration in their lifetime. The aim is to find the optimum decisions based on the cost of maintenance and inspection. The procedure could prevent failures in the structures and reduce consequences caused by late inspections or maintenance as well as early ones to optimize the cost of repair and inspection.

3.3.1. DAMAGE EVOLUTION MODEL FOR THE FATIGUE OF REBARS USING CALIBRATION OF THE S-N MODEL TO THE FM MODEL (PAPER 2)

This section uses the results from the previous section (Paper 1). The aim is to find the crack propagation model as an indicator of decision-making, which can be used in the BN. By using a fracture mechanics (FM) approach, the model for crack propagation is developed in Paper (2) by back calculating from the S-N approach presented in Paper (1). For more details, see Paper (2).

3.3.2. BAYESIAN NETWORK MODEL FOR O&M PLANNING

(Rastayesh, Sønderkær Nielsen, & Dalsgaard Sørensen, 2018) provides an introduction of how BNs could be used as a tool for O&M planning. In this regard, the dynamic influence diagram is proposed as a framework that focuses on risk-based decision-making (Rastayesh, 2019). The damage development model over time is used as the basis for the proposed methodology. The indicator for the risk-based decision-making is the damage size. The initial value is set to "a(0)", meaning crack size at time 0. In this approach, the damage states are considered by intervals as it is not possible to consider continuous distributions while using influence diagrams. Hence, the distribution known from the damage model is discretized.

3.3.3. DISCRETIZATION METHODOLOGY

In case of a normal distribution, it is assumed that 10 intervals is enough to catch the whole distribution from three times sigma from the mean value. In other words, the distribution is truncated from both sides. For other distributions, the power function methodology for discretization is used (Friis-Hansen, 2000). (Straub, 2009) also suggested a discretization methodology for continuous distributions.

Figure 3-1 and Figure 3-2 shows the discretized distributions using Hugin software.

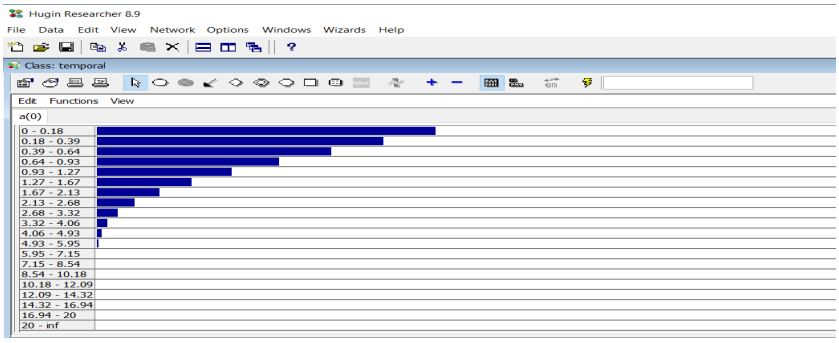

Figure 3-1:Discretization of the exponential distribution for cracks

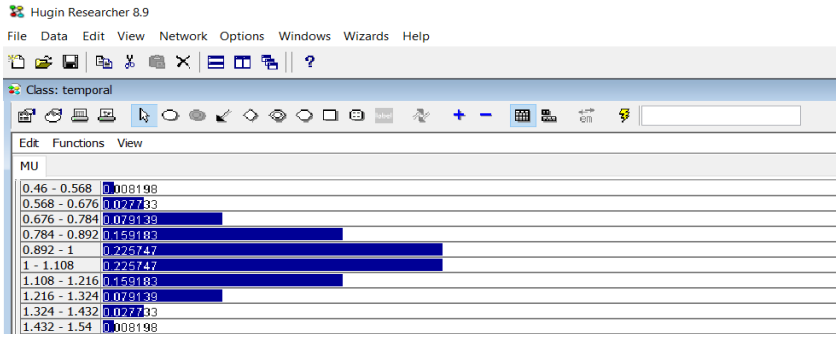

Figure 3-2: Discretization of the normal distribution for model uncertainty

In the damage model, there is always uncertainty associated, which can change over time or could be considered constant for all time steps. For instance, considering load parameter, the load is changing over time. Consequently, if it is modeled by a distribution such as lognormal, the mean and standard deviation could change over time (Sønderkær Nielsen & Dalsgaard Sørensen, 2017). Although in many studies, they are all considered the same over time (Friis-Hansen, 2000). Node, Model Uncertainty, "MU" is taken into account for all resistance and load parameters uncertainty labeled "A", as an example in time step 2, it is shown as A(02).

In this time step, a utility node is added called Cost of Failure, "CF(0)". Failure would happen if the design of the structure fails and causes the collapse or local failure in the infrastructure.

In the next time step, T(02), an assumed two-year interval, an inspection decision will be made in the decision node, Inspection Decision, "Inspect(02)", with two states, inspection or no inspection. In this case study, it is assumed that the inspector starts the first inspection and interval based on the designers' plan described in the design stage. There is always a cost involved with each inspection in the utility node, Cost of Inspection, "CI(02)".

This inspection is assumed to distinguish the damage at four states: finding failure, finding crack, finding nothing, and no inspection. This information is stored in the chance node called Inspection Result, "InspRes(02)". As seen in Figure 3-4, this node is dependent on the Inspection Decision and "a(02)". "a(02)" is calculated the same way as "a(0)" with a damage degradation model over time. Moreover, this node includes a PoD giving the probability of detection of a crack given the crack size.

The uncertainty associated with each inspection is modeled by the probability of the detection curve with an exponential distribution function (Georgiou, 2006). This model is needed to model the fact that there is always more probability to detect larger damages.

The repair strategy is taken into consideration through three states in the node called “a rep(02)”, which is the crack after repair which is assumed to be the same as the initial crack. This node will decide to exchange when the inspection outcome is a failure, meaning the damage state will come back to initial damage if the exchange is done.

The repair node has a cost with a utility node assigned for it named Cost of Repair “CR(02)”.

Some assumptions are considered for simplicity. The focus of this section is to show the dynamic influence diagram approach, which can easily be developed to any other case.

It is assumed that at the initial time step, there is no failure means the “PF(0)” probability of failure is zero for all intervals except the last one; as seen in Figure 3-3. “dPF(02)” is the difference of probability of failures with the previous time step (Friis-Hansen, 2000).

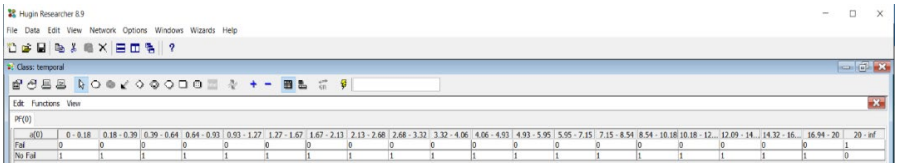

Figure 3-3: Probability of failure at the initial time step

As a conclusion, which is mainly taken from the approach presented in (Friis-Hansen, 2000), a comprehensive DBN using influence diagram is proposed for the risk-based decision-making, where at each time step the damage will be updated after repair. The dynamic BN is built in the Hugin software. The temporal nodes are suggested instead of showing each time step to be calculated for 10 time steps, which allows to easily add more time steps in the calculation to cover more years. The temporal nodes in Figure 3-4 are “T_A(02)”, “T_a(02)” and ”T_a rep(02)”.

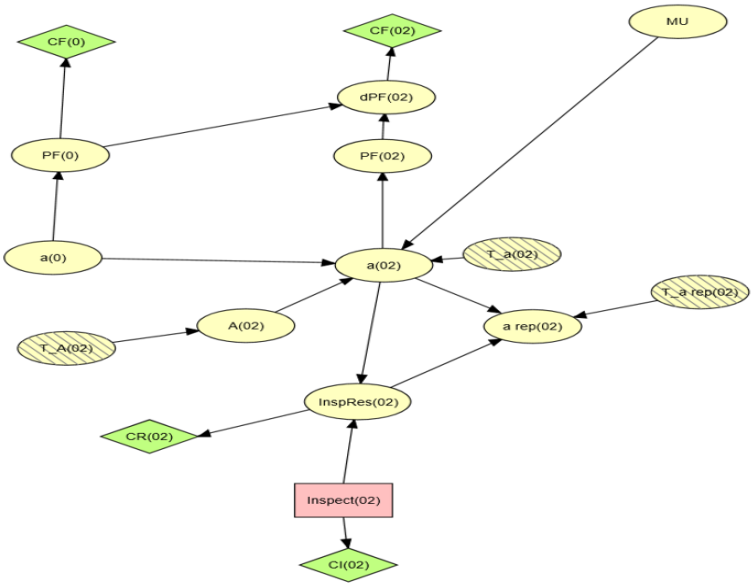

Figure 3-4: Dynamic Influence Diagram as a Framework for Risk-Based Decision-Making

Figure 3-5 is the extension of Figure 3-4 to three time steps.

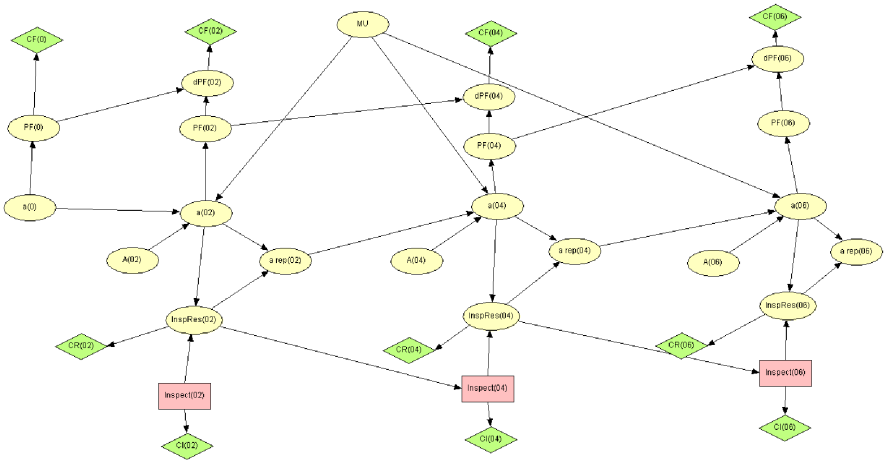

Figure 3-5: The extended form of Figure 3-4 (Friis-Hansen, 2000)

CHAPTER 4. WIND TURBINES

1.1 Introduction

In this chapter, the objectives of the Ph.D. are investigated through case studies for wind turbines, published in Papers 3–6.

There are different approaches in the literature for risk assessment of wind turbines (Asghari, Pourgol Mohammad, & Salehpour Oskouyi, 2015; Hallowell et al., 2018; Hammar, Wikström, & Molander, 2014; Hong & Möller, 2012; Integrated Environmental Data, 2013; Kang, Sun, Sun, & Wu, 2017; Mensah & Dueñas-Osorio, 2012; Rastayesh, Zorzi, Miraglia, & Dalsgaard Sørensen, 2019; Shafiee & Dinmohammadi, 2014; P. Tavner, 2012; P. J. Tavner, Xiang, & Spinato, 2007).

For risk assessment of an adverse event, as mentioned earlier in Chapter 2, the preliminary step can be identifying what caused this risk to happen and then to investigate the effects of the risk. For quantitative risk assessment, a failure probability model could be obtained from the parameters causing this risk event to happen and, subsequently, the consequence modeling to calculate the adverse event risk. The consequences can be put in different main categories, environmental, fatality, and economic impacts. These categories could be categorized in wind turbines as follows: operating expenses (OPEX), capital expenditures (CAPEX), development expenditure (DEVEX), revenue, people, environment, reputation, delay in the project, and, most importantly, production loss during different life-cycles of the wind turbine. For instance, people as one of the categories could be in different forms: injury or fatality. Moreover, the level of the injuries could also be classified as minor and major. Different classifications for each of the consequences mentioned above would help to reach a better result in the risk analysis during the identification. In order to have an accurate risk assessment, the decision-maker must pay close attention to the classification and identification of the risk likelihood and its impact.

There are different methodologies available for risk assessment. Risk analysts should find the best method aimed for the objective of decision-making. In the following, FMEA, FTA, BN and decision tree are investigated for wind turbine case studies as the best practice. However, there is not a unique solution for finding the best method for each decision-making process, as each of them has pros and cons.

4.1. RISK ASSESSMENT OF WIND TURBINES NEAR HIGHWAYS (PAPER 3)

There is always a risk if any failure in the wind turbine leads to throwing one or more than one part or object of the wind turbine off to its surrounding (Braam &

Rademakers, 2004; Gupta, Robinson, Sanderson, & Morrison, 2012; Kaposvari & Weidl, 2015; Rastayesh & Dalsgaard Sørensen, 2018; Sarlak & Nørkær Sørensen, 2016; Seifert, Westerhellweg, & Kröning, 2003). The same scenario in icy conditions (a cold climate) could happen if ice can throw off wind turbines, specifically from the blades (LeBlanc, 2007). Considering a case where these surroundings are located, the risk could have different consequences. There are some countries where there is limited space for placing wind turbines. In this situation, it could be considered to locate wind turbines in areas which there are in the vicinity of a highway (Rastayesh, Long, et al., 2019). As mentioned earlier, based on the location of the wind turbine, the impacts of a risk event (failure of a blade or ice throw) could be different. For instance, if the wind turbines are placed near some houses, the risk could be damage to buildings and people. Other conditions could be if the wind turbines are placed near a highway, and the consequence could be on the cars passing by on the highway, which also means the driver and passengers. These examples could be classified into the impact on the environment, people, and production loss in the consequence categories, as mentioned in section 4.1.

In this chapter, the case study is considered where there is a risk to people in cars when wind turbines are placed near a highway. Figure 4-1 depicted this scenario where the wind turbines are placed near a highway.

Figure 4-1: Wind turbines near a highway

Risk models in three different cases are developed, and a risk model for each scenario is developed (Dalsgaard Sørensen, Nørkær Sørensen, & Lemming, 2012; Rastayesh, Long, et al., 2019). These three failure scenarios are as follow:

Scenario 1: When failure of the blades could lead to throwing off part of the wind turbine blade or the entire blade. In Figure 4-2, the model illustrates the same scenario

when a part of the blade is thrown off the wind turbine and hits a car. Using a function of distance from the wind turbines to the highway, the risk is calculated (Rastayesh, Long, et al., 2019).

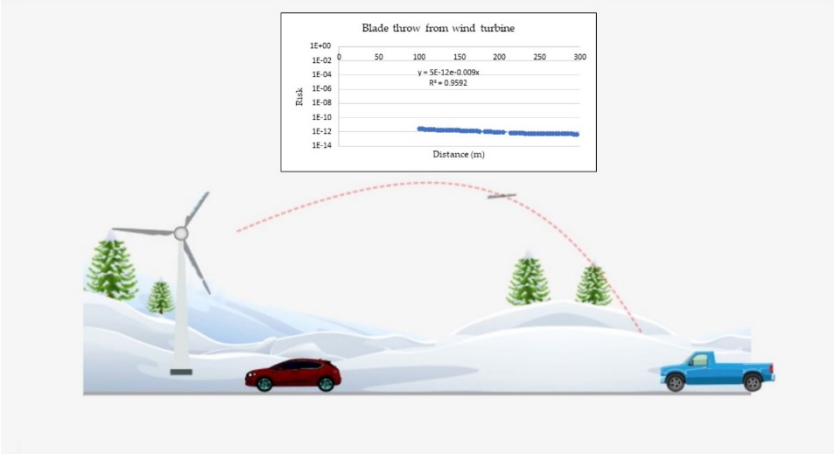

Figure 4-2: Blade thrown off the wind turbine near a highway

In cold climates, ice accretion on the blades could result in throwing ice pieces to the surroundings. In Figure 4-3, the model demonstrates the situation when an ice piece is thrown off a wind turbine and hits a car. Risk is calculated as a function of distance from the wind turbines to the highway (Rastayesh, Long, et al., 2019).

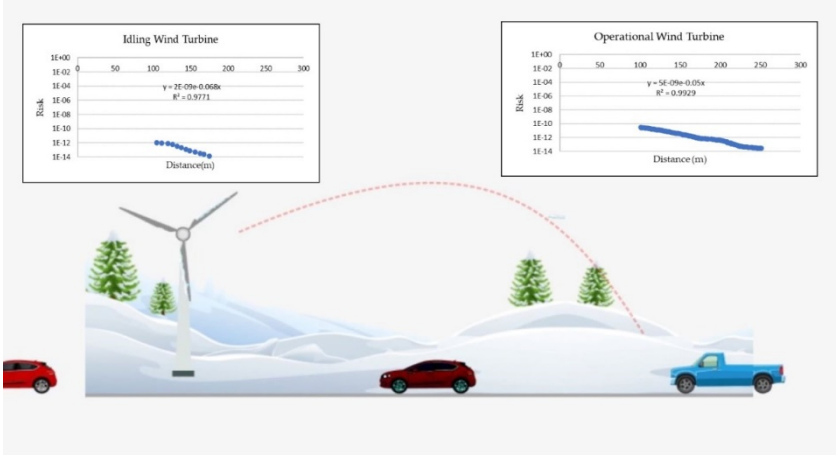

Figure 4-3: Ice from the wind turbine near a highway

There are two different cases in this situation:

Scenario 2: the wind turbines could still be operating, and ice pieces can be thrown off.

Scenario 3: the wind turbine could be in an idling mode, which means a detection system identified the ice condition, and the wind turbine is stopped (Rastayesh, Long, et al., 2019). Although it should be noted since still wind is blowing, it could lead to throwing off ice pieces. Please see the video attached as complementary material to this chapter of the thesis.

An anti-icing or de-icing system in scenarios 2 and 3 could be a solution to avoid or decrease the risk of these events. In this case, it is required to have an ice detection system to give an indication to the de-icing or anti-icing system to start functioning. The aim of this paper is to use the decision tree as a decision tool for risk-based decision-making to find out whether it is worth installing a heating system on blades to avoid the risk of ice being thrown off the wind turbines placed near a highway and hitting a passing car (Rastayesh, Long, et al., 2019). The application of Bayesian decision analysis is discussed in this paper. Considering some assumptions described in detail in Paper (3), the following simplified decision tree is developed. Assuming an ideal ice detection system, Figure 4-4 is the result of the decision tree suggested. The VoA is utilized in this decision-making.

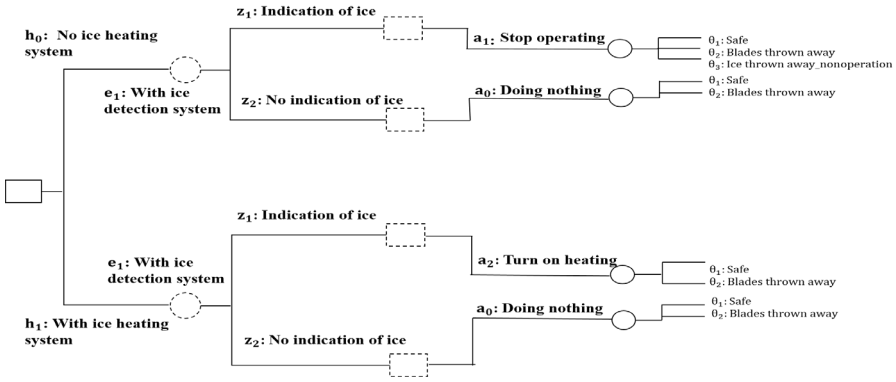

Figure 4-4 simplified decision tree for decision-making whether to use ice heating system (Rastayesh, Long, et al., 2019)

To answer the question if it is worth turning on the heating system or not, Figure 4-4 shows a decision tree for this decision-making process considering two decisions that should be optimized. The first utility u_{h_0} which points out to the decision of whether to shut down the wind turbine, and second one the decision to turn on the heating system u_{h_1}. Eq. 4 is the calculated VoA (Rastayesh, Long, et al., 2019).

$$VoA = u_{h_1} - u_{h_0} \qquad Eq.\ 4$$

In order to solve Eq. 4, using the suggested decision tree, the Bayesian decision theory is applied to maximize the cost of benefits. Each parameter of Eq. 4 is expanded to another detailed equation considering the probability of failure of each scenario presented in Figure 4-2 and Figure 4-3 and their consequences in the form of impact to people or production loss or cost of the heating system during the wind turbine lifetime. The results indicate that such systems should be used in countries that have a relatively high frequency of icy weather. Moreover, the duration of downtime as an essential factor in the results shows that the decision to use the heating system is highly related to this factor.

4.2. RISK ASSESSMENT OF POWER STAGE USED IN WIND-FUEL CELL HYBRID ENERGY SYSTEMS

As mentioned in the introduction, there is not a unique methodology that can be used for the risk assessment of each system to give the best results, as each of these methods has its advantages and disadvantages. The aim in this section, which refers to Papers (4, 5, and 6), is to explore methodologies described in the introduction, including FMEA, FTA, and BN, with a case study that has application in wind turbines. In these three papers, proton exchange membrane fuel cells (PEMFCs) are chosen as a renewable energy source that can be used as a hybrid energy system together with wind turbines. By a system engineering approach and using FMEA, it is possible to identify critical components, failure modes, and failure causes (Bahrebar, Blaabjerg, Wang, Rastayesh, & Zhou, 2018; Bahrebar, Blaabjerg, Wang, Zhou, et al., 2018). The Risk Priority Numbers (RPN) are obtained by means of the FMEA. Moreover, by BN, critical causes of critical components have been explored using the RPNs obtained from FMEA. In addition, the reliability analysis is done applying FTA, by considering exponential and Weibull distributions for failure rates. The importance of obtaining more realistic reliability is highly dependent on the failure data. To see also the influence of the O&M, the FTA is applied for reliability assessment. Repair action shows a great impact on the availability of the system.

4.2.1. LIFETIME ESTIMATION AND FAILURE RISK ANALYSIS IN A POWER STAGE USED IN WIND-FUEL CELL HYBRID ENERGY SYSTEMS (PAPER 4)

This paper presented a failure mechanism analysis of the power stage components as a central part of the power conditioner sub-system in a hybrid wind-fuel cell system using the FMEA and the FTA methods (Rastayesh, Bahrebar, et al., 2019). In this article, the power stage FMEA process and its utilization in ranking the estimated risk priority with various potential failure modes for critical subcomponents is explained. The failure mechanism of power stage components for selected critical

subcomponents is identified and analyzed by the FMEA. Figure 4-5 shows important subcomponents of the power stage in the power conditioner utilized in PEMFC.

Figure 4-1: Critical power stage subcomponents in a power conditioner utilized in PEMFC (Rastayesh, Bahrebar, et al., 2019).

The failure mechanism analysis of the MOSFET as a critical active component is identified with details. Some failure mechanisms have significant effects on system reliability and made some critical failure modes. FMEA identifies some of the failure modes of active subcomponents such as MOSFET and passive subcomponents like electrolyte capacitors. Considering the FMEA results, three main failure parts of the power stage (input filter, power amplifier, and output filter) are considered in the FTA. Utilizing FTA of the power stage, it is identified how failure could happen.

Figure 4-6 is the fault tree of the power stage of PEMFC where the top event is power stage failure. Top event fails if the input filter or power amplifier or output filter fails.

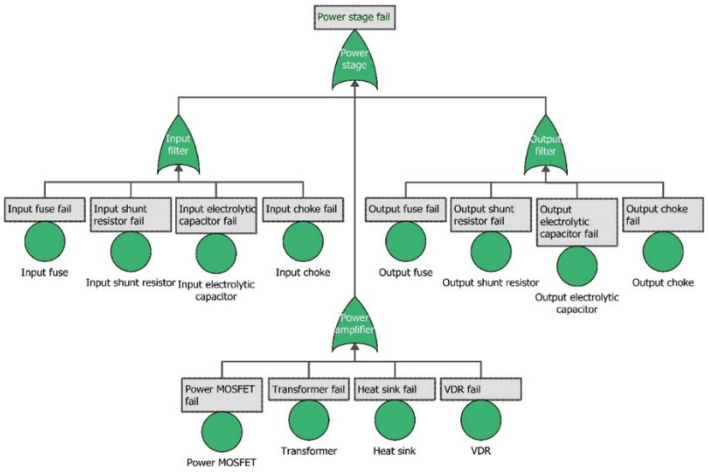

Figure 4-2: Fault tree of the power stage of PEMFC (Rastayesh, Bahrebar, et al., 2019)

The reliability curve of the power stage is estimated for a five years period, consistent with the product guarantee period. The B1 lifetime of the power stage using exponential distribution is concluded to be near two folds smaller than the Weibull distribution. Besides, the Weibull lifetime estimation by applying the Monte Carlo simulation shows closer results to the real experience. Hence, the more realistic reliability analysis results by the Weibull distribution make it a superior distribution compared to exponential distribution. Although the Weibull parameters are usually not available for all components or can prove to be challenging to obtain by reliability tests, the FMEA is still recommended as the method of choice for distinguishing high-risk components and their Weibull parameters for reliability analysis.

4.2.2. A SYSTEM ENGINEERING APPROACH USING FMEA AND BAYESIAN NETWORK FOR RISK ANALYSIS—A CASE STUDY (PAPER 5)

This study proposed a system engineering approach using a comprehensive FMEA analysis by applying the block diagram, function block diagram, and parameter diagram (Rastayesh, Bahrebar, et al., 2020). These methodologies are implemented to provide a better understanding of the power conditioner system for the risk analysis in a PEMFC system.

First, using the FMEA for the PEMFC system, potential failure modes of the components and critical components have been identified. Furthermore, potential risk numbers are assigned to each failure mode. The results have presented risky components based on high RPNs. The highest RPNs correspond to the failure modes in three components with a wide range of failure modes, including high Leakage Current (LC) of the MOSFET, Short Circuit (SC) of the capacitor, and increased LC due to gate oxide of the MOSFET. In other words, short circuits, open circuits, and leakage current are found as the most important failure modes. Besides, the MOSFETs, capacitors, chokes, and transformers are identified as the critical components of the power stage. These components should be considered in the design stage. Lastly, the most critical failure causes among the more important items are identified by the FMEA method and used for BN analysis. The BN is implemented by two states of true and false (failure and success) (García & Gilabert, 2011) to find the most critical failure causes such as high temperature and overvoltage, which have been ascertained utilizing BN. The BN investigates the impact of each failure cause in order to identify the most effective one among other failure causes in the most critical component (MOSFET) at the system. Table 4-1 shows the FMEA of the MOSFET and Figure 4-7, the BN of the MOSFET. In Figure 4-7, the high temperature importance is feasible.

Table 4-1: FMEA table for MOSFET (Rastayesh, Bahrebar, et al., 2020).

Item	Function	Failure Mode	Failure Causes	Failure Effects	S	O	D	RPN
MOSFET	Switch electrical current at desired time interval	Short circuit, loss of gate control, and increased leakage current due to gate oxide	High temperature High electric field Over-voltage	Time dependent dielectric breakdown	9	7	5	**315**
	Control electrical current	High power dissipation, loss of gate control and device burn-out due to silicon die	High electric field Over-voltage Ionizing radiation	Latch-up, Increased forward voltage	8	7	5	**280**
	Rectify current at desired time interval	High leakage current due to substrate interface	High temperature High current Over-voltage High current density	Hot electrons	8	7	8	**448**
	Protection and regulation	Open circuit due to bond wire and die attach	High temperature High current density	Bond-wire cracking, lift-off; delamination of die attach	7	4	6	**168**

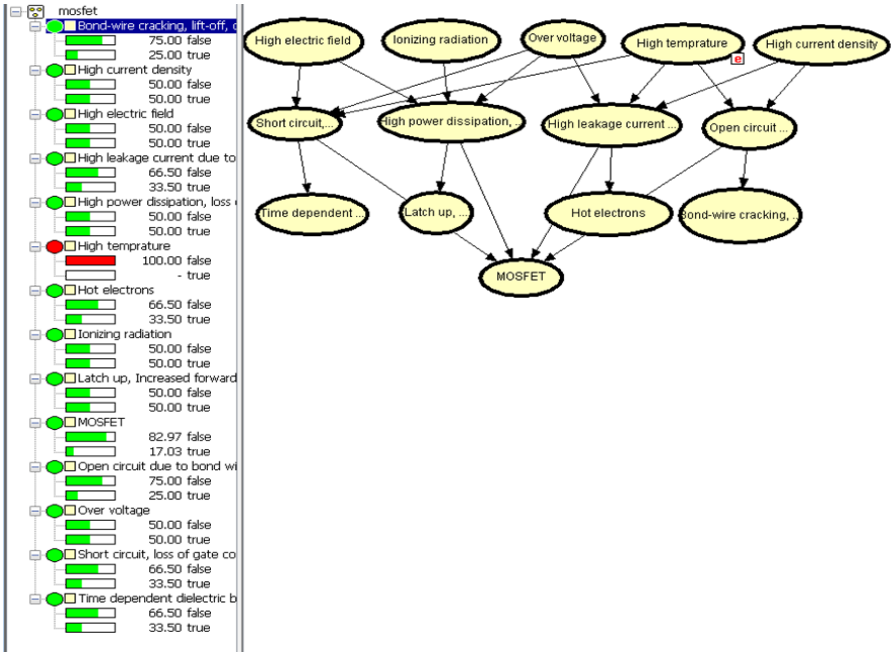

Figure 4-3 High temperature effect failure on the MOSFET (Rastayesh, Bahrebar, et al., 2020).

Finally, some solutions are proposed to reduce the risk of damage to the entire system due to failure modes and causes. Knowing the failure modes will help designers to

pay more attention to terms of use, material properties, and design of various components to avoid failures caused by high temperature and overvoltage.

4.2.3. RELIABILITY ASSESSMENT OF POWER CONDITIONER CONSIDERING MAINTENANCE IN A PEM FUEL CELL SYSTEM (PAPER 6)

In this paper, the reliability and availability issues of the power conditioner system in the PEMFC is investigated by using the FTA (Bahrebar, Zhou, et al., 2018). The methodology – as a conventional approach for reliability assessment – is designed to illustrate the relations between basic events, logical variables, and significant components. The FTA approach is applied as a graphic representation of the different combinations of failures causing the occurrence of a top event (Modarres et al., 2016). FTA is used as a deductive process to analyze five sub-systems in the power conditioner as our top events. Figure 4-8 shows the simplified configuration of the power conditioner.

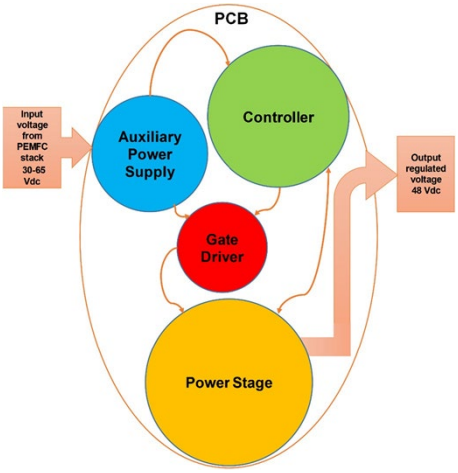

Figure 4-4 The simplified configuration of the power conditioner (Bahrebar, Zhou, et al., 2018).

Aging is one of the major aspects that could affect the system reliability. One of the critical steps in the reliability calculations is choosing an appropriate distribution that helps to show the aging effect. By applying the Monte Carlo simulation and considering maintenance and inspection policies, the availability is calculated for the system during operation. Besides, the reliability curves are compared for five main components of the power conditioner in this case, proving the availability of the system increases under planned maintenance. For decision-makers, one solution to optimize the maintenance is to look at the inspection or monitoring systems by considering the inspection intervals. However, the repair actions for critical components could significantly affect the availability of the system.

CHAPTER 5. CONCLUSION

There is a variety of risk assessment approaches. One of the primary steps is to identify which methodology is the most suitable one in a risk assessment project. The solution is not the same for each industry because of its aim. For wind turbines and bridges, it is the same issue. There is not even a unique answer for the best approach that can be used in the risk assessment. Despite the fact, each method has some pros and cons. One of the main goals of this Ph.D. was to identify and develop illustrative computer tools for decision-making using the applied methodologies for risk assessment for case studies. In order to reach this goal, two different infrastructures – bridge and wind turbines (These two types of structures were given by the INFRSASTAR project) – have been investigated to reach a better approach for risk assessment of each case study described in chapters 3 and 4. Each case study incorporates an investigation of the evaluation of hazards and the recommendation of a plan in order to reach a lower level of risk.

Firstly, for a data set from the fatigue test, different uncertainty methodologies, MLM, Bootstrapping, and Bayesian, are compared. The results from the Bayesian approach had better performance than the others. The results have been used for reliability analysis of a case study of a Swiss bridge as discussed in Chapter 3. The importance of uncertainty analysis and its effect on the reliability analysis has been investigated. Later, using the fracture mechanics approach and inputs from inspections, O&M data including repairs from sensors and condition monitoring, a BN is suggested using dynamic influence diagrams. This case study uses BN, which is based in the Bayesian decision theory, as the illustrative tool to fulfill the goal of the Ph.D., which enables the risk assessment modeling dynamically during the lifetime. In the worst case scenario, cracks could lead to local failure and collapse of the structure as the adverse event in this case.

In the risk assessment of ice and blades thrown off wind turbines near a highway, three cases as adverse events are studied, and finally, using the As Low As Reasonably Practicable (ALARP) principle, the risk is found acceptable. Moreover, using decision trees as the illustrative tool, the application of the heating system as a solution for an icy condition to avoid ice thrown off the wind turbine is investigated. Based on the results in this study, it is better to consider the installation of such systems when the frequency of icing in that area is considerable, although the lack of enough data in this study was challenging. Similarly, Bayesian decision theory as the basis for the decision tree is utilized as the tool for the risk assessment of this case study. The condition monitoring information from sensors (heating system, anemometer…) is used to reach the goal of the Ph.D. in this case study.

In addition, the application of PEMFCs and wind turbines as a hybrid system is investigated. Usage of FMEA is a standard methodology, especially during the design

phase of a project, although it is more qualitative or semi-quantitative. Besides, FTA and BNs are more powerful tools when it comes to quantitative analysis, although both qualitative and quantitative inputs can be feed into BNs. Once more, the Bayesian decision theory is used as the illustrative tool in the BN supported FMEA and FTA to reach the goal in this case study. Moreover, the influence of repairs in the decision making is investigated by FTA for decision-making.

CHAPTER 6. FUTURE WORK

The basic methodologies for risk assessment presented is considered applicable for the case studies considered, especially the application of the Bayesian approach. However, further development is needed to model and assess systems modelling e.g. a wind turbine with many different components or wind farms with many wind turbines, especially development of the computational capabilities are needed.

A major challenge of most risk assessment projects is the lack of diverse data, especially failures, as these are very often confidential in the industries, and even in some situations no data are recorded. Hence, it is recommended to track and record data of failures for the systems considered. Even though the qualitative approaches could be a solution in this regard, the uncertainty is still higher than the quantitative approaches. Moreover, qualitative approaches usually use expert opinions, which itself has uncertainty. It is recommended that if no quantitative data is available to collect, more experts are needed to be involved for qualitative judgment following standards available in this regard in some industries.

Sensors and measurements required for the risk assessments need to be assessed during the design stage. For example, the selection of which kind of sensors can be used as indicators for cracks during the lifetime of a bridge or a wind turbine, and so it may be necessary to install the sensors during the fabrication and execution of the structure. Moreover, the uncertainty of these sensors has an essential impact on the risk assessment that needs to be considered.

There are several methodologies that are not discussed in this project and that industries are using for risk assessment, and the best solution for each could be developed if more data would be available.

The model used for crack propagation in the BN can be further developed. A suitable sensor as an indicator for crack sizes and consideration of their installation during the building phase of the structure could be recommended in order to have a better basis for the decision-making. The assumption here is if cracks can be detected or not. If the information about the size of the crack was available, the analysis could be more reliable. This case could be challenging for concrete structures.

All these aspects could be an advancement to have better risk assessment with less uncertainty.

LITERATURE LIST

Adar, E., İnce, M., Karatop, B., & Bilgili, M. S. (2017). The risk analysis by failure mode and effect analysis (FMEA) and fuzzy-FMEA of supercritical water gasification system used in the sewage sludge treatment. *Journal of Environmental Chemical Engineering*, *5*(1), 1261–1268. https://doi.org/10.1016/j.jece.2017.02.006

Ambühl, S. (2015). *Reliability of wave energy converters*. Aalborg University. https://doi.org/10.13052/rp-9788793379053

Asghari, J., Pourgol Mohammad, M., & Salehpour Oskouyi, F. (2015). Improving dynamic fault tree method for complex system reliability analysis: Case study of a wind turbine. In *ASME International Mechanical Engineering Congress and Exposition, Proceedings (IMECE)* (Vol. 14–2015). Texas: American Society of Mechanical Engineers (ASME). https://doi.org/10.1115/IMECE2015-51307

Ashrafi, M., Davoudpour, H., & Khodakarami, V. (2015). Risk assessment of wind turbines: Transition from pure mechanistic paradigm to modern complexity paradigm. *Renewable and Sustainable Energy Reviews*, *51*, 347–355. https://doi.org/10.1016/j.rser.2015.06.011

Ashrafi, M., Davoudpour, H., & Khodakarami, V. (2016). A Bayesian network based framework to evaluate reliability in wind turbines. *Wind and Structures, An International Journal*, *22*(5). https://doi.org/10.12989/was.2016.22.5.543

Ayala-Uraga, E., & Moan, T. (2007). Fatigue reliability-based assessment of welded joints applying consistent fracture mechanics formulations. *International Journal of Fatigue*, *29*, 444–456.

Bahrebar, S., Blaabjerg, F., Wang, H., Rastayesh, S., & Zhou, D. (2018). Failure modes and effect analysis for risk minimizing in critical components of proton exchange membrane fuel cell system. In *7th Conference on Safety Engineering and HSE Management*.

Bahrebar, S., Blaabjerg, F., Wang, H., Vafamand, N., Khooban, M.-H., Rastayesh, S., & Zhou, D. (2018). A novel type-2 fuzzy logic for improved risk analysis of proton exchange membrane fuel cells in marine power systems application. *Energies*, *11*(4), 721. https://doi.org/10.3390/en11040721

Bahrebar, S., Blaabjerg, F., Wang, H., Zhou, D., & Rastayesh, S. (2018). System-level risk analysis of PEM fuel cell using failure mode and effect analysis. In *5th International Reliability and Safety Engineering Conference*. Shiraz: Arzhang

Printing.

Bahrebar, S., Rastayesh, S., & Sepanloo, K. (2014). Dynamic availability assessment on Tehran research reactor water cooling system. *Indian J.Sci.Res*, *1*(2), 471–474.

Bahrebar, S., Zhou, D., Rastayesh, S., Wang, H., & Blaabjerg, F. (2018). Reliability assessment of power conditioner considering maintenance in a PEM fuel cell system. *Microelectronics Reliability*, *88–90*, 1177–1182. https://doi.org/10.1016/j.microrel.2018.07.085

Bech Andersen, M. (2012). *Improvement of failure mode and effects analysis*. Retrieved from http://docplayer.net/35365885-Improvement-of-failure-mode-and-effects-analysis-june-2012.html

Beržonskis, A., & Dalsgaard Sørensen, J. (2016). Reliability analysis of fatigue fracture of wind turbine drivetrain components. In *Energy Procedia* (Vol. 94). https://doi.org/10.1016/j.egypro.2016.09.209

Braam, H., & Rademakers, L. W. M. M. (2004). Guidelines on the environmental risk of wind turbines in the Netherlands. In *Wind Energy*. Retrieved from ftp://130.112.2.101/pub/www/library/report/2004/rx04013.pdf

Carlson, C. (n.d.). What is FMEA? Retrieved from https://accendoreliability.com/fmea-2/

Chemweno, P., Pintelon, L., Nganga Muchiri, P., & Van Horenbeek, A. (2018). Risk assessment methodologies in maintenance decision making: A review of dependability modelling approaches. *Reliability Engineering & System Safety*, *173*(January), 64–77. https://doi.org/10.1016/j.ress.2018.01.011

Collong, S., & Kouta, R. (2015). Fault tree analysis of proton exchange membrane fuel cell system safety. *International Journal of Hydrogen Energy*, *40*(25), 8248–8260.

Dalsgaard Sørensen, J. (2009). Framework for risk-based planning of operation and maintenance for offshore wind turbines. *Wind Energy*, *12*(5), 493–506. https://doi.org/10.1002/we.344

Dalsgaard Sørensen, J. (2011). *Notes in structural reliability theory and risk analysis*. Aalborg: Aalborg University.

Dalsgaard Sørensen, J. (2017). Reliability analysis and risk-based methods for planning of operation & maintenance of offshore wind turbines. In *Proceedings*

of the International Conference on Offshore Mechanics and Arctic Engineering - OMAE (Vol. 9). American Society of Mechanical Engineers (ASME). https://doi.org/10.1115/OMAE2017-62713

Dalsgaard Sørensen, J., Nørkær Sørensen, J., & Lemming, J. (2012). Risk assessment of wind turbines close to highways. In *European Wind Energy Conference and Exhibition* (pp. 348–356). EWEC.

Dalsgaard Sørensen, J., & Stensgaard Toft, H. (2014). *Safety factors – IEC 61400-1 ed. 4 - background document* (4th ed.). *DTU* (Vol. 0066). DTU Wind Energy. Retrieved from http://orbit.dtu.dk/files/118222161/Database_about_blade_faults.pdf

Decision Tree. (n.d.). Retrieved from https://en.wikipedia.org/wiki/Decision_tree

DNV.GL. (2018). *Standard-DNVGL-ST-0126 -Support structures for wind turbines*. *DNV.GL*. Retrieved from https://rules.dnvgl.com/docs/pdf/DNVGL/ST/2018-07/DNVGL-ST-0126.pdf

Eduard Kostandyan, E. (2013). *Reliability modeling of wind turbines: exemplified by power converter systems as basis for O&M planning*. River Publishers, Aalborg. Retrieved from http://www.windmeasurementinternational.com/wind-turbines/om-turbines.php

EN. (2019). *Dansk standard vindenergianlæg – Del 1 : Konstruktionskrav wind energy generation systems – Part 1 : Design requirements*. DANSK STANDARD Danish Standards Association.

Fenton, N., & Neil, M. (2013). *Risk assessment and decision anlysis with Bayesian networks*. *CRC Press*. CRC Press.

Friis-Hansen, A. (2000). *Bayesian networks as a decision support tool in marine applications*. *DTU*. Technical University of Denmark.

García, A., & Gilabert, E. (2011). Mapping FMEA into Bayesian networks. *International Journal of Performability Engineering*, *7*(6), 525–537.

Gash, M. (2007). The collapsed 35W bridge in Minneapolis seen on August 2, 2007. Retrieved from https://www.npr.org/2017/08/01/540669701/10-years-after-bridge-collapse-america-is-still-crumbling?t=1581208201305

Georgiou, G. A. (2006). *Probability of Detection (PoD) curves derivation, applications and limitations*. London.

Gupta, S., Robinson, C., Sanderson, D., & Morrison, A. (2012). *Den Brook wind farm risk assessment*. *MMI Engineering Limited*.

Hallowell, S. T., Myers, A. T., Arwade, S. R., Pang, W., Rawal, P., Hines, E. M., … Fontana, C. M. (2018). Hurricane risk assessment of offshore wind turbines. *Renewable Energy*, *125*, 234–249. https://doi.org/10.1016/j.renene.2018.02.090

Hammar, L., Wikström, A., & Molander, S. (2014). Assessing ecological risks of offshore wind power on Kattegat cod. *Renewable Energy*, *66*, 414–424. https://doi.org/10.1016/j.renene.2013.12.024

Hansen, L. P., & Heshe, G. (2001). Fire and fatigue tests of ultra high-strength fibre reinforced concrete and ribbed bars. *Journal Nordic Concrete Research*, *26*, 17–37.

Havbro Faber, M. (2007). *Risk and safety in civil engineering*. *ETH*. Zurich: Swiss Federal Institue of Technology Zurich. Retrieved from http://webarchiv.ethz.ch/ibk/emeritus/fa/education/ws_safety/Safety07/Script_secure.pdf

Havbro Faber, M. (2008). *Risk assessment in engineering: Principles, system representation & risk criteria*. *JOINT COMMITTEE ON STRUCTURAL SAFETY, JCSS*. Retrieved from https://www.jcss.byg.dtu.dk/Publications/Risk_Assessment_in_Engineering

Havbro Faber, M. (2012). *Statistics and probability theory* (Vol. 18). Dordrecht: Springer Netherlands. https://doi.org/10.1007/978-94-007-4056-3

Havbro Faber, M., Dalsgaard Sørensen, J., Tychsen, J., & Straub, D. (2005). Field implementation of RBI for jacket structures. *Journal of Offshore Mechanics and Arctic Engineering*, *127*(3), 220–226. https://doi.org/10.1115/1.1951777

Havbro Faber, M., & Stewart, M. G. (2003). Risk assessment for civil engineering facilities: Critical overview and discussion. *Reliability Engineering and System Safety*, *80*(2), 173–184. https://doi.org/10.1016/S0951-8320(03)00027-9

Havbro Faber, M., Straub, D., & A. Maes, M. (2006). A computational framework for risk assessment of RC structures using indicators. *Computer-Aided Civil and Infrastructure Engineering*, *21*(3), 216–230. https://doi.org/10.1111/j.1467-8667.2006.00429.x

Honfi, D., Leander, J., & Björnsson, Í. (2017). Decision support for bridge condition assessment. *The Fourth International Conference on Smart Monitoring,*

Assessment and Rehabilitation of Civil Structures (SMAR 2017), (September).

Hong, L., & Möller, B. (2012). An economic assessment of tropical cyclone risk on offshore wind farms. *Renewable Energy*, *44*, 180–192. https://doi.org/10.1016/j.renene.2012.01.010

Imhof, D. (2004). *Risk assessment of existing bridge structures*. *University of Cambridge*. Cambridge. Retrieved from http://www.nbq.ch/PhD/Thesis.pdf

Integrated Environmental Data, L. (2013). Environmental surveys and risk assessment for the proposed SUNY Canton wind turbine, (July), 1–26.

Jensen, F., Morris, A. S., Levin, M. A., Kalal, T. T., Pascoe, N., & Carlson, C. (2012). *Effective FMEAs*. USA: Wiely.

Jessen Nielsen, J., & Dalsgaard Sørensen, J. (2011). On risk-based operation and maintenance of offshore wind turbine components. *Reliability Engineering and System Safety*, *96*(1), 218–229. https://doi.org/10.1016/j.ress.2010.07.007

Kaminski, M., & Rigo, P. (2018). *Proceedings of the 20Th international ship and offshore structures congress (Issc 2018) Volume 2*. *20h International Ship and Offshore Structures Congress* (Vol. One).

Kang, J., Sun, L., Sun, H., & Wu, C. (2017). Risk assessment of floating offshore wind turbine based on correlation-FMEA. *Ocean Engineering*. https://doi.org/10.1016/j.oceaneng.2016.11.048

Kaplan, S., & Garrick, B. J. (1981). On the quantitative definition of risk. *Risk Analysis*, *1*(1). Retrieved from https://doi.org/10.1111/j.1539-6924.1981.tb01350.x

Kaposvari, M., & Weidl, T. (2015). Assessment of the ice throw and ice fall risks nearby wind energy installations. In *Winterwind*.

Kjaerulff, U. B., & Madsen, A. L. (2008). *Bayesian networks and influence diagrams : a guide to construction and analysis*. Springer.

Krogness Forsnes, M. (2015). *Risk assessment of strait crossing bridges*. NTNU.

Leander, J., Honfi, D., & Björnsson, Í. (2017). Risk-based planning of assessment actions for fatigue life prediction. *Procedia Structural Integrity*, *5*, 1221–1228. https://doi.org/10.1016/j.prostr.2017.07.047

LeBlanc, M. P. (2007). *Recommendations for risk assessments of ice throw and rotor*

blade failure in Ontario. *Garrad Hassan Canada Inc.*

Liu, Y., Xiao, X., Lu, N.-W., & Deng, Y. (2016). Fatigue reliability assessment of Orthotropic bridge decks under Stochastic Truck Loading. *Zhongguo Gonglu Xuebao/China Journal of Highway and Transport*, 10. https://doi.org/10.1155/2016/4712593

Lotsberg, I., & Sigurdsson, G. (2005). Assessment of input parameters in probabilistic inspection planning for fatigue cracks in offshore structures. In *ninth international conference on structural safety and reliability, ICOSSAR'05.* (pp. 1081–1090). Rome: ninth international conference on structural safety and reliability, ICOSSAR'05.

Lotsberg, I., Sigurdsson, G., Fjeldstad, A., & Moan., T. (2016). Probabilistic methods for planning of inspection for fatigue cracks in offshore structures. *Marine Structures*, *46*, 167–192.

Luque, J., & Straub, D. (2019). Risk-based optimal inspection strategies for structural systems using dynamic Bayesian networks. *Structural Safety*, *76*. https://doi.org/10.1016/j.strusafe.2018.08.002

Madsen, H. O., Krenk, S., & Lind, N. C. (2006). *Methods of Structural Safety*. New York: Prentice-Hall.

Magee, J. F. (1964). Decision trees for decision making. Retrieved from https://hbr.org/1964/07/decision-trees-for-decision-making

Mankar, A., Rastayesh, S., & Dalsgaard Sørensen, J. (2018a). Fatigue reliability analysis of Cret De l'anneau viaduct: A case study. In *6th International Symposium on Life-Cycle Civil Engineering, IALCCE 2018*. Ghent.

Mankar, A., Rastayesh, S., & Dalsgaard Sørensen, J. (2018b). Sensitivity and identifiability study for uncertainty analysis of material model for concrete fatigue. In *5th International Reliability and Safety Engineering Conference*. Shiraz: Arzhang Printing.

Mankar, A., Rastayesh, S., & Dalsgaard Sørensen, J. (2019). Fatigue reliability analysis of crêt de l'Anneau viaduct: a case study. *Structure and Infrastructure Engineering*. https://doi.org/10.1080/15732479.2019.1633361

Márquez-Domínguez, S. (2013). *Reliability-based design and planning of inspection and monitoring of offshore wind turbines*. *Rivers Publishers*. Aalborg University.

Márquez-Domínguez, S., & Dalsgaard Sørensen, J. (2012). Fatigue reliability and calibration of fatigue design factors for offshore wind turbines. *Energies*, *5*, 1816–1834. https://doi.org/10.3390/en5061816

Mensah, A. F., & Dueñas-Osorio, L. (2012). A closed-form technique for the reliability and risk assessment of wind turbine systems. *Energies*, *5*(6), 1734–1750. https://doi.org/10.3390/en5061734

Miceli, F. (2013). Geotechnical parameters for WYG foundations design. Retrieved from http://www.windfarmbop.com/geotechnical-parameters-for-wyg-foundations-design/

Misra, K. B. (2008). *Handbook of performability engineering*. (K. B. Misra, Ed.), *Springer*. London. https://doi.org/10.1007/978-1-84800-131-2_50

Moan., Torgeir, Hovde, G. O., & Blanker, A. M. (1993). Reliability-based fatigue design criteria for offshore structures considering the effect of inspection and repair (pp. 591–597). Houston: 25th Offshore Technology Conference. https://doi.org/10.4043/7189-ms

Moan, T. (2005). Reliability-based management of inspection, maintenance and repair of offshore structures. *Structure and Infrastructure Engineering*, *1*(1), 33–62. https://doi.org/10.1080/15732470412331289314

Modarres, M. (1993). *What every engineer should know about reliability and risk analysis*. M. Dekker.

Modarres, M. (2006). *Risk analysis in engineering: Techniques, tools, and trends*. *CRC Press*. USA: CRC Press.

Modarres, M., Kaminskiy, M., & Krivtsov, V. (1999). *Reliability engineering and risk analysis A practical Guide*. *CRC Press* (First). New York: Taylor & Francis Group. https://doi.org/10.1201/9781420008944

Modarres, M., Kaminskiy, M., & Krivtsov, V. (2016). *Reliability engineering and risk analysis: A practical guide*. *CRC Press* (Third). Taylor & Francis Group.

Narayanagounder, S., & Gurusami, K. (2009). A new approach for prioritization of failure modes in design FMEA using ANOVA. *World Academy of Science, Engineering and Technology*, *3*(1), 524–531.

National Academy Press. (1983). *Risk assessment in the federal government: Managing the process*. Washington, DC.

Nowak, A. S. (2007). *Risk analysis for bridges*. *University of Nebraska-Lincoln*.

Nowak, A. S., Kozikowski, M., & Lutomirska, M. (2009). *Risk mitigation for highway and railway bridges*.

Pawar, A., & Chikalthankar, S. B. (2017). Failure mode effect analysis of rollers in Mill Stand. In *International Conference on Recent Trends in Engineering and Science (ICRTES 2017)* (Vol. 6). Jalagon: International Journal of Innovative Research in Science, Engineering and Technology. Retrieved from http://docplayer.net/51640784-Failure-mode-effect-analysis-of-rollers-in-mill-stand.html

Placca, L., & Kouta, R. (2011). Fault tree analysis for PEM fuel cell degradation process modelling. *International Journal of Hydrogen Energy*, *36*(19), 12393–12405. https://doi.org/10.1016/J.IJHYDENE.2011.06.093

Rafiq, M. I., Chryssanthopoulos, M. K., & Sathananthan, S. (2014). Bridge condition modelling and prediction using dynamic Bayesian belief networks. *Structure and Infrastructure Engineering*, *11*(1), 38–50. https://doi.org/10.1080/15732479.2013.879319

Raiffa, H., & Schlaifer, R. (2013). Applied statistical decision theory. *Journal of Chemical Information and Modeling*, *53*(9), 1689–1699. https://doi.org/10.1017/CBO9781107415324.004

Rangel-Ramírez, J. G., & J.D., S. (2010). Framework for probabilistic of calibration of fatigue design factors for offshore wind turbine support structures. In *Proc. of Reliability and Optimization of Structural Systems*. TUM, München, Germany.

Rastayesh, S. (2018). Ph.D. / 11-month status seminar by Sima Rastayesh: Development of methods for risk assessment of wind turbine support structures and bridges. Retrieved from https://www.aau.dk/arrangementer/vis/phd---11-month-status-seminar-by-sima-rastayesh.cid351826

Rastayesh, S. (2019). Bayesian network for risk-based decision making. In *38th International Conference on Ocean, Offshore and Arctic Engineering*. Glasgow: OMAE 2019.

Rastayesh, S., & Bahrebar, S. (2014). Importance analysis of a typical diesel generator using dynamic fault tree. *International Journal of Current Life Sciences*, *4*(2), 697–700. Retrieved from http://www.bretj.com

Rastayesh, S., Bahrebar, S., Bahman, A. S., Dalsgaard Sørensen, J., & Blaabjerg, F.

(2019). Lifetime estimation and failure risk analysis in a power stage used in wind-fuel cell hybrid energy systems. *Electronics*, *8*(12), 1412. https://doi.org/10.3390/electronics8121412

Rastayesh, S., Bahrebar, S., Blaabjerg, F., Zhou, D., & Wang, H. (2020). A system engineering approach using FMEA and Bayesian network for risk analysis — A case study. *Sustainability*, *12*(77). https://doi.org/10.3390/su12010077

Rastayesh, S., Bahrebar, S., & Sepanloo, K. (2014). Time dependent reliability of emergency diesel generator station. *Indian J.Sci.Res*, *1*(2), 453–460.

Rastayesh, S., & Dalsgaard Sørensen, J. (2017). Development of methods for risk assessment of wind turbine support structures and bridges. Retrieved from https://infrastar.eu/research-framework/wp3-reliability-approaches-for-decision-making/esr11-aau/

Rastayesh, S., & Dalsgaard Sørensen, J. (2018). Risk analysis for wind turbines near highways. In *The 4th Society for Risk Analysis (SRA) Nordic Conference*. Stavanger: University of Stavanger.

Rastayesh, S., & Dalsgaard Sørensen, J. (2019). Dynamic influence diagrams for risk-based decision making for rebars. In *5th Society for Risk Analysis (SRA) Nordic Conference 2019: Risk Management for Innovation* (p. 31). Copenhagen: DTU.

Rastayesh, S., Long, L., Dalsgaard Sørensen, J., & Thöns, S. (2019). Risk assessment and value of action analysis for icing conditions of wind turbines close to highways. *Energies*, *12*(14), 2653. https://doi.org/10.3390/en12142653

Rastayesh, S., Mankar, A., & Dalsgaard Sørensen, J. (2018). Comparative investigation of uncertainty analysis with different methodologies on the fatigue data of rebars. In *5th International Reliability and Safety Engineering Conference*. Shiraz: Arzhang Printing.

Rastayesh, S., Mankar, A., Dalsgaard Sørensen, J., & Bahrebar, S. (2020). Development of stochastic fatigue model of reinforcement for reliability of concrete structures. *Applied Sciences*, *10*(604). https://doi.org/10.3390/app10020604

Rastayesh, S., Sønderkær Nielsen, J., & Dalsgaard Sørensen, J. (2018). Bayesian network methods for risk-based decision making for wind turbines. 14th EAWE PhD Seminar on Wind Energy 18-20 September 2018 Vrije Universiteit Brussel, Belgium: European Academy of Wind Energy.

Rastayesh, S., Zorzi, G., Miraglia, S., & Dalsgaard Sørensen, J. (2019). Risk

assessment of adverse events for wind turbines caused by strong winds. In *Wind Energy Science Conference 2019*. Cork: University College Cork.

Rouhan, A., Goyet, J., & Havbro Faber, M. (2004). Industrial implementation of risk based inspection planning lessons learned from experience (2) the case of steel offshore structures. In *Proceedings of the International Conference on Offshore Mechanics and Arctic Engineering - OMAE* (Vol. 2, pp. 565–572). American Society of Mechanical Engineers Digital Collection. https://doi.org/10.1115/OMAE2004-51573

Sarlak, H., & Nørkær Sørensen, J. (2016). Analysis of throw distances of detached objects from horizontal-axis wind turbines. *Wind Energy*, *19*(1). https://doi.org/10.1002/we.1828

Seifert, H., Westerhellweg, A., & Kröning, J. (2003). Risk analysis of ice throw from wind turbines. In *Boreas VI* (pp. 1–9). Pyhä. Retrieved from http://www.mi-group.ca/files/boreas_vi_seifert_02.pdf

Shabakhty, N., Haselibozchaloee, D., & Correia, J. A. F. O. (2020). Investigation on fatigue damage calibration factors of steel members in offshore structures. *Proceedings of the Institution of Civil Engineers - Maritime Engineering*, 1–36. https://doi.org/10.1680/jmaen.2020.17

Shafiee, M., & Dinmohammadi, F. (2014). An FMEA-based risk assessment approach for wind turbine systems: A comparative study of onshore and offshore. *Energies*, *7*(2), 619–642. https://doi.org/10.3390/en7020619

Sønderkær Nielsen, J. (2013). *Risk-based operation and maintenance of offshore wind turbines*. *Rivers Publishers*. Aalborg University.

Sønderkær Nielsen, J., & Dalsgaard Sørensen, J. (2010). Bayesian networks as a decision tool for O&M of offshore wind turbines. *ASRANet : Integrating Structural Analysis, Risk & Reliability : 5th International ASRANet Conference*, (1), 1–8.

Sønderkær Nielsen, J., & Dalsgaard Sørensen, J. (2017). Computational framework for risk-based planning of inspections, maintenance and condition monitoring using discrete Bayesian networks Computational framework for risk-based planning of inspections, maintenance and condition monitoring using discrete Bayes. *Structure and Infrastructure Engineering Maintenance, Management, Life-Cycle Design and Performance*. https://doi.org/10.1080/15732479.2017.1387155

Spitzer, C., Schmocker, U., & Dang, V. N. (Eds.). (2004). Probabilistic safety

assessment and management. In *PSAM 7 — ESREL 04* (Vol. 6). Berlin: Springer London. https://doi.org/10.1007/978-0-85729-410-4

Stewart, M. G., & Melchers, R. E. (1997). *Probabilistic risk assessment of engineering systems*. Chapman & Hall.

Straub, D. (2009). Stochastic modeling of deterioration processes through dynamic Bayesian networks. *Journal of Engineering Mechanics*, *135*(10), 1089–1099. https://doi.org/10.1061/(asce)em.1943-7889.0000024

Straub, D., & Havbro Faber, M. (2006). Computational aspects of risk-based inspection planning. *Computer-Aided Civil and Infrastructure Engineering*, *3*(21), 179–192.

Sutrisno, A., Gunawan, I., & Tangkuman, S. (2015). Modified Failure Mode and Effect Analysis (FMEA) model for accessing the risk of maintenance waste. *Procedia Manufacturing*, *4*, 23–29. https://doi.org/10.1016/j.promfg.2015.11.010

Tavner, P. (2012). *Offshore wind turbines: Reliability, availability and maintenance*. *Institution of Engineering and Technology*. https://doi.org/10.1049/pbrn013e

Tavner, P. J., Xiang, J., & Spinato, F. (2007). Reliability analysis for wind turbines. *Wind Energy*, *10*(1). https://doi.org/10.1002/we.204

Thoft-Christensen, P., & Dalsgaard Sørensen, J. (1987). Optimal strategy for inspection and repair of structural systems. *Civil Engineering Systems*, *4*(2), 94–100. https://doi.org/10.1080/02630258708970464

Urban, S., Strauss, A., Schütz, R., Bergmeister, K., & Dehlinger, C. (2014). Dynamically loaded concrete structures - Monitoring-based assessment of the real degree of fatigue deterioration. *Structural Concrete*, *15*(4). https://doi.org/10.1002/suco.201300095

Velarde, J., Kramhøft, C., Sørensen, J. D., & Zorzi, G. (2020). Fatigue reliability of large monopiles for offshore wind turbines. *International Journal of Fatigue*, *134*. https://doi.org/10.1016/j.ijfatigue.2020.105487

Vinnem, J.-E. (2014). *Offshore risk assessment vol 1. Principles, modelling and applications of QRA studies*. (H. Pham, Ed.), *Springer Series in Reliability Engineering* (Third, Vol. 1). Stavanger: Springer. https://doi.org/10.1007/978-1-4471-5213-1

Vrouwenvelder, A., & Holicky, B. (2001). *Risk assessment and risk communication*

in civil engineering. Retrieved from http://web.cvut.cz/ki/710/pdf/1812.pdf

Whiteley, M., Dunnett, S., & Jackson, L. (2016). Failure mode and effect analysis, and fault tree analysis of polymer electrolyte membrane fuel cells. *International Journal of Hydrogen Energy*, *41*(2), 1187–1202. https://doi.org/10.1016/j.ijhydene.2015.11.007

Ye, X. W., Su, Y. H., & Han, J. P. (2014). A state-of-the-art review on fatigue life assessment of steel bridges. *Hindawi Publishing Corporation Mathematical Problems in Engineering*.

Zhou, X.-Y., Treacy, M., Schmidt, F., Brühwiler, E., Toutlemonde, F., & Jacob, B. (2015). Effect on bridge load effects of vehicle transverse in-lane position: A case study. *Journal of Bridge Engineering*, *20*(12). https://doi.org/10.1061/(asce)be.1943-5592.0000763

APPENDICES

Appendix A. Journal Papers

Paper 1:

Title:

Development of Stochastic Fatigue Model of Reinforcement for Reliability of Concrete Structures

Authors:

Sima Rastayesh, Amol Mankar, John Dalsgaard Sørensen and Sajjad Bahrebar

Published in:

Applied Sciences 2020, 10, 604; doi:10.3390/app10020604

applied sciences

MDPI

Article

Development of Stochastic Fatigue Model of Reinforcement for Reliability of Concrete Structures

Sima Rastayesh [1,*], Amol Mankar [1], John Dalsgaard Sørensen [1] and Sajjad Bahrebar [2]

[1] Department of Civil Engineering, Aalborg University, 9100 Aalborg, Denmark; ama@civil.aau.dk (A.M.); jds@civil.aau.dk (J.D.S.)

[2] Department of Mechanical Engineering, Technical University of Denmark, 2800 Lyngby, Denmark; sajbahr@mek.dtu.dk

* Correspondence: sir@civil.aau.dk

Received: 15 November 2019; Accepted: 8 January 2020; Published: 14 January 2020

Abstract: This paper presents recent contributions to the Marie Skłodowska-Curie Innovative Training Network titled INFRASTAR (Innovation and Networking for Fatigue and Reliability Analysis of Structures-Training for Assessment of Risk) in the field of reliability approaches for decision-making for wind turbines and bridges . Stochastic modeling of uncertainties for fatigue strength parameters is an important step as a basis for reliability analyses. In this paper, the Maximum Likelihood Method (MLM) is used for fitting the statistical parameters in a regression model for the fatigue strength of reinforcement bars. Furthermore, application of the Bootstrapping method is investigated. The results indicate that the latter methodology does not work well in the considered case study because of run-out tests within the test data. Moreover, the use of the Bayesian inference with the Markov Chain Monto Carlo approach is studied. These results indicate that a reduction in the statistical uncertainty can be obtained, and thus, better parameter estimates are obtained. The results are used for stochastic modelling in reliability assessment of a case study with a composite bridge. The reduction in statistical uncertainty shows high impact on the fatigue reliability in a case study on the Swiss viaduct Crêt De l'Anneau.

Keywords: Bayesian inference; bootstrap method; Maximum Likelihood Method; reinforced-concrete; uncertainty; fatigue-resistance

1. Introduction

This paper presents statistical analyses performed on fatigue data obtained from [1], where laboratory fatigue tests were performed on reinforcement bars (rebars).

General methods and techniques utilized for risk and reliability assessment of civil engineering structures are presented [2–18].

Statistical analyses of the data are an essential step for the stochastic modeling of the material fatigue uncertainties, which can next be used as a basis for a probabilistic modeling and reliability analysis [19] of structures with reinforced concrete components, such as wind turbines and bridges [20,21]. Usually, foundations for onshore wind turbines are constructed by the use of reinforced concrete, which is also used in many bridges. Therefore, the development of stochastic models for the fatigue limit state and estimation of the resulting reliability can be considered as a contribution to reliability assessment of these types of structures, with respect to fatigue failure and also as the basis for the development of optimal strategies for the maintenance of wind turbines and bridges. [22].

Several methodologies can be used to estimate the statistical parameters. For instance: Maximum Likelihood Method (MLM), moment method, least square method, and Bayesian statistics. In the literature, there are some recommendations indicating which of these methods could be more

suitable. At the same time, there is no unique answer to this question, especially for a fatigue case study on rebars. On the reliability assessment, choosing a specific method has a direct influence. In the reliability assessment, there is a need to have stochastic modeling for the material-resistance as well as for the loads. In this paper, the material-resistance model is presented in detail, and at the end, using a generic stochastic model for the fatigue load reliability results of a composite bridge are presented.

The MLM is chosen in this study as it gives an estimate of the statistical uncertainties [23]. MLM is considered for fitting the statistical parameters [2] in a regression model for fatigue strength. Typically, the statistical analyses are based on a limited number of data, for which MLM can provide estimates of the uncertainties associated with each of these parameters and the correlation between the parameters [24]. This paper also presents the use of the Bootstrap method, which generates synthetic data based on the available measurements from the experiment.

Further, Bayesian statistics is considered taking subjective/prior information into account. This is done with application of Bayesian inference with a Markov Chain Monte Carlo implementation [25–27]. Bayesian updating is an appropriate tool to update the structural performance function for fatigue by applying the information from the structural health monitoring and the prior information about different fatigue parameters. The aim is to compare the results of different methodologies and to provide information in order to select an appropriate method.

To study the effect of uncertainty of fatigue resistance model on the fatigue reliability of a structure, a case study of Swiss viaduct Crêt De l'Anneau is presented. For this structure, long term strain monitoring data on critical reinforcement is available.

2. Materials and Methods

2.1. Test Data

Test data on the fatigue strength test for steel reinforcement from the lab tests were done at Aalborg University by Hansen and Heshe [1]. It is utilized for the statistical analysis to determine typical fatigue strength uncertainties (see Table 1, where 1 indicated run-out/no failure and 0 indicates failure). The lab tests are performed with steel reinforcement bars with 16 mm of diameter and yields strengths of 570 MPa. The S-N curve for this data is presented in Figure 1. Run-outs are depicted in orange and failures in gray.

Table 1. Data [1].

Data Number (Index)	Number of Cycles to Failure	Stress Range [MPa]	Run-out
1	7,875,829	337	1
2	4,485,923	335	1
3	9,182,542	391	1
4	3,981,071	385	1
5	347,328	396	0
6	589,346	403	0
7	441,005	405	0
8	371,852	408	0
9	341,454	408	0
10	238,658	405	0
11	255,509	408	0
12	255,509	420	0
13	273,550	430	0
14	215,443	430	0
15	411,921	439	0
16	398,107	419	0
17	411,921	424	0
18	255,509	467	0

19	184,784	488	0
20	161,215	488	0
21	161,215	494	0
22	131,376	503	0
23	114,619	505	0
24	129,154	506	0
25	158,489	507	0
26	140652	536	0
27	105,250	536	0
28	80,113	561	0
29	53,201	572	0
30	48,026	572	0
31	50,547	572	0

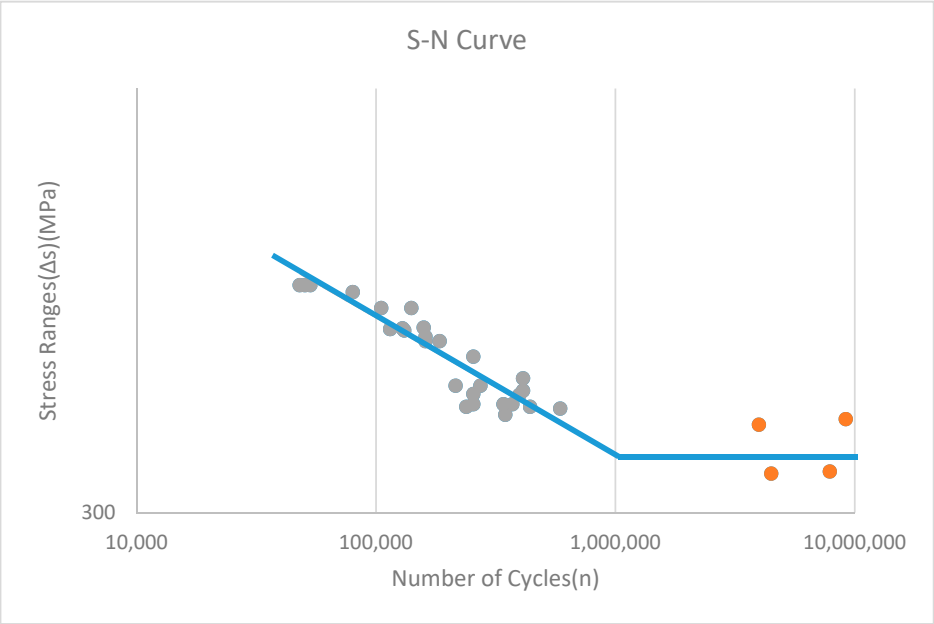

Figure 1. S-N curve for rebar data [1].

2.2. Statistical Analysis of Fatigue Data of Steel Reinforcing Bars

For steel reinforcement bars used in concrete S-N, curves are recommended by various international codes (such as Model code 2010, Model code 1990, DNV OS C 502, EN 1992-1) [28–31] and are generally written as:

$$n_i = K\,\Delta s_i^{-m}, \tag{1}$$

or

$$\log(n_i) = \log(K) - m\log(\Delta s_i), \tag{2}$$

where n_i is the number of cycles to failure with stress range Δs_i in test number, i. K and m are fatigue parameters to be fitted by MLM here using test data [31].

To account for uncertainties in fatigue life, Equation (2) can be rewritten [22]:

$$\log(n_i) = \log(K) - m\log(\Delta s_i) + \varepsilon, \tag{3}$$

where ε represents the uncertainty of the fatigue life model and is modelled by a stochastic variable with mean value equal to zero and standard deviation, σ_ε. ε is often assumed to have a Normal distributed [31].

The Likelihood function to be used to estimate the optimal values of the parameters K, m, and σ_ε from test data is written [22]:

$$L(K,m,\sigma_\varepsilon) = \prod_{i=1}^{n_F} P[\log(K) - m\log(\Delta s_i) + \varepsilon = \log(n_i)] \times \prod_{i=n_F+1}^{n_F+n_R} P[\log(K) - m\log(\Delta s_i) + \varepsilon > \log(n_i)]. \quad (4)$$

Here, n_i is the number of stress cycles to failure or to run-out with stress range Δs_i in test number i. n_F is the number of tests where failure occurs, and n_R is the number of tests where failure did not occur after n_i stress cycles (run-outs). The total number of tests is $n = n_F + n_R$. K, m, and σ_ε are obtained from the optimization problem $max_{K,m,\sigma_\varepsilon} L(K,m,\sigma_\varepsilon)$, which can be solved using a non-linear optimization algorithm [31].

Run-outs contain information which from a statistical point of view has to be included in the statistical modelling in order to be consistent with all tests performed. This paper describes how run-outs can be included using the MLM. The number of cycles where the tests are stopped are often chosen in order to limit the costs and time used for the test campaign.

The terms in Equation (4) can be obtained from Equation (5) [22]:

$$P[\log(K) - m\log(\Delta s_i) + \varepsilon = \log(n_i)] = \frac{1}{\sqrt{2\pi}\sigma_\varepsilon} exp\left(-\frac{1}{2}\left(\frac{\log(K) - mlog(\Delta s_i) - \log(n_i)}{\sigma_\varepsilon}\right)^2\right),$$
$$P[\log(K) - m\log(\Delta s_i) + \varepsilon > \log(n_i)] = \Phi\left(\frac{\log(K) - m\log(\Delta s_i) - \log(n_i)}{\sigma_\varepsilon}\right). \quad (5)$$

The parameters K, m, and σ_ε are generally determined using a limited number of data. Consequently, the estimates are subject to statistical/parameter uncertainty. Since the parameters are estimated by the MLM, they become asymptotically (number of data should be >25–30). Normal distributed stochastic variables with expected values equal to the maximum-likelihood estimator and a covariance matrix equal to [32]:

$$C_{K,m,\sigma_\varepsilon} = \left[-H_{K,m,\sigma_\varepsilon}\right]^{-1} = \begin{bmatrix} \sigma_K^2 & \rho_{K,m}\sigma_K\sigma_m & \rho_{K,\sigma_\varepsilon}\sigma_K\sigma_{\sigma_\varepsilon} \\ \rho_{K,m}\sigma_K\sigma_m & \sigma_m^2 & \rho_{m,\sigma_\varepsilon}\sigma_m\sigma_{\sigma_\varepsilon} \\ \rho_{K,\sigma_\varepsilon}\sigma_K\sigma_{\sigma_\varepsilon} & \rho_{m,\sigma_\varepsilon}\sigma_m\sigma_{\sigma_\varepsilon} & \sigma_{\sigma_\varepsilon}^2 \end{bmatrix}. \quad (6)$$

$H_{K,m,\sigma_\varepsilon}$ is the Hessian matrix with second-order derivatives of the log-likelihood function. σ_K, σ_m, and $\sigma_{\sigma_\varepsilon}$ denote the standard deviations of K, m, and σ_ε, respectively, and e.g., $\rho_{K,m}$ is the correlation coefficient between K and m.

2.3. Bootstrap Method

The Bootstrap method developed by Efron [33] may be used for smaller samples and is quite flexible concerning the assumptions made. The Bootstrap method applies the actual distribution of the measurement errors, which are then propagated using an appropriate Monte Carlo scheme. That is, the Bootstrap method can be used to estimate the statistical (parameter) uncertainty.

Fatigue tests take very long time as it can take millions of cycles before the failure of one specimen, and changing the frequency of load application could lead to erroneous results. The Bootstrap method can be used to generate more synthetic data, which can then be used to estimate the parameter uncertainties as an alternative to the use of MLM described above.

Residuals are estimated by subtracting the calculated number of cycles to failure from the observed number of cycles in logarithmic scale. These residuals are plotted in Figure 2a, considering the case when run-outs are not included. This histogram indicates that an assumption of residuals as white noise is satisfactory and it is uniformly distributed with a mean value equal to zero. In this case, the Bootstrap method can be used, but in applications where run-outs are part of the data, the Bootstrap method cannot be used directly, as seen in Figure 2b.

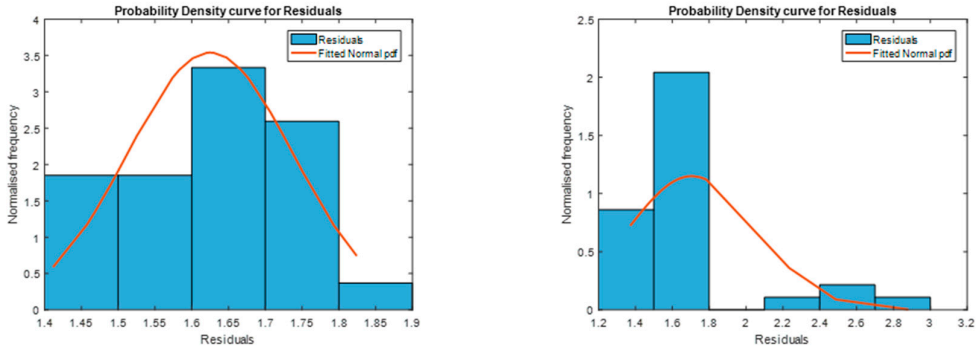

(**a**) (**b**)

Figure 2. Histogram for Residuals: (**a**) without Run-outs; (**b**) with Run-outs.

If we plot the residuals along with their index (data number), they are random without considering run-outs, which is a basic requirement for using the Bootstrap method, as seen in Figure 3a. Random in this context means that residuals should not follow a pattern [34]. Whereas in Figure 3b with run-outs, residuals are following a pattern, so this requirement to apply the Bootstrap method is not fulfilled here.

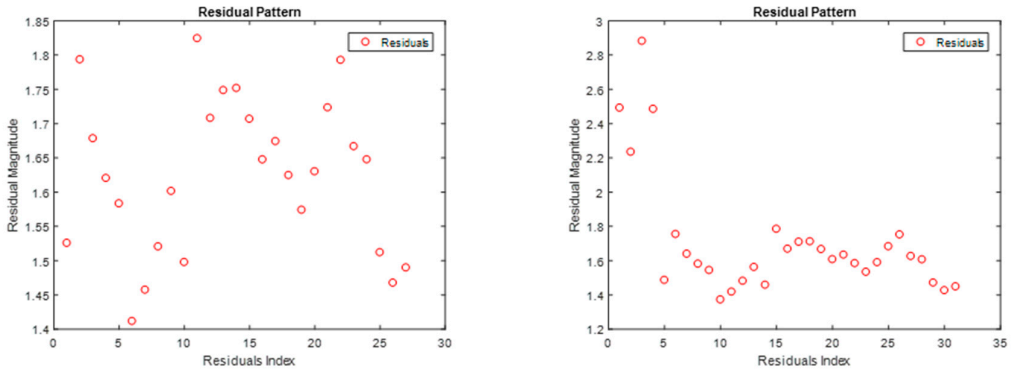

(**a**) (**b**)

Figure 3. Residuals Pattern: (**a**) without Run-outs; (**b**) with Run-outs.

Therefore, it can be concluded that Bootstrapping can be used for estimating parameter uncertainty only in the case of no run-outs.

2.4. Bayesian Inference with Markov Chain Monte Carlo Implementation

Bays' rule provides the mathematical basis to update beliefs (prior information) about a variable, θ, given observations, y. By Bays' rule, the posterior probability of θ given observations, $p(\theta|y)$ is obtained as follows [35,36]:

$$p(\theta|y) = \frac{p(\theta)p(y|\theta)}{p(y)}, \quad (7)$$

Future predictions for y^* given observations y is obtained from the predictive distribution

$$p(y^*|y) = \int p(y^*|\theta)p(\theta|y)d\theta, \quad (8)$$

Thus, future predictions are modeled using the updated probability density function $p(\theta|y)$ similar to making a prediction for y^* using a single value of θ in the classical statistical sense. Equation (8) can be estimated using Monte Carlo simulation strategies such as the Markov-Chain Monte-Carlo algorithm [36].

By definition, a Markov chain simulation is a sequence of random variables $\theta^1, \theta^2, \theta^3, \ldots$ for which for any k, the distribution of θ^k depends only on the most recent one θ^{k-1}. In practice, several independent sequences of Markov chain simulations are created. The Metropolis algorithm is used to obtain the transition distribution function [31]. It is an adaption of a random walk that uses an acceptance/rejection rule to converge to the specified target distribution. The step-by-step procedure is as follows [27]:

1. Select initial parameter vector
2. Iterate as follows for $k = 1, 2, 3, \ldots$
    a. Create a new trial position $\theta^* = \theta^{k-1} + \Delta\theta$, where $\Delta\theta$ is randomly sampled from the jumping distribution $q(\Delta\theta)$.
    b. Create the Metropolis ratio.

$$r = \frac{\pi\left((\theta^*|y)\right)}{\pi\left((\theta^{k-1}|y)\right)}, \tag{9}$$

3. Accept a new sample if:

$$\theta^k = \begin{cases} \theta^* & \text{with probability } \min(r, 1) \\ \theta^{k-1} & \text{otherwise} \end{cases}, \tag{10}$$

Note that this requires the jumping distribution to be symmetric: $q\,(\theta^*, \theta^{k-1}) = q\,(\theta^{k-1}, \theta^*)$. If the jumping distribution is not symmetric, then the Metropolis-Hasting algorithm [37] can be used where both sides jumping distributions are part of the ratio.

Since the posterior distribution can be calculated by Equation (7), where $p(y)$ is a normalizing constant, it also follows that the posterior density function can be written as:

$$p(\theta|y) \propto p(\theta)p(y|\theta), \tag{11}$$

i.e., the posterior distribution is proportional to the product of the prior and the likelihood functions.

If it is assumed that the prior distribution is the multivariate Normal distribution, then the Likelihood function becomes:

$$p(y|\theta, \sigma^2) = \frac{1}{\sigma\sqrt{2\pi}} exp\left(-\frac{1}{2\sigma^2} SS(\theta)\right), \tag{12}$$

where,

$$SS(\theta) = \sum_i^n \left(y - f(S, \theta)\right)^2, \tag{13}$$

The Metropolis ratio becomes:

$$r = \frac{p\left(\theta^*|y, \sigma^2\right)}{p\left(\theta^{k-1}|y, \sigma^2\right)} = exp\left(-\frac{1}{2\sigma^2}\left(SS(\theta^*) - SS(\theta^{k-1})\right)\right), \tag{14}$$

The scale reduction factor *R* indicates a potential scale reduction for the considered distribution when the number of samples goes to infinity (see [38] for theory and more detailed descriptions). The sampling is said to converge if *R* is close to one. Therefore, the number of simulations should be chosen such that *R* becomes as close to one as possible, and thereby, the Monte Carlo sampling error close to zero.

The parameters fitted in the SN-curve in Equation (1) are K and m. The correlation between them is illustrated in Figure 4. Here, the Markov Chain Monte Carlo algorithm is used. Furthermore, the Metropolis algorithm is applied for obtaining the transition distribution. Based on Reference [36], the scale reduction factor R is also calculated to 1.0007.

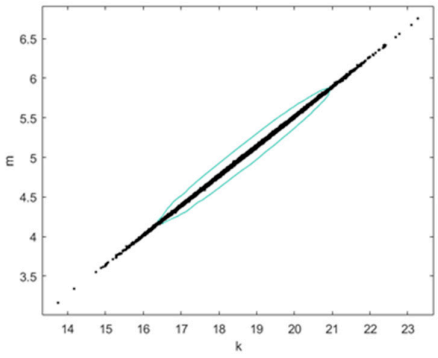

Figure 4. Correlation between k and m

3. Results of Uncertainty Modelling.

Table 2 shows a comparison between the results obtained by the methods presented above. This includes results obtained for the statistical parameters by MLM accounting for run-outs. Furthermore, a characteristic, 5% quantile is estimated using the MLM estimates resulting in $\log k = 18.77$, which is larger than the characteristic value equal to 17.054 specified in the Eurocodes (see [38,39], and Table 2).

Table 2. Results.

Parameter	Mean by MLM	Mean by Bayesian Approach	Standard Deviation by MLM	Standard Deviation by Bayesian Approach	Distribution	Remark
ε	0	0	---	---	Normal	Error term
σ_ε	0.39	0.21	0.06	0.04	Normal	Standard deviation of error term
$\log k$	18.77	18.72	0.07	0.05	Normal	Location parameter in Wöhler curve
m	Fixed to 5	5.03	---	0.02	Fixed/Deterministic	Slope of Wöhler curve
$\rho_{\log k,\sigma_\varepsilon}$			0.06	0.03	Deterministic	Correlation coefficient between location and standard deviation of error

The Markov Chain Monte Carlo simulation results in Figure 5a show that $\log k$ is mostly in the interval 18–19, and in Figure 5b, m is close to 5, which is in agreement with the fixed value used for MLM. It should be noted that m is assumed fixed in the reliability section. The Posterior marginal density function is also shown in Figure 6.

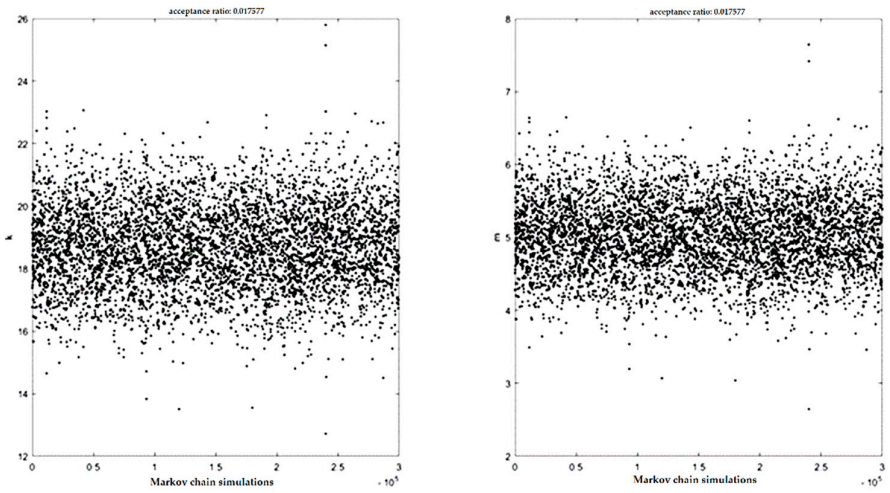

(**a**) (**b**)

Figure 5. Markov Chain Simulation for: (**a**) k; (**b**) m.

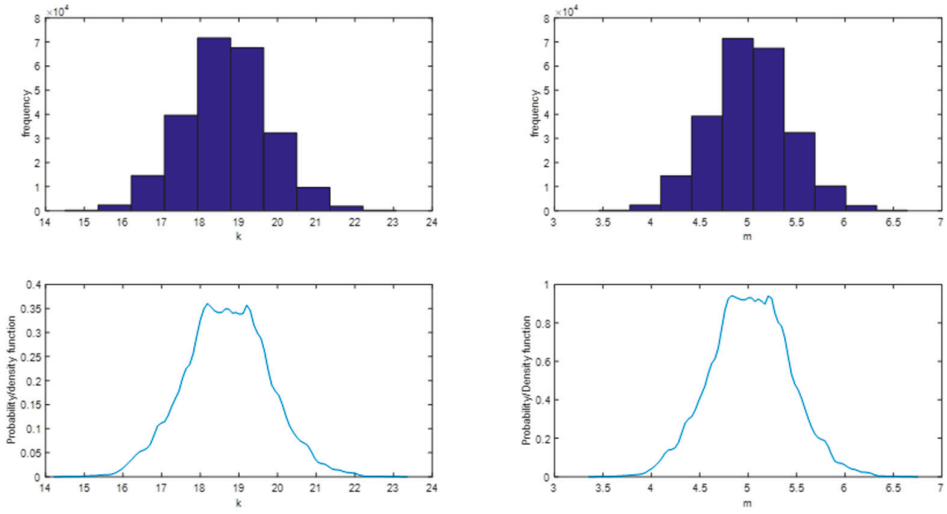

(**a**) (**b**)

Figure 6. Posterior marginal density functions: (**a**) k; (**b**) m.

4. Case Study: Crêt De l'Anneau Viaduct

To illustrate the effect of change of model uncertainty of $\log k$, i.e., σ_ε on the fatigue reliability of a structure, a case study of a composite (reinforced concrete deck and steel box girders) viaduct in Switzerland is chosen as seen in Figure 7.

Figure 7. A view of Crêt De l'Anneau.

The identified fatigue critical location of this composite bridge is the reinforced concrete slab, as shown in [40] pp.41. The fatigue behavior of the reinforced concrete deck slab is mainly governed by transverse bending between two girders. It contributes also to local longitudinal bending under vehicle rolling wheel loads, thus it is double bending behavior. The MCS department at EPFL has installed electrical strain gauges on reinforcement bars at critical location. This monitored strain data is used as action effects to perform fatigue reliability analysis of the viaduct, a reliability framework presented in [41] is used for the purpose.

4.1. Limit State Equation

A limit state equation for fatigue failure of critical reinforcement in the viaduct is formulated based on the Palmgren-Miner rule [42,43] assuming linear damage accumulation, Equation (15), and [41,44].

$$g(t) = \Delta - \sum_{i=1}^{j} \frac{X_n n_i t}{10^{\epsilon} \cdot k} (X_w R_D \Delta s_i)^m = 0, \quad (15)$$

where

t indicates time $0 < t < T_L$ in years,
T_L is the service life time of the structure,
R_D is modelling the ratio of design parameters, here the section modulus of the deck slab,
Δs_i is the stress range for the ith load bin.
All other terms in the limit state equation are explained in Table 3.

Table 3. Stochastic model for Wöhler curve.

Parameter	Distribution	Mean	Standard Deviation	Remark
Δ	Lognormal	1	0.30	Model uncertainty related to PM Rule [1]
X_w	Lognormal	1	0.05	Uncertainty in strain measurements
X_n	Lognormal	1	0.01	Uncertainty in number of vehicles
$logk$	Normal	18.77	0.07	Location parameter in Wöhler curve
m	Fixed	5	---	Slope of Wöhler curve fixed to 5 [2]
ϵ	Normal	0	σ_ε	Error term taken from Table 2
σ_ε	Normal	0.39/0.21 [3]	0.06/0.004 [3]	Standard deviation of error term taken from Table 2
$\rho_{logk,\sigma\varepsilon}$	Deterministic	0.06/0.003 [3]	---	Correlation coefficient between location and standard deviation of error taken from Table 2

[1] model uncertainty obtained by fitting lognormal distribution to test data in [45]; [2] slope of Wöhler curve fixed to 5 as $\log k$ and m are highly correlated with correlation coefficient equal to 0.9997; [3] two

values are used for analysis first one from MLM approach, while the second one is from Bayesian approach.

4.2. Reliability Analysis

The First Order Reliability Method (FORM) is used for reliability analysis [2,46]. An open-source MATLAB-based toolbox, namely the FERUM (Finite Element Reliability Using MATLAB), is used for performing all FORM calculations [47]. The cumulative (accumulated) probability of failure in time interval [0, t] is obtained by Equation (16):

$$P_F(t) = P(g(t) \leq 0), \tag{16}$$

The probability of failure is estimated by FORM [47]. The corresponding reliability index $\beta(t)$ is obtained by Equation (17):

$$\beta(t) = -\phi^{-1}\big(P_F(t)\big), \tag{17}$$

where, $\phi()$ is standardized normal distribution function.

The annual probability of failure is obtained by:

$$\Delta P_F(t) = P_F(t) - P_F(t - \Delta t), t > 1year, \tag{18}$$

where Δt = one year. The corresponding annual reliability index is denoted $\Delta\beta$.

4.3. Reliability Results

The cumulative reliability index along the service life of the structure is presented in Figure 8 for the case where uncertainty in vehicle number X_n is 1% and CoV for log$K$ is as 0.39 (MLM) and 0.2 (Bayesian).

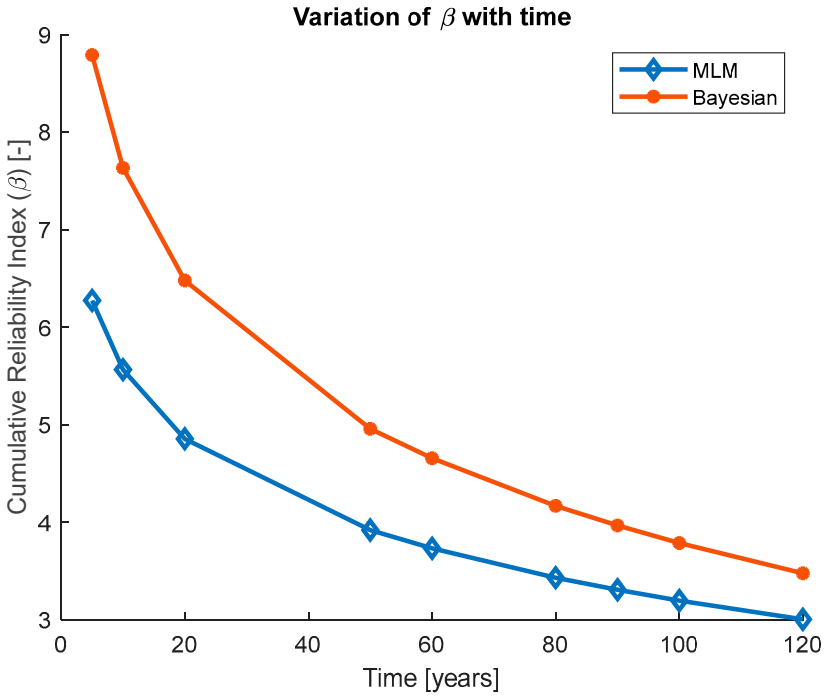

Figure 8. Reliability index as function of time.

Corresponding annual reliability index at 120 years is presented in Table 4.

Table 4. Annual reliability index as function of CoV of $\log k$.

CoV of $\log k$	Annual Reliability Index at 120 Years
0.39 (MLM)	3.90
0.20 (Bayesian)	4.25

The actual stress in slab of viaduct is very low, thus exhibiting a very high fatigue reliability. Current results are shown for the case of scaled stresses. Even after the scaling of the stresses annual reliability index is within acceptable levels, which is more than 3.7 (for the case of very high consequence and low efficiency of intervention, [48]). Furthermore, it can be seen from the results that CoV for $logK$ has a very high influence on reliability index. Thus, estimating the CoV with great accuracy is very important in order to estimate the safety of the structures reasonably.

5. Conclusions

In this paper, for stochastic modeling of uncertainties for fatigue strength parameter, MLM as a common methodology is utilized to fit the statistical parameters in a regression model based on available test data. The Bootstrapping method is used to generate synthetic data. Example investigations in this paper indicate that Bootstrapping cannot be used if run-out data are to be accounted for. Thus, further steps are not proceeded to estimate statistical parameters. It should be mentioned that if the Bootstrapping method was fulfilled the requirement (random pattern), another methodology such as least square method or even Bootstrapping could be used for parameter estimation in the next step. Subsequently, the use of Bayesian inference with the Markov Chain Monto Carlo approach is studied.

Reliability analysis of a selected detail in the Cret De l'Anneau Viaduct is used to illustrate and compare different stochastic models obtained by the statistical methods. The results obtained by MLM is used in reliability analyses and is assumed as a prior for Bayesian. The results show difference in the reliability indices, indicating the importance of accurate estimation of the model uncertainty of the SN-curve. The results emphasize the choice of statistical method as it influences the reliability analyses. In this case study, Bayesian provided better statistical uncertainty, hence better fatigue reliability assessment.

Authors Contributions: The main idea for the paper was proposed by S.R. S.R. wrote the first draft of the paper, except Section 4 which was drafted by A.M. S.R., A.M. and S.B. provided literature review. S.R. developed the methodology wrote relevant codes for Maximum likelihood method, Markov Chain Monte Carlo, Bayesian inference and Bootstrap and reviewed by A.M. A.M. developed the reliability framework with relevant codes with input for stochastic model from S.R. S.R. and A.M. post-processed the results. J.D.S. supervised the findings of this work and reviewed methodology. S.R., A.M., J.D.S. and S.B. contributed for articulate the research work in its current form as full research manuscript. All authors discussed the results and contributed to the final results. All authors have read and agreed to the published version of the manuscript.

Funding: Current work is carried out under the project INFRASTAR (infrastar.eu), which has received funding from the European Union's Horizon 2020 research and innovation program under the Marie Skłodowska-Curie grant agreement No. 676139. The grant is gratefully acknowledged.

Acknowledgments: These current codes were further developed based on codes provided in DTU Summer School on Uncertainty and sensitivity analysis of numerical models—7–11 August 2017, lecturer: Gurkan Sin, to suit current application.

Conflicts of Interest: The authors declare no conflict of interest.

References

1. Hansen, L.P.; Heshe, G. Static, Fire and Fatigue Tests of Ultra High-Strength Fibre Reinforced Concrete and Ribbed Bars. *J. Nord. Concr. Res.* **2001**, *26*, 17–37.
2. Sørensen, J. *Notes in Structural Reliability Theory and Risk Analysis*; Aalborg University: Aalborg, Denmark, 2011.

3. Madsen, H.O.; Krenk, S.; Lind, N.C. *Methods of Structural Safety*; Prentice-Hall: Upper Saddle River, NJ, USA, 1986.
4. Ditlevsen, O.; Madsen, H. *Structural Reliability Methods*; Wiley: Hoboken, NJ, USA, 1996.
5. Faber, M.H. Risk Assessment in Engineering (Principles, System Representation & Risk Criteria). https://www.jcss.byg.dtu.dk/-/media/Subsites/jcss/english/publications/risk_assessment_in_engineering/jcss_riskassessment.ashx?la=da&hash=F4BD53E6E9C2AD6242FD54762719D55BD251A995 (accessed on 15 November 2019).
6. Kaplan, S.; Garrick, B.J. On the Quantitative Definition of Risk. *Risk Anal.* **1981**, *1*, 11–27.
7. Modarres, M. *Risk Analysis in Engineering: Techniques, Tools, and Trends*; CRC Press: Boca Raton, FL, USA, 2006.
8. Zio, E.; Baraldi, P.; Cadini, F. *Basics of Reliability and Risk Analysis: Worked Out Problems and Solutions*, World Scientific Publishing Co. Pte. Ltd: Singapore, 2011.
9. Zio, E. Introduction To The Basics Of Reliability And Risk Analysis [Elektronisk resurs], World Scientific Publishing Co. Pte. Ltd: Singapore, 2007.
10. Chemweno, P.; Pintelon, L.; Muchiri, P.N.; Van Horenbeek, A. Risk assessment methodologies in maintenance decision making: A review of dependability modelling approaches. *Reliab. Eng. Syst. Saf.* **2018**, *173*, 64–77.
11. Aven, T.; Zio, E. *Knowledge in Risk Assessment and Management*; John Wiley & Sons: Hoboken, NJ, USA, 2018.
12. Pham, H. *Bayesian Inference for Probabilistic Risk Assessment*; Springer: Berlin, Germany, 2005.
13. Fenton, N.; Neil, M. *Risk Assessment and Decision Anlysis with Bayesian Networks*; CRC Press: Boca Raton, FL, USA, 2013.
14. Singpurwla, N.D. *Reliability and Risk. A Bayesian Perspective*; John Wiley & Sons, Ltd: Chichester, UK, 2006.
15. Aven, T. Risk assessment and risk management: Review of recent advances on their foundation. *Eur. J. Oper. Res.* **2016**, *253*, 1–13.
16. Lair, J.; Rissanen, T.; Sarja, A. Methods for Optimisation and Decision Making in Lifetime Management of Structures. 2004, Available online: https://www.scribd.com/document/342349363/METHODS-FOR-OPTIMISATION-AND-DECISION-MAKING-IN-LIFETIME-MANAGEMENT-OF-STRUCTURES (accessed on 15 November 2019).
17. Vrouwenvelder, A.; Holicky, B.M.; Tanner, C.P.; Lovegrove, D.R.; Canisius, E.G. Risk Assessment and Risk Communication in Civil Engineering. 2001. Available online: https://www.irbnet.de/daten/iconda/CIB14314.pdf (accessed on 15 November 2019).
18. Bhattacharya, B. *Risk and Reliability in Bridges. Innovative Bridge Design Handbook*; Elsevier: Amsterdam, The Netherlands, 2016.
19. Bahrebar, S.; Zhou, D.; Rastayesh, S.; Wang, H.; Blaabjerg, F. *Microelectron. Reliab. J.* **2018**, *88–90*, 1177–1182.
20. Rastayesh, S.; Bahrebar, S.; Bahman, A.S.; Dalsgaard Sørensen, J.; Blaabjerg, F. Lifetime Estimation and Failure Risk Analysis in a Power Stage Used in Wind-Fuel Cell Hybrid Energy Systems. *Electronics* **2019**, *8*, 1412.
21. Rastayesh, S.; Long, L.; Dalsgaard Sørensen, J.; Thöns, S. Risk Assessment and Value of Action Analysis for Icing Conditions of Wind Turbines Close to Highways. *Energies* **2019**, *12*, 2653.
22. Màrquez-Dominguez, S. *Reliability-Based Design and Planning of Inspection and Monitoring of OffshoreWind Turbines*; Aalborg University: Aalborg, Denmark, 2013.
23. Mankar, A.; Rastayesh, S.; Dalsgaard Sørensen, J. Sensitivity and Identifiability Study for Uncertainty Analysis of Material Model for Concrete Fatigue. In Proceedings of the 5th International Reliability and Safety Engineering Conference, Shiraz University, Shiraz, Iran, 9–10 May 2018.
24. Seber, G.; Wild, C. *Non-Linear Regression*; Wiley: Hoboken, NJ, USA, 1989.
25. Rastayesh, S.; Bahrebar, S.; Blaabjerg, F.; Zhou, D.; Wang, H.; Dalsgaard Sørensen, J. A System Engineering Approach Using FMEA and Bayesian Network for Risk Analysis—A Case Study. *Sustainability* **2020**, *12*, 77.
26. Rastayesh, S.; Sønderkær Nielsen, J.; Dalsgaard Sørensen, J. Bayesian Network Methods for Risk-Based Decision Making for Wind Turbines. In Proceedings of the EAWE PhD Seminar on Wind Energy, Brussel, Belgium, 18–20 September 2018.
27. Metropolis, N.; Ulam, S. The Monte Carlo method. *J. Am. Stat. Assoc.* **1949**, *44*, 335–341.
28. *MC1990, FIB Model Code for Concrete Structures 1990*; Ernst & Sohn: Berlin, Germany, 1993.
29. *MC2010, FIB Model Code for Concrete Structures 2010*; Ernst & Sohn: Berlin, Germany, 2013.

30. Høvik, S. *DNV OS C 502, DNV OS C 502, Offshore Concrete Structures;* DNVGL: Høvik, Norway, 2012.
31. Rastayesh, S.; Mankar, A.; Sørensen, J.D. Comparative investigation of uncertainty analysis with different methodologies on fatigue data of rebars. In Proceedings of the 5th International Reliability and Safety Engineering Conference, Shiraz University, Shiraz, Iran, 9–10 May 2018.
32. Lindley, D. *Introduction to Probability and Statistics from a Bayesian Viewpoint, vol. 1+2*; Cambridge University Press: Cambridge, UK, 1976.
33. Efron, B. Bootstrap Methods: Another Look at the Jackknife. *Ann. Stat.* **1979**, *7*, 1–26.
34. Sin, G.; Gernaey, K.V. Data Handling and Parameter Estimation. In *Experimental Methods in Wastewater Treatment*; IWA publishing: London, UK, 2016; Volume 281780404745.
35. Alfredo, H.; Tang, W.H. *Probability Concepts in Engineering: Emphasis on Applications in Civil & Environmental Engineering*, 2nd ed.; Wiley: Hoboken, NJ, USA, 2007.
36. Gelman, A.; Carlin, J.B.; Stern, H.S.; Dunson, D.B.; Vehtari, A.; Rubin, D. *Bayesian Data Analysis*; A Champman & Hall Book: New York, NY, USA, 2003.
37. E. 1990, Eurocode 0: Basis for Structural Design; Cen: Brussels, Belgium, 2002.
38. Hastings, W.K. Monte Carlo sampling methods using Markov chains and their applications. *Biometrika* **1970**, *57*, 97–109.
39. *E. 1992-1-1, Eurocode 2: Design of Concrete Structures - Part 1-1: General Rules and Rules for Buildings*; Cen: Brussels, Belgium, 2004.
40. MCS. *Surveillance du Viaduc du Crêt de l'Anneau par un Monitoring à Longue Durée*; MSC: Lausanne, Switzerland, 2017.
41. Mankar, A.; Rastayesh, S.; Dalsgaard Sørensen, J. Fatigue reliability analysis of Crêt de l'Anneau viaduct: A case study. *Struct. Infrastruct. Eng.* **2019**, doi:10.1080/15732479.2019.1633361.
42. Palmgren, A. Die lebensdauer von kugellagern (The life of ball bearings). *Zeitschrift Des Vereins Deutscher Ingenieure* **1924**, *68*, 339–341.
43. Miner, M.A. Cumulative damage in fatigue. *Am. Soc. Mech. Eng. J. Appl. Mech.* **1945**, *12*, 159–164.
44. Mankar, A.; Rastayesh, S.; Dalsgaard Sørensen, J. Fatigue Reliability analysis of Cret De l'Anneau Viaduct: A case study. In Proceedings of the IALCCE 2018, Ghent, Belgium, 18–31 October 2018.
45. CEB 1988. *Fatigue of Concrete Structures - State of Art Report*; CEB: Zurich, Switzerland, 1989.
46. Madsen, H.O.; Krenk, S.; Lind, N.C. *Methods of Structural Safety*; Dover Publications: New York, NY, USA, 2006.
47. FERUM. *Finite Element Reliability Using Matlab*; University of California Berkeley: Berkeley, CA, USA, 2010.
48. *SIA-269, Existing Structures–Bases for Examination and Interventions*; Swiss Society of Engineers and Architects: Zurich, Switzerland, 2016.

Paper 2:

Title:

Fatigue reliability analysis of cre^t de l'Anneau viaduct: a case study

Authors:

Amol Mankar, Sima Rastayesh, John Dalsgaard Sørensen

Published in:

Structure and Infrastructure Engineering 2019; doi:10.1080/15732479.2019.1633361

Taylor & Francis
Taylor & Francis Group

Structure and Infrastructure Engineering
Maintenance, Management, Life-Cycle Design and Performance

ISSN: 1573-2479 (Print) 1744-8980 (Online) Journal homepage: https://www.tandfonline.com/loi/nsie20

Fatigue reliability analysis of crêt de l'Anneau viaduct: a case study

Amol Mankar, Sima Rastayesh & John Dalsgaard Sørensen

To cite this article: Amol Mankar, Sima Rastayesh & John Dalsgaard Sørensen (2019): Fatigue reliability analysis of crêt de l'Anneau viaduct: a case study, Structure and Infrastructure Engineering, DOI: 10.1080/15732479.2019.1633361

To link to this article: https://doi.org/10.1080/15732479.2019.1633361

STRUCTURE AND INFRASTRUCTURE ENGINEERING
https://doi.org/10.1080/15732479.2019.1633361

Fatigue reliability analysis of crêt de l'Anneau viaduct: a case study

Amol Mankar, Sima Rastayesh, and John Dalsgaard Sørensen

Department of Civil Engineering, Aalborg University, Aalborg, Denmark

ABSTRACT

Fatigue of reinforced concrete is often not considered for civil engineering structures since the self-weights of reinforced concrete structures are very high (in case of normal strength concrete) while live loads are relatively small, which leads to very small stress variations during service duration of the structure. However, particularly for bridge structures with increased use of high strength concrete and increase in traffic loads, this scenario is reversed and fatigue verification becomes much more important for the safety. This paper presents a probabilistic approach for reliability assessment of existing bridges along with reliability-based calibration of fatigue-design-factors based on the S-N approach, calibration of S-N approach with fracture-mechanics approach and reliability updating using inspections along with a case study for the Crêt de l'Anneau viaduct in Switzerland. It has been observed that, a designer needs to design the structure for fatigue life of 3.5–4.5 times the planned service life, in order to achieve the target annual reliability index of 3.7 at the end of the service life. Further, the presented framework can easily be extended to any other viaducts to estimate the fatigue reliability and maintain the safety level throughout the entire service duration.

ARTICLE HISTORY
Received 25 February 2019
Revised 23 May 2019
Accepted 7 June 2019

KEYWORDS
Reliability; fatigue; fracture mechanics; reinforced concrete; bridges; calibration

1. Introduction

Until 1960, it was believed to be impossible to get any fatigue failure in reinforced concrete structures with mild steel as reinforcement within the level of permitted stresses at that time, (Mallet, 1991). Most of the bridges in Switzerland built during the last 50 years are reinforced concrete bridges and they typically experience more than 100 million cycles of fatigue load during design lifetime. This is especially the case for reinforced concrete decks of such bridges exposed to traffic loads during their lifetime, which are not designed for fatigue (Schläfli & Brühwiler, 1998, p. 1).

Currently bridge engineers in the industry use Palmgren & Miner's rule of linear damage accumulation along with Wöhler curves from codes and standards (e.g. SIA-261, 2003) for new structures and (SIA-269, 2016) for existing structures. The result might often be the replacement of the existing bridge or atleast its deck. On strength side, the fatigue tests exhibit large scatter, and on action side, codes defining heavy vehicles as actions/loads may lead to non-economical and non-ecological solutions.

A better way forward could be the use of reliability methods (probabilistic approach) to assess the bridge, by quantifying all possible uncertainties in loads and resistance and thereby form a better basis for decision-making. This requires to formulate a stochastic material model from the fatigue test data and a stochastic load model using among others, the monitoring of strains in the structure at critical locations. By this approach, it is possible to quantify the level of damage and the remaining useful fatigue life of the structure. Further, in order to maintain the reliability above acceptable level throughout the service life, it can be important to perform inspections and use the outcomes of the inspections to update the reliability and proceed with mitigation actions, if necessary.

Fatigue reliability assessment of the steel components of bridges is studied in many references where Weight In Motion data (WIM) are used to estimate the reliability of orthotropic bridge decks (see e.g. Yang, Xinhui, Naiwei, & Yang, 2016). Kihyon and Dan (2010) focussed on fatigue reliability assessment of steel bridges by using probability density functions of the equivalent stress range based on the field monitoring data. Saberi, Rahai, Sanayei, and Vogel (2016) estimated the bridge fatigue service life using operational strain measurements. Furthermore, probabilistic reliability assessment of steel structures exposed to fatigue is studied by Krejsa (2014). Sain and Chandra Kishen (2008) presented a probabilistic approach for assessment of fatigue crack growth in Steel Reinforced Concrete (SRC). Petryna, Pfanner, Stangenberg, and Kratzig (2002) proposed a time variant reliability framework, at component level along with a material model for reinforced concrete; however, the obtained results show its inapplicability to system level.

Based on the literature review, it can be seen that, most of the research work for fatigue of bridges is limited to steel bridges or its components, very few researchers focus on concrete bridges. Further, most of the researchers limit to determinstic approaches, when using monitoring results. To estimate fatigue reliability of a reinforced concrete bridge by taking care of all possible uncertainties in load and fatigue

CONTACT Amol Mankar ama@civil.aau.dk

strength, in a probabilistic way, this paper presents a reliability-based framework for assessment with respect to fatigue failure of Crêt de l'Anneau viaduct as a case study. where the Labourator of Maintenance, Construction and Safety of the structures (MCS) department at École polytechnique fédérale de Lausanne (EPFL), Lausanne, Switzerland has installed a long-term monitoring system for estimating strains in the structure deck slab. As part of reliability-based framework, stochastic modelling of fatigue strength of reinforcing bars along with stochastic modelling of fatigue loads is presented as well as the calibration of fatigue safety factors. The reliability indices obtained are compared with target values indicated in SIA-269 (2016), the Swiss standard for existing structures.

Further, a probabilistic fracture-mechanics (FM) approach (damage evolution model) for the tensile reinforcement is developed based on Ayala-Uraga and Moan (2007), Lotsberg and Sigurdsson (2005), Madsen, Krenk, and Lind (2006), Moan, Hovde, and Blanker (1993) and Paris and Erdogan (1963). The FM approach is calibrated to the probabilistic S-N model using the annual probability of failure. To maintain the required target reliability level, a reliability-based-inspection-planning approach is presented.

2. Crêt de l'Anneau viaduct and its monitoring system

2.1. Salient features

Crêt de l'Anneau viaduct is an eight span composite bridge with a total length of 194.8 m, built in 1957. It has a reinforced concrete deck slab with a thickness of 170 mm at mid-span. The deck is supported by two parallel steel box girders, which have an average height of 1.3 m. These box girders are connected to each other by articulation at about 4 m from the support. The concrete used during construction had a cube strength of 40 MPa, which now may be estimated, approximately to 50 MPa (gain in strength due to continued hydration during ~60 years of life).

The deck slab has an orthogonal grid reinforcement serving for double bending (sagging) behaviour in transverse and longitudinal direction. An orthogonal grid is also present in the hogging bending section, near the longitudinal and transverse supports (near and above the box girders). The grid reinforcement consists of different diameters ranging from 10 mm, 14 mm and 18 mm. 18 mm at 500 mm and 14 mm at 100 mm reinforcement are used in the main transverse bending direction between two girders. Out of the two diameters, 18 mm reinforcement in transverse direction is considered in the current study, where strain gauges are installed. Clear cover to reinforcement is 20 mm.

2.2. Fatigue behaviour

The identified critical part of this composite bridge is the reinforced concrete slab (MCS, 2017, p. 41). The fatigue behaviour of the reinforced concrete deck slab is mainly governed by transverse bending between two girders; it contributes also to local longitudinal bending under vehicle rolling wheel loads, thus it is a double bending behaviour. The stress levels in the steel box girder are very low and below the endurance limit for the steel. Therefore, the current study focuses only on reinforced concrete deck slab, and especially on fatigue of the reinforcement in the tension zone, since fatigue of concrete in the compression zone is unlikely to occur (Rocha & Brühwiler, 2012, p. 1) if concrete is not suffering from any other deterioration mechanisms like frost or aggregate alkali reaction. The behaviour of the viaduct is studied considering:

- Fatigue of steel-reinforcement in tension zone and fatigue of concrete in compression zone, using deterministic approach (Bayane, Mankar, Brühwiler, & Sørensen, 2019).
- Fatigue reliability of concrete in compression zone, using probabilistic approach (Mankar, Bayane, Sørensen, & Brühwiler, 2019).

The results of these studies show that, for this particular viaduct, fatigue of steel-reinforcement in tension zone is critical compared to fatigue of concrete in compression zone.

2.3. Monitoring system

The MCS department at EPFL has installed eight electrical strain gauges on longitudinal and transverse reinforcement bars of two spans of the viaduct, at halfway between articulation and support. Two more strain gauges are installed to capture the response of the steel box girders. First, on the bottom side of the top flange and second, on the bottom side of the bottom flange. Furthermore, thermocouples are installed to measure temperature variations in concrete and steel parts of the viaduct. For details about monitoring system, reference is made to MCS (2017), as shown in Figures 1 and 2.

3. Results of monitoring and stochastic load model

3.1. Measurement of strain and calculation of stresses

A study of influence line diagram for the bridge shows that the maximum stress range for the live loads due to traffic can be expected at the mid-span between articulation and support. At the same location strain, gauges are installed to measure strain variations with a frequency of 50–100 Hz. This high frequency of the strain measurement captures all the vehicles and the associated peaks in the responses. Along with this high-frequency-traffic-strain measurements, the strain gauges also capture a low-frequency-strain change due to the temperature variation and the associated structural response. The two responses can be separated since their frequencies vary largely. Figure 3 depicts strain measurements and corresponding temperature effect.

Figure 1. Monitoring system installed on Crêt de l'Anneau viaduct, a view from bottom of viaduct. (Strain gauges locations are highlighted with explosions.)

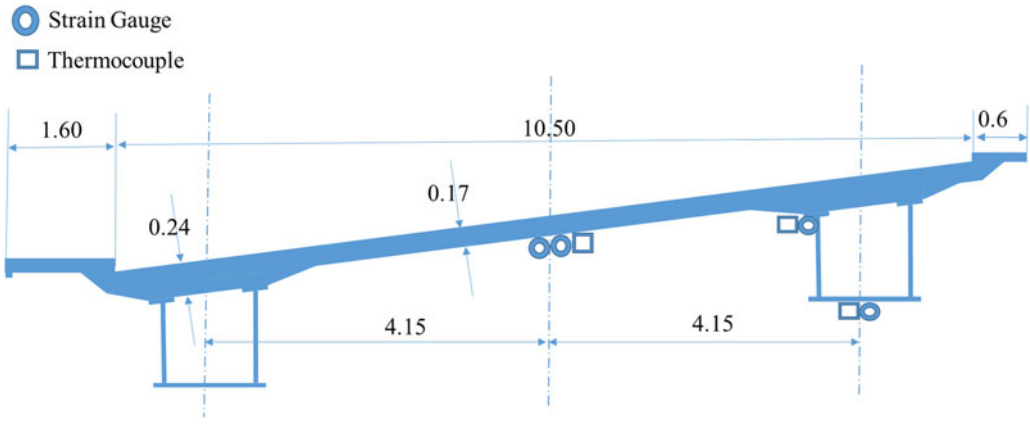

Figure 2. Crêt de l'Anneau viaduct cross section (all dimensions are in m).

The temperature effect can easily be removed from the total response in order to obtain the response due to vehicles only. Five to 10 min averaging time for calculating the mean temperature effect is generally sufficient. Moving average method can be employed using Equation (1) (National-Instruments, 2012). Once the temperature effect is removed from the strains, stresses in the steel-reinforcement can easily be obtained:

$$f(y_i) = \frac{1}{2n+1} \sum_{k=i-n}^{k=i+n} y_k \ for \ N - n > i > n \qquad (1)$$

where

$f(y_i)$ = mean temperature effect,
n = averaging time chosen,
N = total number of data points.

3.2. Rain-flow counting and stress histogram

The stress histogram is obtained by rain-flow counting of the strain data for a monitoring duration of 303 days. The number of cycles required for failure are related only to the stress range (and not to the mean-stress), which is similar to the welded steel. The stress range histogram of transverse reinforcement is shown in Figure 4. The fatigue life of the

viaduct can be estimated using the stress range histogram (Figure 4) along with Equation (2) and Miner's rule. As the actual stresses (Figure 4) in the bridge are very low and the bridge has a very high fatigue life. The reliability analysis is illustrated through the actual histogram, which is scaled such that the design equation, with characteristic values and safety factors-DFF, presented in Section 4.2, is exactly fulfilled. The scaling is performed on the stress range as well as on the number of cycles.

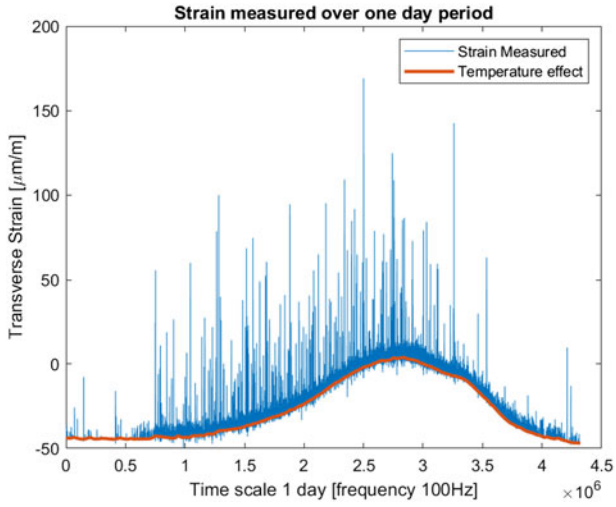

Figure 3. Effect of temperature on strain measurements.

3.3. Stochastic load model for reliability analysis

Uncertainty in the fatigue load (for this specific case, traffic load) covers different aspects and each of them can be modelled independently. These different aspects could be e.g. measurement uncertainty in the strain measurements, as these measurements are very accurate, a very small uncertainty associated with measurement is assumed and modelled as lognormal with a mean of 1.0 and a standard deviation of 0.05, see X_w in Table 1.

Other uncertainties can be related to:

- Extrapolation of results to another location in the structure based on measurement at a certain location (this is not considered here as strain gauges are installed at exactly the same location).
- Extrapolation of the available results to a full year fatigue load based on 303 days observations.
- Extrapolation of the results to the remaining life, which includes year-to-year variations and increase in traffic load and frequency with time.

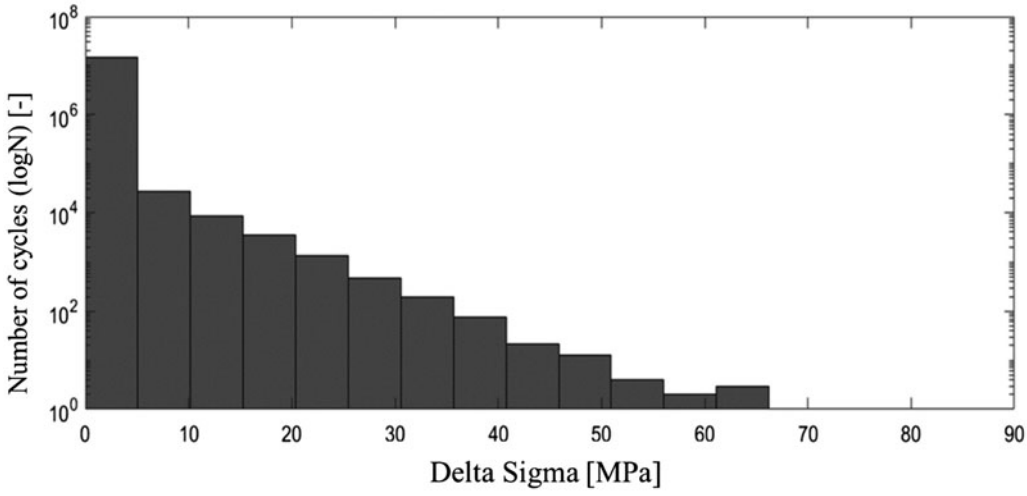

Figure 4. Stress histogram for transverse reinforcement.

Table 1. Stochastic model for Wöhler curve.

Parameter	Distribution	Mean	Standard deviation	Remark
Δ	Lognormal	1	0.30	Model uncertainty related to PM Rule*
X_w	Lognormal	1	0.05	Uncertainty in strain measurements
X_n	Lognormal	1	**0.01** –0.1++	Uncertainty in number of vehicles
logk	Normal	18.77	0.07	Location parameter in Wöhler curve
m	Fixed	5	–	Slope of Wöhler curve fixed to 5+
ϵ	Normal	0	$\sigma\varepsilon$	Standard deviation of the error term
σ_ε	Normal	**0.39**/0.20**	0.06	Standard deviation of the error term
$\rho_{logk,\sigma\varepsilon}$	Deterministic	0.06	–	Correlation coefficient between location and standard deviation of error

*Model uncertainty obtained by fitting lognormal distribution to test data in (CEB 1988, 1989).
+slope of Wöhler curve fixed to 5 as logk and m are highly correlated with correlation coefficient equal to 0.9997.
++Variation in reliability index as function of standard deviation of X_n values is studied.
**Variation in reliability index as function of standard deviation of *logK* values is studied.
Values in bold indicates base values used for reliability analysis.

Available traffic data for 303 days are extrapolated to the total life of the structure by making the assumption of a constant traffic over the entire completed life of 60 years; this is a conservative assumption, as the traffic in the early service duration of the structure is low compared to the present traffic. For the future life of the structure, which is 60 years, 1% increase in the traffic volume each year is assumed. Uncertainties associated with this extrapolation are modelled as lognormal with a mean of 1.0 and standard deviation of 0.10, see X_n in Table 1.

4. Reliability framework

The First Order Reliability Method (FORM) is used for the reliability analysis (Madsen et al., 2006; Sørensen 2011) through the open source Matlab-based toolbox FERUM (Finite Element Reliability Using Matlab) (FERUM, 2010).

4.1. Stochastic material reinforcement in reliability analysis

The deterministic Wöhler curves are recommended by various international codes for the verification of reinforcement fatigue (e.g. DNV OS C 502, 2012; (EN 1992-1, 2004; MC1990, 1993; MC2010, 2013, etc.). These are used as basis for establishing stochastic models together with statistical analysis of the available test data for reinforcement fatigue (Hansen & Heshe, 2001).

For reinforcement fatigue, the number of cycles required for fatigue failure can be calculated based on Wöhler curve, as follows:

$$N = k\Delta\sigma^{-m}$$

or

$$\log N = \log k - m \cdot \log\Delta\sigma + \varepsilon \tag{2}$$

where ε models the uncertainty related to the SN-curve and is assumed Normal distributed with the mean value and the standard deviation equal to 0 and σ_ε respectively. The values of $logk$, m, σ_ε are obtained by the Maximum Likelihood Method (MLM) (Sørensen & Toft, 2010). As these parameters are estimated based on limited set of the data there is a statistical uncertainty, which is presented in Table 1. The use of the MLM provides the option to include run-outs. For more details about probabilistic model for fatigue strength of reinforcing bars and associated uncertainties, reference is made to Rastayesh, Mankar, and Sørensen (2018).

4.2. Design equation and limit state equation

The design equation for reinforcement fatigue is developed based on Equation (2) and Miner's rule, as follows:

$$G = 1 - \sum_{i=1}^{j} \frac{n_i T_F}{k^c} \mathrm{R}_D \Delta\sigma_i^m = 0 \tag{3}$$

where
k^c is the characterisitc value of k;
$logk^c = logk^{mean} - 1.64 \cdot \sigma_\epsilon$; $logk^c$ corresponds to 95% quantile;
n_i is the number of cycles experienced by the structure—for the i^{th} stress range bin $\Delta\sigma_i$;
j *is the total number of bins*;
T_F is the fatigue life; $T_F = FDF \cdot T_L$; FDF is the fatigue-design factor; T_L is the service life time of the structure;
R_D is modelling the ratio of design parameters, here the section modulus of the deck slab;
$\Delta\sigma_i$ is the stress range for the i^{th} bin.

Stress range for each bin is obtained directly by rain-flow counting of the strain gauge measurements, see Section 3.2. Stress range in each bin is multiplied by the ratio of the design parameters (New design parameter/Original design parameter). A specific value of Fatigue-Design Factor (FDF) can be obtained by changing the ratio of design parameter. The design equation (Equation (3)) can be transformed to a limit state equation by introducing the stochastic variables, as follows:

$$g(t) = \Delta - \sum_{i=1}^{j} \frac{X_n n_i t}{10^\epsilon \cdot k} (X_w R_D \Delta\sigma_i)^m = 0 \tag{4}$$

where t indicates the time $0 < t < T_L$ in years. All other terms in the limit state equation are explained in Table 1.

4.3. Calculation of reliability index

As explained in Section 3.2, the actual stresses in the bridge are very low and the bridge has a very high fatigue life. Therefore, the reliability analyses are performed using the scaled fatigue load. The cumulative (accumulated) probability of failure $P_F(t)$ in the time interval [0, t] is obtained:

$$P_F(t) = P\big(g(t) \le 0\big) \tag{5}$$

The probability of failure is estimated by FORM (see Madsen et al., 2006). The corresponding reliability index $\beta(t)$ is obtained:

$$\beta(t) = -\phi^{-1}(P_F(t)) \tag{6}$$

where $\Phi()$ is the standardised normal distribution function. The annual probability of failure is obtained based on the cumulative probability of failure:

$$\Delta P_F(t) = P_F(t) - P_F\big(t - \Delta t\big), t > 1 \text{ year} \tag{7}$$

where Δt = 1year. The corresponding annual reliability index is denoted $\Delta\beta$.

5. Reliability results with the S-N approach

The current age of the bridge is 60 years, and it is investigated if the bridge can be used for additional 60 years, i.e. a total of 120 years. The reliability is assessed for the reinforced concrete deck slab with respect to fatigue failure of the reinforcement.

Table 2. Stochastic parameters in FM Model.

Parameter	Distribution	Mean	Std-Dev	Remark
a_{cr}	Normal	10.8 mm	1.8 mm	Crack size at unstable fracture (SB)
a_d	Exponential	0.5, 1 ,5* mm	0.5, 1, 5* mm	PoD assumed for AE_Tomography
log$C$	Normal	−12.738	0.11	Material parameter C, (DNVGL)
X_S	LogNormal	1	0.05	Uncertainty in monitored stress
X_n	LogNormal	1	0.05	Uncertainty in number of vehicles

SB: Schläfli and Brühwiler, (1998); DNVGL: DNVGL RP 0001 (2015).
*A sensitivity study is performed for different values of PoD.

5.1. Code requirements for reliability analysis

The Swiss standard (SIA-269, 2016) provides guidelines for assessing the safety of existing structures by a probabilistic approach and presents a target reliability level in the form of reliability indices based on the consequence of failure and the efficiency of interventions (a unity value for the coefficient of efficiency of interventions is recommended by SIA-269 (2016), when it is not determined during the examination phase, see table 2 in Appendix B of SIA-269, 2016). In this study, a low efficiency of intervention is assumed considering that costs to rehabilitate an existing structure as very high and consequences of structural failure are assumed to be serious, which leads to a target annual reliability index of 3.7. Efficiency of safety-related interventions is expressed as the ratio of the risk reduction to the safety costs, which is similar to relative cost of safety measure as explained in probabilistic model code JCSS (2000).

EN 1990 (2002) provides some aspects for assessment of new structures by a probabilistic approach and presents an indicative target accumulated reliability index for life time of 50 years against fatigue. It provides a range of target reliability from 1.5 to 3.8, based on the degree of inspect-ability, repair-ability and damage tolerance (see table C2 in Appendix C of EN 1990, 2002).

5.2. Results of reliability analysis

Results of reliability analysis are presented for different values of Coefficient of Variation (CoV) of $logK$. CoV of $logK$ represents the variability in fatigue performance of the steel-reinforcement. It may vary for different deliveries of the steel-reinforcement. Lower the quality control in production of the steel-reinforcement, larger the CoV and lower the fatigue reliability. For current reliability analysis, CoV of 0.39 is used, which is obtained from test results (Hansen & Heshe, 2001). While, CoV of 0.2 is standard CoV recommended by DNVGL RP C203 (2016).

The variation of the cumulative reliability index along the service life of the structure is presented in Figure 5 for the case where the uncertainty in the vehicle number X_n is 1% and CoV for $logK$ is 0.39. The annual reliability index $(\Delta\beta)$ as a function of the FDF for different CoV values of $logK$ representing reinforcement from an arbitrary delivery is presented in Figure 6. It is observed that the CoV of $logK$ has a large influence on the reliability index values. To meet a target annual reliability index of 3.7 with planned design life of 120 years, the required FDF is of the order of 3.8 for CoV of 0.2 for $logK$, while the needed FDF is of order of 4.4 for CoV of 0.39 for $logK$.

The annual reliability index (β) as a function of the FDF for different CoV values of $logK$ is presented in Figure 7 for

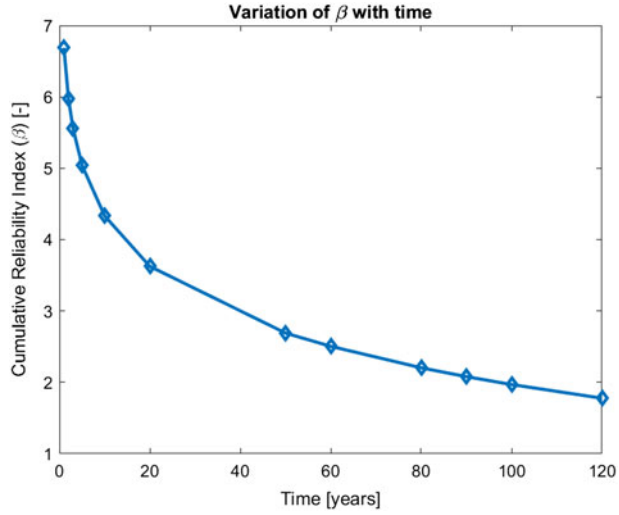

Figure 5. Variation in Cumulative reliability index along service duration of structure (FDF∼2 and T_L=120 years).

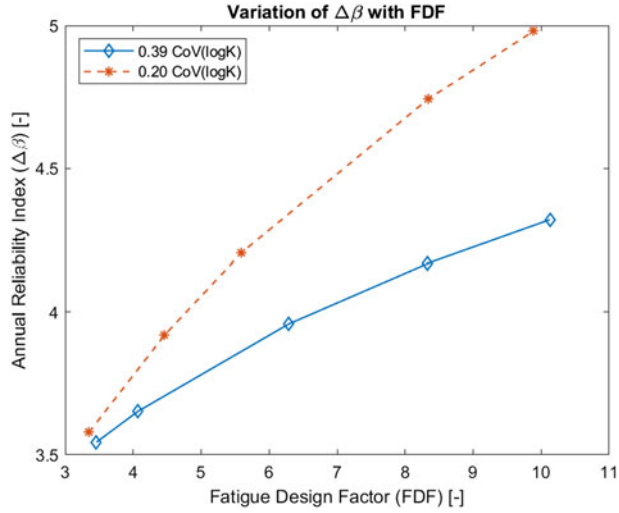

Figure 6. Annual reliability index as function of FDF.

120 years of design life. The cumulative reliability indices in Figure 7 can be compared to the target reliability indices indicated in EN 1990 (2002). A range of fatigue safety factors (FDF) required to achieve the accumulated target reliability index can be obtained from Figure 7.

6. Fracture-mechanics (FM) approach

6.1. FM model for crack growth

This section presents a generic crack growth model based on Paris-Erdogan law (Paris & Erdogan, 1963), for the main

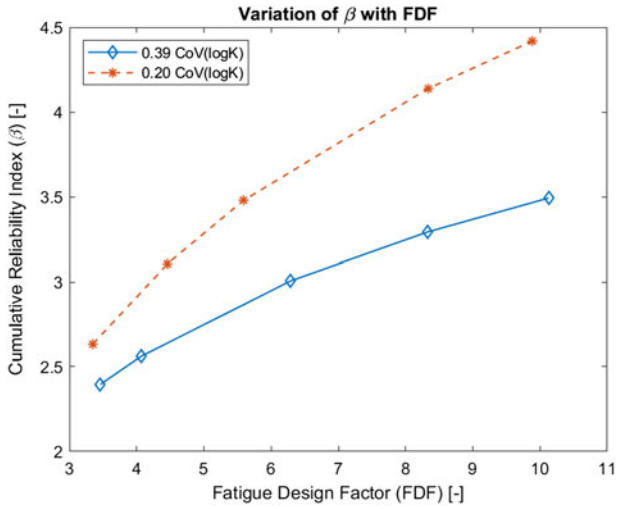

Figure 7. Cumulative reliability index as function of FDF ($T_L = 120$ years for mean values of σ_ε equal to 0.20 and 0.39).

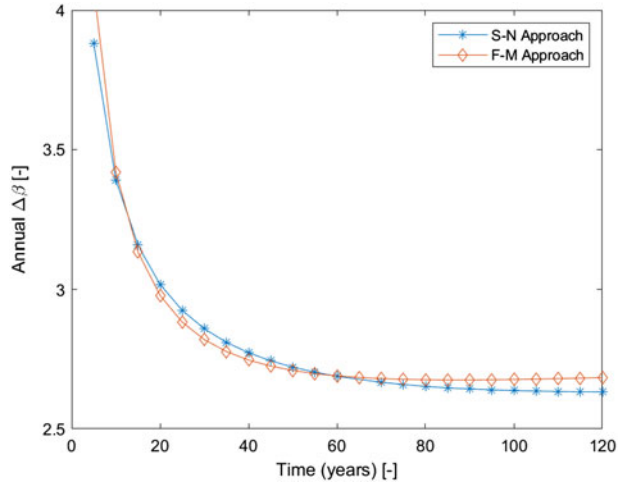

Figure 8. Calibration of FM approach with S-N approach (FDF = 1.5).

reinforcement of 18 mm, at a critical fatigue location. Experimental investigations show that the increment of crack per stress cycle can be approximated as follows:

$$\Delta a = C\left(\sqrt{\pi a}\Delta\sigma Y\right)^m \tag{8}$$

The crack length increment Δa is often very small compared to the variation of $a^{m/2}$, therefore Δa can be idealised to be the differential quotient da/dN, where N is the number of cycles considered as a continuous parameter and then, the solution $a_{(T)}$ is given by Equation (9) (Ditlevsen & Madsen, 1996). The geometry function or shape factor (Y) is assumed to be 1.0 in Equation (9) and it shows sufficiently accurate calibration with S-N approach (see Section 6.3):

$$a_{(T)} = \left[a_0^{\frac{(2-m)}{2}} + \left(\frac{2-m}{2}\right)\cdot C\cdot \pi^{\frac{m}{2}}\cdot \Delta\sigma^m \cdot n\cdot T\right]^{\left(\frac{(2-m)}{2}\right)^{-1}} \tag{9}$$

where
$a_{(T)}$ crack length at time T (years);
a_0 initial crack length back calculated based on calibration (see Section 6.3);
m & Cparameters in Paris' law;
n Number of stress cycles per year with stress range $\Delta\sigma$.

6.2. Limit state equation for FM

A limit state equation corresponding to FM model explained in Section 6.1 can be written as Equation (10). This limit state equation corresponds to the state when the crack size $(a_{(T)})$ in the year under consideration reaches the critical crack size (a_C). The critical crack size is the crack size where the unstable brittle fracture of reinforcement occurs or when rupture occurs. This critical crack size (a_C) can be calculated as the ultimate level of stress based on extreme value theory, however for this paper critical crack size is assumed as normal distributed with a mean value of 60% of the diameter of reinforcement and a CoV of 0.1 (see Table 2 and Rocha & Brühwiler, 2012):

$$g(T) = a_c - \left[a_0^{\frac{(2-m)}{2}} + \left(\frac{2-m}{2}\right)\cdot C\cdot\left(\sqrt{\pi}\cdot\Delta\sigma\right)^m\cdot n\cdot T\right]^{\left(\frac{2-m}{2}\right)^{-1}} \tag{10}$$

6.3. FM calibration

An outcome of an inspection cannot be related directly to the damage obtained from the S-N approach. Therefore, the FM approach with Paris-Erdogan law is used, where an inspection outcome can be related to the crack size, which is obtained from the FM approach. However, calculated fatigue lives based on S-N data are more reliable than those based on FM, as S-N data are derived directly from fatigue tests; while FM is based on calculations where additional parameters are required as input to the analysis. Thus, it is reasonable to make a calibration such that the probability of a fatigue failure based on fracture mechanics follows that of S-N data (test data) until the first in-service inspection. After the first inspection, the results will depend on the FM model and the reliability of inspection method. The calibration purpose, it is assumed that crack growth starts at the first stress cycle and then, the distribution of initial crack size (a_0) is calibrated such that probability of a fatigue failure at a given number of stress cycles is similar to S-N fatigue test data. Thus, this initial crack size is "fictitious" as it can hardly correspond to real physical crack sizes (DNVGL RP 0001, 2015).

Figure 8 presents the calibration of the FM approach with S-N approach. Calibration for the current study is performed such that the reliability index at the inspection year for FM approach is achieved as for the S-N approach. For the rest of the years, the calibration is performed, using a least square fitting method. Two parameters are used here for the calibration, namely the initial crack size (a_0) and the FM approach (m). The resulting amount of required in-service inspection is highly correlated with this calibration (Lotsberg, Sigurdsson, Fjeldstad, & Moan, 2016).

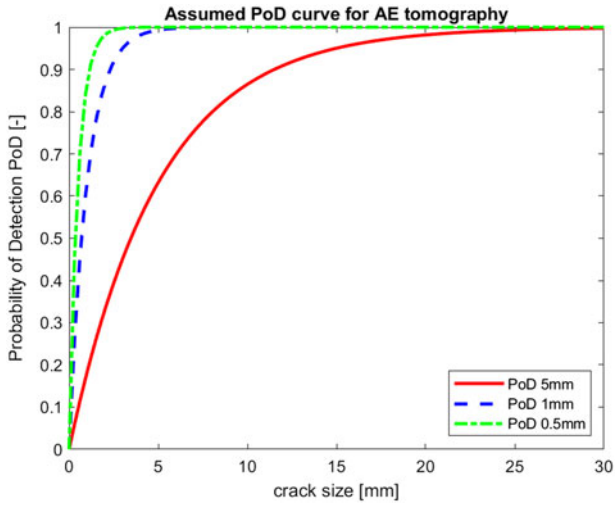

Figure 9. Assumed PoD for AE tomography.

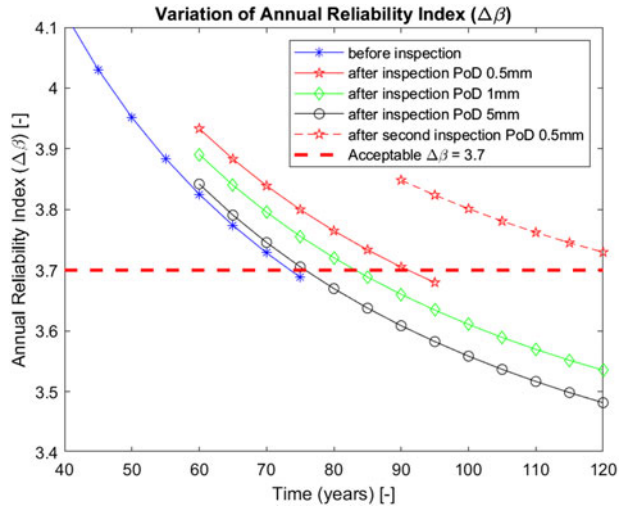

Figure 10. Reliability updating based on AE tomographic inspections for FM approach (FDF∼30).

6.4. Reliability updating using inspections

In order to maintain the reliability level, periodic inspections need to be performed. Information available through inspections can be used to assess the current 'health' of the structure as well as to predict its behaviour, by updating the future failure probabilities. Currently, researchers focus more on understanding fracture surface of reinforcement after failure to know the crack propagation over the diameter. Thus, these present techniques lack to measure the crack size in reinforcement. However, researchers believe that it is possible with Acoustic Emission (AE) tomography (which could be part of a future work for other researchers). In the current study, it is assumed that it is possible to measure the crack size with unknown uncertainty, for the purpose a sensitivity study is performed with different values of uncertainty ranging from 0.5 to 5 mm. The crack size obtained from inspection is used to update the reliability indices, similar to offshore steel structures (DNVGL RP 0001, 2015). It is assumed that the reliability associated with the AE tomography technique is described by a Probability of Detection (PoD) curve (Sergio & Sørensen, 2012), see Figure 9 and Equation (11), where a_d models the smallest detectable crack size:

$$POD(a) = F_{a_d}(a) = 1 - e^{\left(-\frac{a}{b}\right)} \tag{11}$$

where b is the expected value of a_d and is assumed to be equal to 0.5, 1 and 5 mm.

The limit state equation corresponding to an inspection event (h), where no cracks are observed (crack size is less than the detectable crack size a_d), is modelled (see Equation (12)). The inspection event (h) smaller than zero implies that crack size is smaller than the detection ability of inspection method, resulting in no detection of crack while (h) larger than zero implies that crack size is larger than the smallest detectable crack:

$$h\left(T_{insp}\right) = a(T) - a_d \leq 0 \tag{12}$$

The failure probability P_F after an inspection event is updated by calculating the conditional probability of failure, given the inspection event is performed. Bayes' rule is used to obtain the updated failure probability, P_F^U, as follows:

$$P_F^U = P\left(g(T) \leq 0 | h\left(T_{insp}\right) \leq 0\right)$$
$$P_F^U = \frac{P\left(g(T) \leq 0 \cap h\left(T_{insp}\right) \leq 0\right)}{h\left(T_{insp}\right) \leq 0} \tag{13}$$

The numerator in the above equation $P\left(g(T) \leq 0 \cap h\left(T_{insp}\right) \leq 0\right)$ is calculated as the probability of failure of a parallel system by FORM (Madsen et al., 2006). The corresponding updated annual reliability index can be obtained:

$$\Delta\beta^U(\mathrm{T}) = -\emptyset^{-1}\begin{pmatrix} P\left(g(T) \leq 0 | h\left(T_{insp}\right) \leq 0\right) - \\ P\left(g(T-1) \leq 0 | h\left(T_{insp}\right) \leq 0\right) \end{pmatrix}$$
$$T > T_{insp} \tag{14}$$

Figure 10 illustrates the variation of annual reliability index along the service life the structure, at about 75 years of life the annual reliability index is lower than threshold value of 3.7 specified in SIA-269 (2016), thus it is assumed that an inspection of reinforcement near the critical fatigue location is performed at 60 years of life (current year) with AE tomography and no crack was found. The failure probability is updated after the inspection event at 60th year, and thus updated annual reliability after 60th year is obtained for remaining service life until planned future life of 120 years.

It is seen that for AE tomographic inspection with high uncertainty, i.e. mean value of 5 mm for PoD, there is no gain in the form of updated failure probability (P_F^U). The updated failure probability follows almost the same trend as if there is no inspection performed. While with reduction in the uncertainty for AE tomographic inspection to 0.5 mm, the gain in updated probability of failure (P_F^U) is significant. The updated failure probability (P_F^U) crosses the target reliability threshold at about 90 years of life instead of 75 years. Further, if a second inspection is performed at 90 years with

an assumed outcome of no crack detection, then for the remaining service life, the structure meets the requirement of the minimum acceptable level of annual reliability index of 3.7.

7. Conclusions

In this paper, the probabilistic framework for estimating fatigue reliability of bridges is presented. As a case study, fatigue reliability of Crêt de l'Anneau viaduct is presented by formulating the stochastic models for action effects (strain/stress) based on monitoring data and for fatigue resistance of steel-reinforcement based on fatigue test data of steel-reinforcement. It has been observed that the reliability indices for the structure are larger than the acceptable level. As the structure considered in the case study exhibits a very high reliability level with respect to fatigue failure of the reinforcement, the traffic load on the structure can be increased along with the life extension of the structure.

CoV of *logK* has been found to have a large influence on the reliability index values. To meet a target annual reliability index of 3.7 with a planned design life of 120 years, the required FDF is of the order of 3.8 for CoV of 0.2 for *logK*, while the needed FDF is of order of 4.4 for CoV of 0.39 for *logK*. FDF of 3.8 can be interpreted deterministically as the designer should consider designing the structure with a fatigue life of $3.8 * 120 = 456$ years to achieve a target annual reliability index of 3.7 at the end of 120 years of service life when CoV of *logK* is 0.2 while a fatigue life of $4.4 * 120 = 528$ years needs to be used if CoV of *logK* is 0.39.

No noticeable variation in the reliability index is observed for a sensitivity study of the uncertainty associated with vehicle numbers X_n with CoV ranging from 1% to 10%. However, it is seen that changes in uncertainty associated with *logK* result in large variations in the reliability index. Thus, focus should be on reducing the uncertainty in *logK* in order to take decisions. It is observed that calibration of FM approach with S-N approach works well for reinforcement as well similar to offshore oil and gas steel structures using Paris-Erdogan law.

Furthermore, updating the reliability using inspection information by the FM approach is a very useful tool to assess the reliability of the existing assets, however it should be noted that outcome of these updates in safety assessment (or failure probability) is highly dependent on the uncertainty associated with the inspection technique and more work is needed to develop inspection techniques for reinforcements, especially methods that can give indirect information on the fatigue damage state of the reinforcement. The current approach uses only fatigue limit state at the component level reliability, it would be interesting to see the results which include the system level reliability coupled with the ultimate failure of bridge decks.

Funding

The project INFRASTAR (infrastar.eu) has received funding from the European Union's Horizon 2020 research and innovation programme under the Marie Skłodowska-Curie grant agreement No. 676139.

ORCID

Amol Mankar 0000-0003-4015-041X
Sima Rastayesh 0000-0001-9536-3469
John Dalsgaard Sørensen 0000-0001-6987-6877

References

Ayala-Uraga, E., & Moan, T. (2007). Fatigue reliability-based assessment of welded joints applying consistent fracture mechanics formulations. *International Journal of Fatigue*, *29*, 444–456. doi:10.1016/j.ijfatigue.2006.05.010

Bayane, I., Mankar, A., Brühwiler, E., & Sørensen, J. D. (2019). Quantification of traffic and temperature effects on the fatigue safety of a reinforced-concrete bridge deck based on monitoring data. *Engineering Structures*, in press.

CEB 1988. (1989). *Fatigue of concrete structures - State of Art Report*. Zurich: CEB.

Ditlevsen, O., & Madsen, H. (1996). *Structural reliability methods* (1st ed.). Chichester, UK: John Wiley & Sons Ltd.

DNV OS C 502. (2012). *DNV OS C 502, Offshore concrete structures*. Høvik: DNVGL.

DNVGL RP 0001. (2015). *Probabilistic methods for planning of inspection for fatigue cracks in offshore structures*. Oslo: DNVGL.

DNVGL RP C203 (2016). *DNVGL RP C203 Fatigue design of offshore steel structures*. Høvik: DNVGL.

EN 1990 (2002). *EN 1990 Basis of structural design*. Brussels: European Committee for Standardisation.

EN 1992-1 (2004). *Design of concrete structures – Part 1-1: General rules and rules for buildings*. Brussels: European Committee for Standardisation.

FERUM. (2010). *Finite Element Reliability Using Matlab*. Berkeley: University of California.

Hansen, L. P., & Heshe, G. (2001). Fibre Reinforced Concrete and Ribbed Bars. *Nordic Concrete Research*, *26*, 17–37.

JCSS. (2000). *JCSS probabilistic model code*. Joint Committee on Structural Safety JCSS. ISBN: 978-3-909386-79-6.

Kihyon, K., & Dan, M. F. (2010). Bridge fatigue reliability assessment using probability density functions of equivalent stress range based on field monitoring data. *International Journal of Fatigue*, *32*, 1221–1232.

Krejsa, M. (2014). Probabilistic reliability assessment of steel structures exposed to fatigue. In *Safety, reliability and risk analysis: Beyond the horizon*. Boca Raton, London, New York, Lejden: CRC Press.

Lotsberg, I., & Sigurdsson, G. (2005). Assessment of input parameters in probabilistic inspection planning for fatigue cracks in offshore structures. In Proceedings of the 9th International Conference on Structural Safety and Reliability, ICOSSAR'05, Rome, Italy.

Lotsberg, I., Sigurdsson, G., Fjeldstad, A., & Moan, T. (2016). Probabilistic methods for planning of inspection for fatigue cracks in offshore structures. *Marine Structures*, *46*, 167–192. doi:10.1016/j.marstruc.2016.02.002

Madsen, H. O., Krenk, S., & Lind, N. C. (2006). *Methods of structural safety*. New York: Dover Publications.

Mallet, G. P. (1991). *Fatigue of reinforced concrete (state of the art review)*. Stationery Office Books (TSO). ISBN-10: 0115509798, ISBN-13: 978-0115509797

Mankar, A., Bayane, I., Sørensen, J. D., & Brühwiler, E. (2019). Probabilistic reliability framework for assessment of concrete fatigue of existing RC bridge deck slabs using data from monitoring. *Engineering Structures*, in press.

MC1990. (1993). *FIB model code for concrete structures 1990*. Berlin: Ernst & Sohn.

MC2010. (2013). *FIB model code for concrete structures 2010*. Berlin: Ernst & Sohn.

MCS. (2017). *Surveillance du Viaduc du Crêt de l'Anneau par un monitoring à longue durée*. Lausanne: MSC.

Moan, T., Hovde, G., & Blanker, A. (1993). *Reliability-based fatigue design criteria for offshore structures considering the effect of inspection and repair* (II, pp. 591–600). Houston, TX: 25th Offshore Technology Conference.

National-Instruments. (2012). *Smoothing functions*. Retrieved from http://zone.ni.com/reference/en-XX/help/370859K01/genmaths/genmaths/calc_smoothfunctions/

Paris, P., & Erdogan, F. (1963). A critical analysis of crack propagation laws. *Journal of Basic Engineering*, *85*, 528–534. doi:10.1115/1.3656900

Petryna, Y. S., Pfanner, D., Stangenberg, F., & Kratzig, W. B. (2002). Reliability of reinforced concrete structures under fatigue. *Reliability. Engineering and System Safety*, *77*, 253–261. doi:10.1016/S0951-8320(02)00058-3

Rastayesh, S., Mankar, A., & Sørensen, J. D. (2018). Comparative investigation of uncertainty analysis with different methodologies on the fatigue data of rebars. In *IRSEC2018*. Arzhang Printing: Shiraj, Iran.

Rocha, M., & Brühwiler, E. (2012). Prediction of fatigue life of reinforced concrete bridges using Fracture. In Bridge Maintenance, Safety, Management, Resilience and Sustainability. London: CRC Press.

Saberi, M. R., Rahai, A. R., Sanayei, M., & Vogel, R. M. (2016). Bridge fatigue service-life estimation using operational strain measurements. *Journal of Bridge Engineering*, *21*, 04016005. doi:10.1061/(ASCE)BE.1943-5592.0000860

Sain, T., & Chandra Kishen, J. M. (2008). Probabilistic assessment of fatigue crack growth in concrete. *International Journal of Fatigue*, *30*, 2156–2164. doi:10.1016/j.ijfatigue.2008.05.024

Schläfli, M., & Brühwiler, E. (1998). Fatigue of existing reinforced concrete bridge deck slabs. *Engineering Structures*, *20*, 991–998.

Sergio, M.-D., & Sørensen, J. D. (2012). Fatigue reliability and calibration of fatigue design factors for offshore wind turbines. *Energies*, *5*, 1816–1834. doi:10.3390/en5061816. doi:10.3390/en5061816

SIA-261. (2003). *SIA 261 – Action on structures*. Zurich: Swiss Society of Engineers and Architects.

SIA-269. (2016). *Existing structures – Bases for examination and interventions*. Zurich: Swiss Society of Engineers and Architects.

Sørensen, J. D. (2011). *Notes in structural reliability theory and risk analysis*. Denmark: Aalborg University.

Sørensen, J. D., & Toft, H. S. (2010). Probabilistic design of wind turbines. *Energies*, *3*, 241–257. doi:10.3390/en3020241

Yang, L., Xinhui, X., Naiwei, L., & Yang, D. (2016). Fatigue reliability assessment of orthotropic bridge decks under stochastic truck loading. *Shock and Vibration*, *2016*(3), 1–10.

Paper 3:

Title:

Risk Assessment and Value of Action Analysis for Icing Conditions of Wind Turbines Close to Highways

Authors:

Sima Rastayesh, Lijia Long, John Dalsgaard Sørensen and Sebastian Thöns

Published in:

Energies 2019, 12, 2653; doi:10.3390/en12142653

energies

MDPI

Article

Risk Assessment and Value of Action Analysis for Icing Conditions of Wind Turbines Close to Highways

Sima Rastayesh [1,*], Lijia Long [1,2], John Dalsgaard Sørensen [1] and Sebastian Thöns [2,3]

[1] Department of Civil Engineering, Aalborg University, 9220 Aalborg, Denmark
[2] Department 7: Safety of Structures, Federal Institute of Materials Research and Testing, 12205 Berlin Germany
[3] Technical University of Denmark, 2800 Lyngby, Denmark
* Correspondence: sir@civil.aau.dk; Tel.: +45-9940-3833

Received: 30 May 2019; Accepted: 1 July 2019; Published: 10 July 2019

Abstract: The paper presents research results from the Marie Skłodowska-Curie Innovative Training Network INFRASTAR in the field of reliability approaches for decision-making for wind turbines and bridges. This paper addresses the application of Bayesian decision analysis for installation of heating systems in wind turbine blades in cases where an ice detection system is already installed in order to allow wind turbines to be placed close to highways. Generally, application of ice detection and heating systems for wind turbines is very relevant in cases where the wind turbines are planned to be placed close to urban areas and highways, where risks need to be considered due to icing events, which may lead to consequences including human fatality, functional disruptions, and/or economic losses. The risk of people being killed in a car passing on highways near a wind turbine due to blades parts or ice pieces being thrown away in cases of over-icing is considered in this paper. The probability of being killed per kilometer and per year is considered for three cases: blade parts thrown away as a result of a partial or total failure of a blade, ice thrown away in two cases, i.e., of stopped wind turbines and of wind turbines in operation. Risks due to blade parts being thrown away cannot be avoided, since low strengths of material, maintenance or manufacturing errors, mechanical or electrical failures may result in failure of a blade or blade part. The blade (parts) thrown away from wind turbines in operation imply possible consequences/fatalities for people near the wind turbines, including in areas close to highways. Similar consequences are relevant for ice being thrown away from wind turbine blades during icing situations. In this paper, we examine the question as to whether it is valuable to put a heating system on the blades in addition to ice detection systems. This is especially interesting in countries with limited space for placing wind turbines; in addition, it is considered if higher power production can be obtained due to less downtime if a heating system is installed.

Keywords: risk assessment; value of action analysis; icing conditions; wind turbine; blade; probability; highway

1. Introduction

Wind energy is one of the leading sources of renewable energy in Denmark and other countries. Wind energy is increasingly being used in cold climate locations [1] where icing can be a significant issue that should be taken into account in a risk assessment related to the area around wind turbines. An environmental impact assessment has to be performed, e.g., when it is planned to locate wind turbines in areas where people are living and in cases where it is planned to place wind turbines near a road or highway. Generally, the safety factors used for the design of wind turbines do not cover such situations, since safety factors have been calibrated assuming that there is no or almost no risk of human fatalities in case of the failure of parts of a wind turbine. Ice accretion could have a direct

impact on wind turbine operation, such as measurement errors, power losses, mechanical and electrical failures, and safety hazard problems [2]. Several investigations are ongoing in order to establish rules and guidelines related to icing. For instance, icing could affect the functionality of anemometers if they are unheated, see [3]. In Germany, wind turbines are not allowed to operate during icing situations, see [4]. Several reports are available showing that some wind turbines in Sweden during the 2002 and 2003 winters were forced to stop for seven weeks. Statistics from Sweden show that in winter months, 92% of full stops are caused because of icing [5]. In Germany, 85% of full stops of wind turbines in the mountains were caused by icing [6]. During the design stage, a functional ice detection system can be planned to be installed; subsequently, the wind turbine will be shut down if icing is detected by the ice detection systems.

Most of the de-icing and anti-icing techniques used for wind turbines are inspired by the aviation industry; all these techniques can be classified into two types: passive and active. As an example, for passive techniques, ice-phobic and hydrophobic coatings can be used; furthermore, for active techniques, electrothermal blade heating, heating with microwaves, warm air heating can be applied. However, all of them have some disadvantages. These systems are generally unreliable, and therefore energy losses occur, and the effectiveness of the system decrease [2,7,8].

Ice detection systems are needed to make de-icing and anti-icing systems work. Double anemometer and vibration sensors are often used, as they are cheap; however, they have some weak points. For example, in double anemometers, since humidity is measured relatively, it may lead to an incorrect prediction of icing, which will then affect the wind turbine operation [9]. Another weakness point for double anemometers is related to the location of where they are installed; since icing is increasing with height, a double anemometer will always predict less icing compared to the amount of icing at the most critical location, especially when the turbine is parked [10]. Another shortcoming occurs due to increased measurement errors in case of low temperatures for unheated anemometers [11]. Furthermore, vibration sensors cannot detect icing during stall operation [10]. Optical sensors or video cameras seem more reliable than the aforementioned instruments, e.g., Remote Ice Detection Equipment (RIDE) [12].

In this paper, we consider whether it is worthwhile putting heating systems on the blades when there is the possibility of icing. Situations are considered in which an ice detection system is already installed. Different failure scenarios related to blade failures and icing will be presented in Section 2. In Section 3, risk assessment is described taking to account the distance of wind turbines to highways. Risk is estimated as the probability (per km and per year) that a person in a car will be hit (and killed) by ice pieces or parts of wind turbine blades. It is assumed that a row of wind turbines is placed along the highway. The risk is determined as a function of the distance from the wind turbines to the highway. Our results could provide decision-makers with a tool for deciding whether wind turbines should be placed near a highway and whether heating systems should be installed. This risk assessment and a case study are presented in Sections 3 and 4, and can be used as decision support for designers at sites with limited space and in which wind turbines need to be placed as close as possible to highways. In Section 5, the Value of Action approach is presented as the basis for quantifying whether it is worthwhile installing a heat detection system for wind turbine blades exposed to icing, and in Section 6, a case study is presented to illustrate the decision problem and how it can be solved.

2. Failure Scenarios

The following scenarios are considered in the assessment of risks for the surroundings of a wind turbine:

(1) A part of a wind turbine blade or the whole blade may fail/collapse and be thrown away from the turbine;
(2) Icing may occur when the wind turbine is in operation, and ice pieces may be thrown away;
(3) The wind turbine may be stopped in situations with icing, but ice pieces may be thrown away due to high wind speeds.

The reasons for wind turbine blade failures may be the extremely low strength of the materials (within random variations of strength parameters), manufacturing errors, maintenance errors or extreme environmental conditions (within random variations of environmental parameters and accounting for the effect of the control system). Ice throw can be considered to be similar to a slingshot effect. Ice may be blown from the rotor blades in cases with strong wind when the wind turbine is parked or idling, or thrown away when the wind turbine is in operation. In a risk assessment, mechanical and electrical failures may lead to blade or blade fragment failures; fire and ice risks may be considered as similar events with the main difference between them in the risk assessment being related to their frequency of occurrence [13]. An icing event of a wind turbine near a highway is depicted in Figure 1.

Figure 1. Icing in a wind turbine near a highway.

A conservative rule suggested by Seifert states that the risk of ice-throw from an operational wind turbine has to be investigated for roads, paths or other objects of interest if the wind turbine is placed within the following distance from a road [3]:

$$1.5\ (\text{rotor diameter} + \text{hub height}), \quad (1)$$

To determine the probability of adverse events in the affected area around the wind turbine, the following parameters should be considered [14]:

- Hub height
- Rotor diameter
- Rotor revolution under icing conditions
- Wind properties (distribution of wind speed and direction)
- Ice fragment properties

In [15], an icing model is proposed based on measurements in Germany. Some challenges were observed by this study for ice forecasting, such as the high sensitivity to parameters like liquid water content, droplets median diameter, wind, and temperature.

Ice properties/ice pieces are often classified into four scenarios based on a study by TÜV [14]:

- Rime ice, mass: 90 g (scenario A), and 240 g (scenario B);
- Clear ice, mass: 70 g (scenario C) and 180 g (scenario D).

Based on the TÜV study, which considered a typical wind turbine of 141 m hub height and 117 m rotor diameter, scenario B and D are identified as scenarios that can cause fatalities, and in cases of 90 g rime ice (Scenario A) and 70 g clear ice (Scenario C), slight injuries might occur [14].

In another study, rime ice was classified into five cases [16]: (1) 0 to 0.5 kg/m, (2) 0.5 to 0.9 kg/m, (3) 0.9 to 1.6 kg/m, (4) 1.6 to 2.8 kg/m and (5) 2.8 to 5.0 kg/m, for which observations from wind turbines in Quebec showed that the second class could be dangerous [17].

In the WECO (Wind Energy Production in Cold Climate) project [18], the frequency of ice fall events is estimated based on observations from a wind turbine by counting ice pieces around a test site in Switzerland, where 200 ice falls over three winters were measured.

3. Risk Assessment

Risk has a variety of definitions, see, e.g., the glossary of the Society for Risk Analysis (SRA) [19]. The International Risk Governance Council (IRGC) refers to risk as an uncertain and severe consequence of an event or activity [20]. Zio [21] presented a quantitative definition of risk taking into consideration accident scenarios, consequences, uncertainty, and body of knowledge. In this paper, the approach by JCSS [22] is basically applied; here, risk is defined considering an activity with n events, each with probabilities P_i and with potential consequences C_i. The risk R is defined as the sum of the products of the probabilities and the consequences [23]:

$$R = \sum_{i=1}^{n} P_i \cdot C_i \tag{2}$$

In Figure 2, the process of risk-based decision analysis in this case study is shown. First, it is necessary to consider the scenarios in an icing event to determine the influencing parameters, e.g., ice can be thrown away from the wind turbine when it is operating, or ice can be thrown away from the stopped or idling wind turbine. Furthermore, it has to be included that the wind turbine blade parts can be thrown away because of the partial or total failure of the blades. Next, the model is linked to a car passing on a highway near the wind turbine, and its properties, such as speed and number of passengers. Afterward, it is necessary to take into account possible ice detection and blade heating systems. Subsequently, risk scenarios are identified by the concept above for calculating risk, and in parallel, sensitive parameters in the model are identified. The calculated risks are compared with the accepted risks, and, using the ALARP (As Low As Reasonably Practicable) principle, risks can be considered to be acceptable or not. This process can be expanded using information from SHM (Structural Health Monitoring).

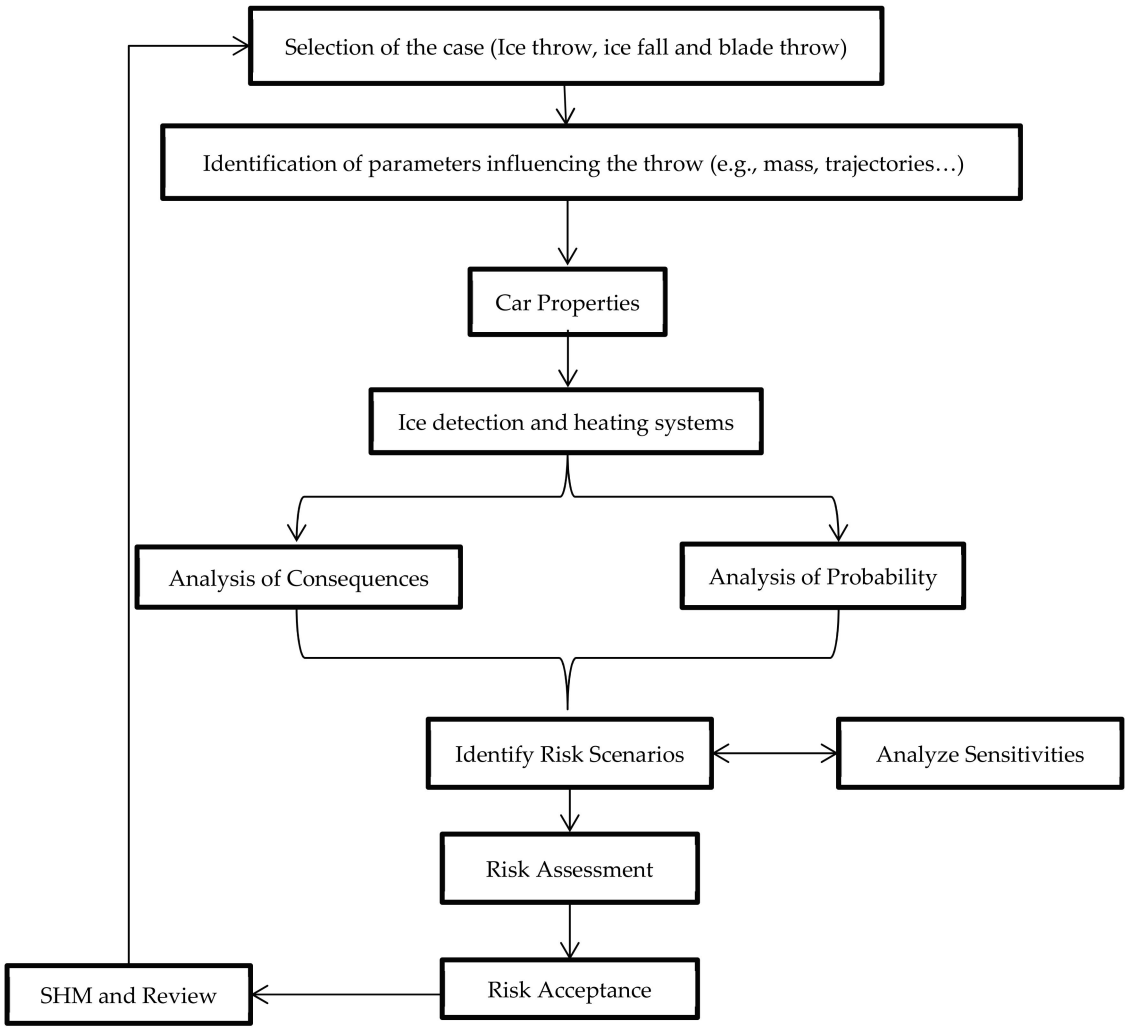

Figure 2. Risk-based decision analysis in this case study.

4. Case Study—Risk Assessment

An example of risk assessment for wind turbines close to highways in Denmark is presented in this section, accounting for the risks mentioned above from falling parts from wind turbine blades in conditions of total or partial damage, as well as ice thrown from wind turbine blades in the case of icing.

In [24], the occurrence of icing was divided into four conditions: heavy, moderate, light, and no icing; Denmark can be considered as a country with moderate icing conditions. It is presumed that a row of wind turbines is placed along a highway with a typical total height of 150 m and a spacing of 500 m along the road. Data is collected from wind turbines both in Denmark and overseas [25].

The following assumptions are made [25]:

- The average drag coefficient of ice pieces is assumed to be 0.6, the density of air is assumed at 1.3 kg/m^3 and that of ice is assumed to be 800 kg/m^3;
- Ice pieces need to be more than 2 cm in thickness in order to be thrown away without being split to smaller pieces on the way;
- The mean speed of vehicles is assumed to 88 km/h on Danish highways (based on Danish road statistics);
- 1.5 people will die in the case of hitting parts (based on Danish road statistics, on average 1 or 2 people usually sits in cars, the average is considered in this case study);

- The probability of being killed when an ice piece or blade part hits a car is assumed to be one, since only large objects are considered;
- The 10-min mean wind speeds, v_i, are assumed to discretized to 5, 10, 15, 20 and 25 m/s;
- The area of a vehicle is assumed to be 10 m^2, which is average for a passenger car;
- Ice pieces larger than 3 mm are used with an occurrence rate of 0.175 times per year (in Denmark). This modeling is subject to considerable uncertainty, since the ice pieces can become larger on the blades because of wind speed or during blade rotation.

In the following figures, models for each of the above three cases are derived based on the models described in [25], as well as ballistic calculations using the models in [26].

The probability (per km per year) that a car is hit by ice pieces, P_A, is estimated in icing conditions based on the following model [25]:

$$P_A = \sum_{v_i=5,\ 10,\ 15,\ 20,\ 25} \left[\frac{1}{V_0}\frac{1}{365\cdot\ 24\cdot\ 3600}\int_S P_Z(s,v_i)A(s)ds\ \frac{1}{D}\right] P(V=v_i) \quad (3)$$

where

V_0 speed of the vehicle
S length of road section considered
$A(s)$ area of a car
D spacing between the wind turbines placed along the highway
$P_Z(s,v_i)$ probability (per km per year) that an ice piece lands in the distance s from the wind turbine if the mean wind speed is v_i. A uniform probability distribution is assumed within the throwing distance R_i at the mean wind speed v_i. Furthermore, using a uniform directional distribution of the wind speed, $P_Z(s,v_i)$ is determined by

$$P_Z(s,v_i) = \nu\frac{1}{R_i} \quad (4)$$

ν number of icing events per year
$P(V=v_i)$ probability that the mean wind speed at hub height in connection with icing is equal to v_i.

The risk, here introduced as the expected number of persons, R_A, per year per kilometer that will be killed by a wind turbine, is estimated by

$$R_A = 1.5\ P_A\ P_D \quad (5)$$

where it is conservatively assumed that the probability of being killed when an ice piece or blade part hits a vehicle is P_D = 1.

A similar equation is presented by [25] for the last scenario.

Figure 3 shows R_A for ice throw from an operational wind turbine as a function of distance (d) to a road (in m) with the tower height of 100 m and the total height of 150 m. Approximately,

$$R_{A,TO} = 5{\cdot}10^{-9}e^{-0.050\ d} \quad (6)$$

Figure 4 illustrates R_A for an idling (parked) wind turbine as a function of distance (d) to a road (in m) with a tower height of 100 m and a total height of 150 m. Approximately

$$R_{A,TI} = 2{\cdot}10^{-9}e^{-0.068\ d} \quad (7)$$

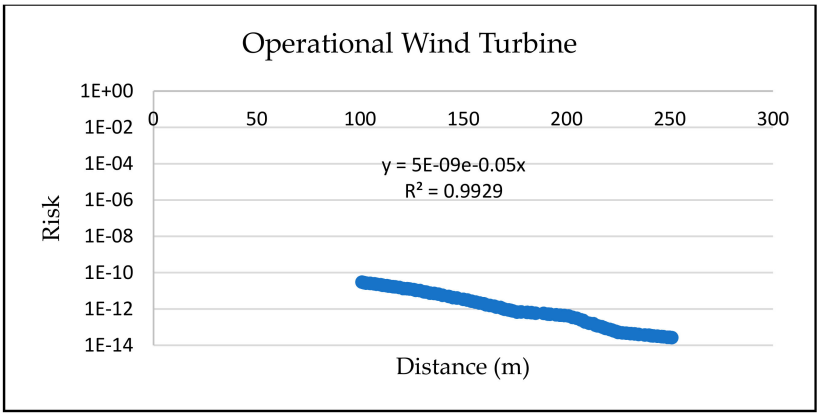

Figure 3. The risk $R_{A,TO}$ per year per kilometer due to icing events as a function of distance to the road for wind turbines in parked position, from [25].

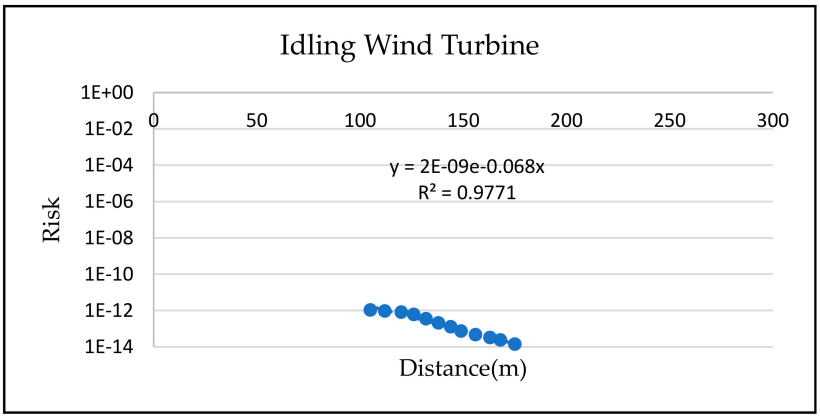

Figure 4. The risk $R_{A,TI}$ per year per kilometer due to icing events as function of distance to road for wind turbines in parked position, from [25].

Figure 5 shows R_A due to total or partial failure/collapse of a wind turbine as a function of distance (d) to a road (in m), with a tower height of 100 m and a total height of 150 m. Approximately

$$R_{A,BT} = 5{\cdot}10^{-12} e^{-0.009\ d} \tag{8}$$

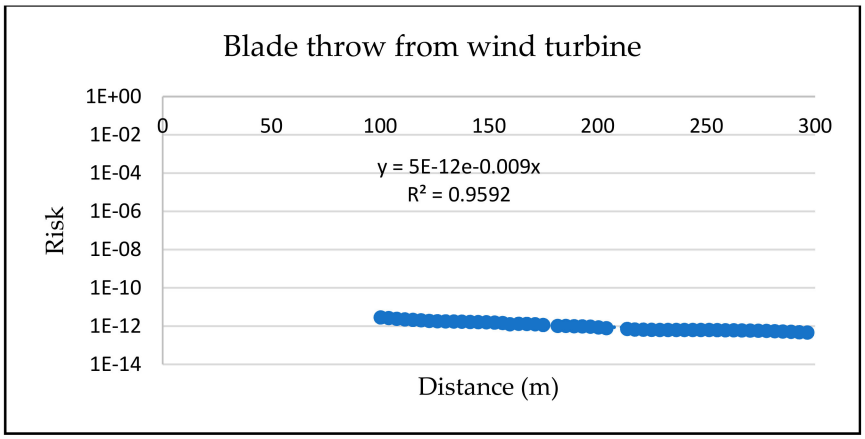

Figure 5. The risk $R_{A,BT}$ per year per kilometer as function of distance to the road for blade parts thrown away from the wind turbine, from [25].

Based on these probabilistic models, the next section presents the basis for decision making and for estimating the Value of Action (VoA). The decision problem that will be considered is whether a heating system should be implemented, assuming that an ice detection system has already been established. This is done for different distances between the road and the row of wind turbines, and can be used as a basis for determining the acceptable distance to the highway using an ice detection system, and next, whether a heating system should be installed.

5. Value of Action Analysis

The concept of Value of Action (VoA) was introduced by Thöns and Kapoor, see [27,28], and constitutes a further development of the Value of Information (VoI) analysis from Raiffa and Schlaifer in [29] and its application in engineering, see e.g., [30–33]. The VoI is defined as the expected utilities gained by obtained (conditional) or predicted (expected) information, including their costs and consequences, while the VoA is different in that the expected utility is gained only on the basis of predicted or implemented actions. The quantification of VoA can be calculated as the difference between the expected utilities of the predicted action and a system state analysis. Based on quantification of VoA, it is possible to provide a decision basis as to whether to implement an action or not. To figure out whether it is beneficial to install the heating systems on the wind turbine blades following the risk assessment results above, a VoA analysis was carried out.

As discussed above, when it is planned to locate a wind turbine location near to highways, one of the interests from owners' perspectives is in reducing risk owing to falling parts from wind turbines in the event of total or partial damage, and from ice thrown from the wind turbines in the case of icing, as shown in Figure 6. The general objective is to ensure normal and steady energy generation, which can be achieved with additional investments in SHM techniques, such as implementing an ice detection system and a blade heating system. Initial investments in SHM techniques can increase the cost of the wind turbine. However, the shutdown of the wind turbine will result in loss of energy production, thus reducing the income of the owner or reputation loss. The major constraints regarding wind turbines close to highways are that falling parts from wind turbines may lead to a traffic accident, damage to cars, and even to the injury or fatality of people. To minimize the overall cost of wind turbine management, it is essential to decide whether to implement an ice detection system, and when to turn on the blade heating system.

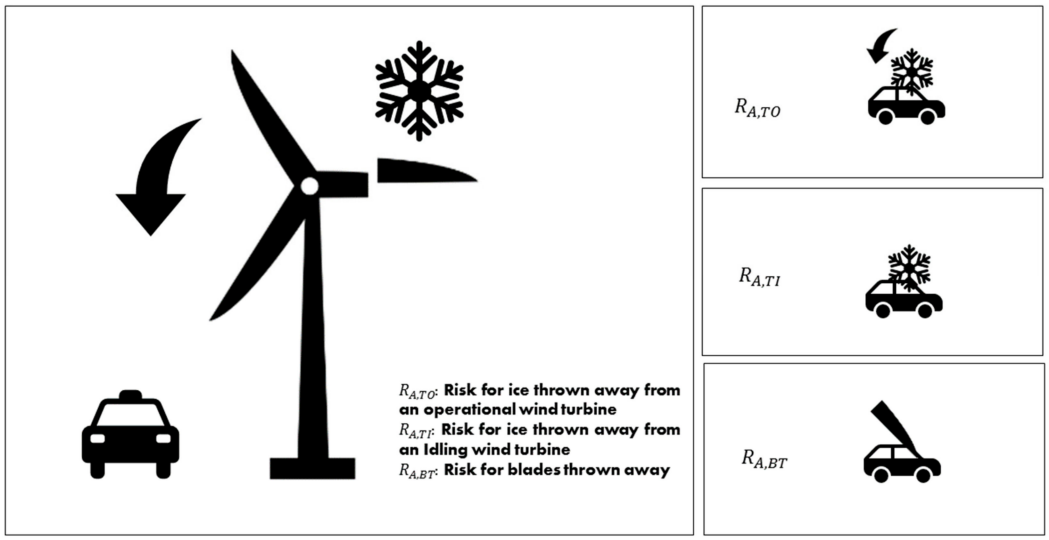

Figure 6. Illustration of risk scenarios of wind turbines close to highways.

A situation is considered in which the risks due to parts being thrown from failed/collapsed wind turbine blades are assumed to be difficult to reduce; therefore, only the reduction of risk due to icing

can be reduced. It is assumed that an ice detection system has already been installed. The question is: is it worthwhile installing a heating system in the blades? When ice is detected, should the wind turbine be shut down directly, or should the ice heating system be turned on? The application of the value of action analysis with regard to the installation of heating systems in wind turbine blades in cases where an ice detection system has already been installed aims at answering the question as to whether it is of value putting a heating system on the blades.

The illustration of the full decision tree is shown in Figure 7. The decision choice is h_0, no heating system, or h_1, with the heating system. By installing the heating, there would be a heating system cost C_H. The decision choice of action will be a_0, do nothing, a_1, stop operating, and a_2, turn on the heating system; moreover, if operation stops, there will be a production loss C_L. Given the monitoring strategy e_1, with ice detection system, data of the ice mass will be collected, and when the mass of ice is over a certain threshold, a warning will be given. Two monitoring outcomes will be provided: z_1, indicating ice, and z_2, not indicating ice. For different choices of actions based on the monitoring outcomes, the wind turbine could be under different states; for example, θ_1, safe state, θ_2, at risk of blades being thrown away, θ_3, at risk of ice being thrown away when the wind turbine is non-operational, and θ_4, at risk of ice being thrown away when the wind turbine is operating. The owners' decisions with respect to actions regarding the wind turbine are based on the indication of ice detection, and the consequences, benefits, and costs. The consequences of parts falling from wind turbines may include traffic accidents, damage of cars, and even the injury or fatality of people, C_F. The most important consequences related to whether a heating system is used or not are those which affect the risk of a person in a vehicle potentially being killed due to falling parts or ice pieces from a wind turbine. If a heating system has not been installed, downtimes can last several days or even weeks due to persistent ice on the blades [34]. Therefore, the production loss C_L can range from hundreds to thousands of Euro. If a heating system is installed, the wind turbine can continue working with benefits B_L per year.

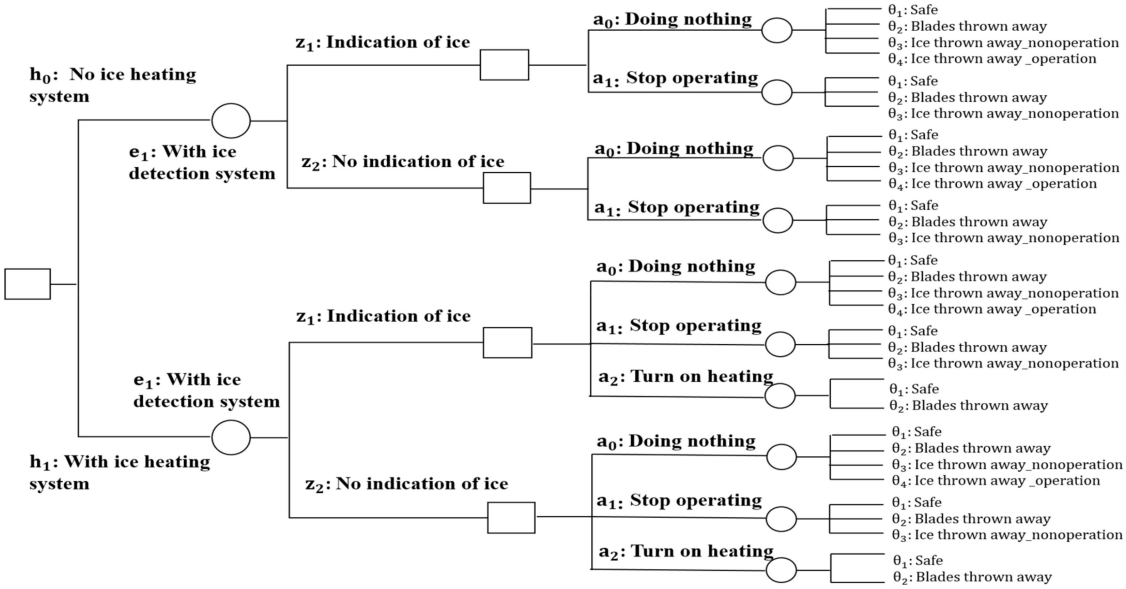

Figure 7. Illustration of the full decision tree for risk assessment of the value of action in the framework of wind turbines close to highways.

It is assumed that the ice detection system provides precise and accurate information. Therefore, if equipped with an ice heating system, when ice is detected, the choice of action could be to a_2, turn on the heating system. The wind turbine will continue working when the heating system is turned on, but there will be a cost for installation of the heating system C_H. The ice will melt after turning on the heating system, and the only risk left in this case will be the risk of blades being thrown away $R_{A,BT}$. If no ice heating system has been installed, when ice is detected, the choice of action could be a_1,

stop operating; there will be a production loss during the downtime, but the risk of ice being thrown away under operation condition $R_{A,TO}$ will be reduced. However, there is still the risk of ice being thrown away under no operation condition $R_{A,TI}$, as well as the risk of blades being thrown away $R_{A,BT}$. If the ice detection system did not indicate ice, whether a heating system has been installed or not, the choice of action will be a_0, do nothing. An illustration of the choice of decision action scenario for wind turbines in icing events close to highways is shown in Figure 8.

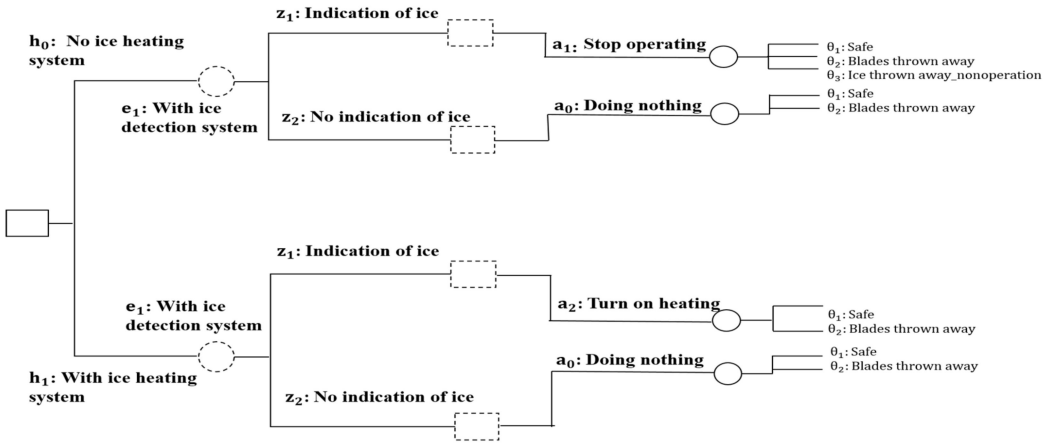

Figure 8. Illustration of the modeled decision scenario and utilized models. A dashed decision node (rectangle) stands for the use of a decision rule and a dashed chance node (circle) for the use of perfect information provided by the ice detection system.

Following the choice of decision scenario in Figure 9, when the ice detection system detects the ice, the choice of action when there is no ice heating system will be to stop operating, which leads to a utility u_{h_0}. The choice of action if the ice heating system is installed will be to turn on the heating, which results a utility u_{h_1}; the value of installing the heating system will be calculated as:

$$VoA = u_{h_1} - u_{h_0} \tag{9}$$

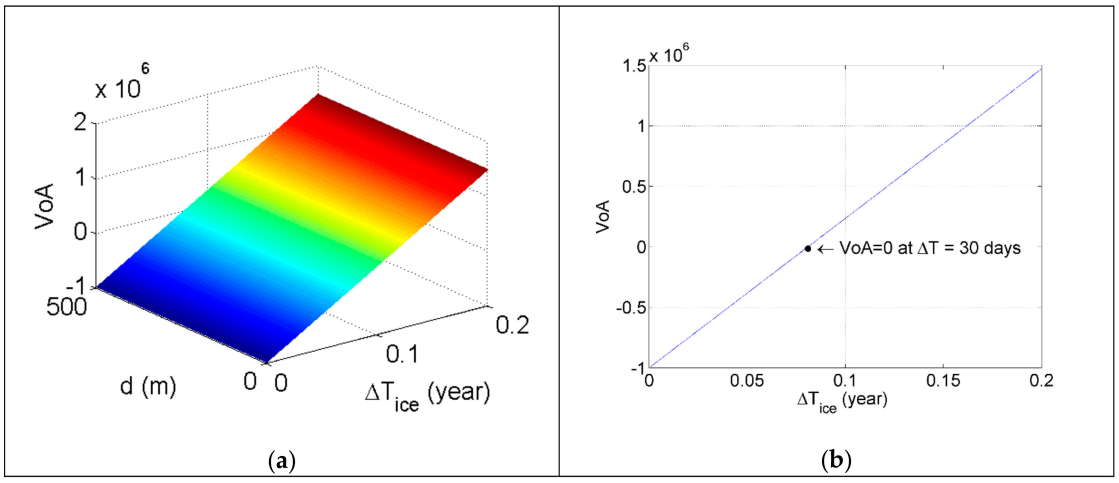

Figure 9. Computational results of VoA in dependence of percentage of downtime per year due to icing ΔT and distance of wind turbine to a highway d (**a**) and VoA with critical down time point when VoA = 0 (**b**).

It is assumed that when the ice heating system is turned on, the ice will melt, and if the ice is thrown away, the risks under both operation and non-operation will be significantly reduced, leaving only the risk of blades thrown away $R_{A,BT}$ remaining, so that, considering the service life T_{SL}, the cost

of the heating system C_H, the cost of possible fatality C_F and the benefits of production B_L, the spacing between wind turbines placed along a highway D, and discounting factor γ, the utility of the heating system u_{h_1} can be obtained by adding the contributions from each year T:

$$u_{h_1} = \sum_{T=1}^{T_{SL}} (1 - P_{A,BT}\,\Delta T_{BT})\,D\,B_L\,\frac{1}{(1+\gamma)^T} - \sum_{T=1}^{T_{SL}} (R_{A,BT}\,D\,C_F + P_{A,BT}\,D\,B_L\,\Delta T_{BT})\frac{1}{(1+\gamma)^T} - C_H. \quad (10)$$

Here, the ratio of downtime per year in which the wind turbine will be stopped ΔT_{BT}. for blade repair if blade has been thrown away is assumed.

When there is no ice heating system, and the wind turbine stops operating, given the ice detection warning, the risk of consequences of ice being thrown away under operation will be reduced, and the remaining risk will be of ice being thrown away under non-operation $R_{A,TI}$ and the risk of blades being thrown away $R_{A,BT}$. Considering the production loss C_L. during this period, the number of icings per year ν, and the ratio of down time per year due to icing ΔT_{ice}, the utility of stop operation u_{h_0} will be:

$$\begin{aligned} u_{h_0} &= \sum_{T=1}^{T_{SL}} (1 - P_{A,TI}\,\Delta T_{ice} - P_{A,BT}\,\Delta T_{BT})\,D\,B_L\,\frac{1}{(1+\gamma)^T} \\ &- \sum_{T=1}^{T_{SL}} ((R_{A,TI} + R_{A,BT})\,D\;\;C_F + P_{A,BT}\,D\,B_L\,\Delta T_{BT} + \nu\,C_L\,\Delta T_{ice})\frac{1}{(1+\gamma)^T} \end{aligned} \quad (11)$$

The estimate of the benefits of production B_L ($C_L = B_L$) per year is based on [35]:

$$B_L = P\;A\;f\;(S + a)\,365{\cdot}24 \quad (12)$$

where P is the rated power of the machine MW, A is the turbine availability factor, f is the capacity factor, A is the sales price of electricity kW/h and a is the feed-in-tariff.

6. Case Study—Value of Action Analysis

The summary of the probability (per km) that a car will be hit by ice or a blade thrown away, as well as the costs and benefits analysis parameters, are shown in Tables 1 and 2, respectively. Table 2 is from [35]; the power of the wind turbine is 3.6 MW, a capacity factor of 0.45 is assumed, turbine availability factor is 0.95, feed-in-tariff is €0.12/kWh, with a rough electricity price of €0.3/kWh, so that there will be $5.66{\cdot}10^6$. Euro per year of production benefit. The total costs of the wind turbine C_I is €$2\cdot10^7$. The discounting factor γ is 0.05. The cost of heating C_H is assumed to be on the order of 5% of the total costs of the wind turbine, considering the equipment costs, installation costs and energy consumption costs [34], which are assumed to be 10^6 Euro. The fatality costs of 1.5 person in a vehicle being killed are assumed to be $3{\cdot}10^6$. Euro, based on [36].

Table 1. Summary of probability (per km) that a car will be hit by ice or blade thrown away.

Remark	Parameter	Equation
The probability (per km) that a car is hit by ice pieces due to ice thrown from an operational wind turbine as a function of distance d to a highway	$P_{A,TO}$	$P_{A,TO} = 3.33{\cdot}10^{-9}e^{-0.005\,d}$
The probability (per km) that a car is hit by ice pieces due to ice thrown from an idling wind turbine as a function of distance d to a highway	$P_{A,TI}$	$P_{A,TI} = 1.33{\cdot}10^{-9}e^{-0.068\,d}$
The probability (per km) that a car is hit by total or partial failure/collapse of a wind turbine blade as a function of distance d to a highway	$P_{A,BT}$	$P_{A,BT} = 3.33{\cdot}10^{-12}e^{-0.009d}$

Table 2. Summary of costs and benefits analysis parameters.

Parameter and Remark	Value	Parameter and Remark	Value
C_F Cost of fatality for 1.5 person	€3 ·10^6	P Power of wind turbine	3.6 MW
C_H Cost of the heating system	€1·10^6	A Turbine availability factor	0.95
γ Discounting factor	0.05	f Capacity availability factor	0.45
T_{SL} service life	20 years	S Electricity price: Euro per-kWh	€0.3/kWh
ν Number of icings per year	0.175	a feed-in-tariff	€0.12/kWh
D spacing between wind turbines	500 m	ΔT_{BT} down time due to blade repair if blade thrown away	1 year

Following Equations (8)–(12) and Tables 1 and 2, the computational results of VoA are shown in Figure 10. When VoA < 0, it means that it is not worthwhile installing the heating system. When VoA > 0, it is recommended that the heating system be installed. Based on Figure 9a, the VoA will increase with the increase in downtime, which means that it will be more beneficial to install the heating system if the downtime due to icing on the blades is longer. However, the impact of the distance of the wind turbine from a highway d is comparably small, which can be explained by the low variation of risk model independence of distance in Section 5. The critical downtime in the case study when VoA = 0 is at $\Delta T =$. 30 days, as shown in Figure 9b. Therefore, if the down time due to ice on the blades is less than 30 days, it is beneficial to just shut down the wind turbine instead of installing a heating system. If the downtime is longer than 30 days, it is worthwhile installing the ice heating system on the blades.

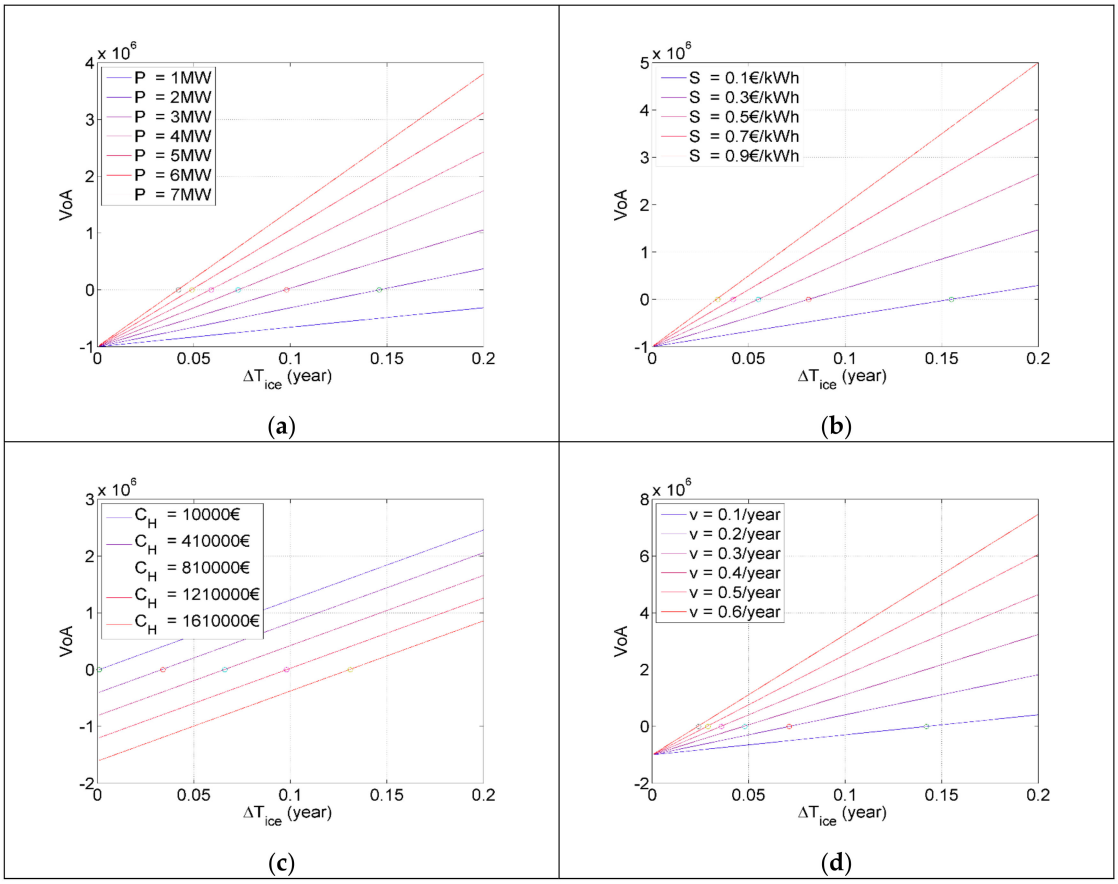

Figure 10. Parametric analysis regarding Value of Action (VoA) with respect to the power of the wind turbine (**a**), electricity price (**b**), cost of the heating system (**c**), and number of icings per year (**d**).

To investigate how the model factors, for example, the power of the wind turbine P, the electricity price S, the cost of the heating system C_H, the number of icings per year ν, and the influence the choice

of action, a parametric analysis is carried out. The results are shown in Figure 10. If the down time is the same, based on Figure 10a, the higher the power of wind turbine P is, the higher the VoA will be, which means that it will be more beneficial to install a heating system on larger wind turbines. The same trend goes for the electricity sales price S in Figure 10b; it is more beneficial to install the heating system when the electricity sales price is high. This also applies to the number of icings per year, ν, in Figure 10c; it is more worthwhile installing a heating system when icing per year is greater. Meanwhile, in Figure 10d, the higher the cost of the heating system, C_H, is, the smaller the benefit of VoA will be.

7. Conclusions

A probabilistic model and a risk assessment model are described for the assessing the consequences related to icing and the associated risk of ice pieces being thrown away from a wind turbine and potentially hitting a vehicle on a road near the wind turbine. In addition, the risk from blades and parts of blades being thrown away from a wind turbine in case of blade failures also needs to be accounted in the risk assessment. This paper considers the application of Bayesian decision analysis for decision-making with respect to the installation of heating systems in wind turbine blades in cases where ice detection systems have already been installed in order to allow wind turbines to be placed close to highways.

Furthermore, the application of Value of Action (VoA) is presented for the decision problem related to installation of a heating system in situations where an ice detection system is already available. Decision trees for the VoA are developed, together with the corresponding utility functions, making it possible to quantify whether it is valuable to put a heating system on the blades in addition to the ice detection systems. This is especially interesting in countries with limited space for placing wind turbines. The model makes it possible to investigate, e.g., whether higher power production can be obtained with less downtime when a heating system is installed.

An illustrative case study is considered, presenting the details of the risk modelling and the Value of Action. Risk is calculated as a function of distance from the wind turbines to the highways. The risk owing to ice throw in operation mode is slightly higher than in the parked position. The spacing between the wind turbines and the height of them did not have a major impact.

The case study with regard to quantification of the Value of Action on wind turbines close to highways with respect to icing events provides a general decision basis for deciding whether or not to install ice heating systems given the condition that ice detection systems have already been installed. The results show that the decision result is highly dependent on the duration of downtime due to ice on the blades.

Author Contributions: S.R. wrote the first draft of the paper. S.R. developed the methodology and results in Sections 1–4; and L.L. in Sections 5 and 6. J.D.S. and S.T. supervised the findings of this work. All authors discussed the results and contributed to the final results.

Funding: The project INFRASTAR (infrastar.eu) has received funding from the European Union's Horizon 2020 research and innovation programme under the Marie Skłodowska-Curie grant agreement No 676139. The grant is gratefully acknowledged.

Acknowledgments: The support of COST Action TU1402 on Quantifying the Value of Structural Health Monitoring is gratefully acknowledged.

Conflicts of Interest: The authors declare no conflicts of interest.

References

1. Frohboese, P.; Anders, A. Effects of icing on wind turbine fatigue loads. *J. Phys. Conf. Ser.* **2007**, *75*, 012061. [CrossRef]
2. Parent, O.; Ilinca, A. Anti-icing and de-icing techniques for wind turbines: Critical review. *Cold Reg. Sci. Technol.* **2011**, *65*, 88–96. [CrossRef]

3. Seifert, H.; Westerhellweg, A.; Kröning, J. Risk analysis of ice throw from wind turbines. Paper presented at Boreas VI, Pyhä, Finland, 9—11 April 2003; pp. 1–9.
4. *German Guideline—Richtlinie für Windenergieanlagen, Liste der Technischen Baubestimmungen*; Wissenschaftliche Dienste des Deutschen Bundestages: Berlin, Germany, 2012.
5. Lamraoui, F.; Fortin, G.; Benoit, R.; Perron, J.; Masson, C. Atmospheric icing impact on wind turbine production. *Cold Reg. Sci. Technol.* **2014**, *100*, 36–49. [CrossRef]
6. Durstewitz, M. A Statistical Evaluation of Icing Failures in Germany "250 MW Wind"-Programme-Update 2005. 2005. Available online: https://www.osti.gov/etdeweb/biblio/20902671 (accessed on 26 June 2019).
7. Zinmickas, V.; Gecevičius, G.; Markevičius, A. A Literature Review of Wind Turbines Icing Problems. In Proceedings of the CYSENI, International Conference on Energy Issues, Kaunas, Lithuania, 26–27 May 2016.
8. Boinovich, L.B.; Emelyanenko, A.M. Anti-icing potential of superhydrophobic coatings. *Mendeleev Commun.* **2013**, *23*, 3–10. [CrossRef]
9. Laakso, T.; Talhaug, L.; Ronsten, G.; Horbaty, R.; Baring, I.; Lacroix, A.; Peltola, E. *Wind Energy Projects in Cold Climates*; Iea wind: Espoo, Finland, 2005.
10. Tammelin, B.; Dobesch, H.; Durstewich, M.; Ganander, H.; Kury, G.; Laakso, T.; Peltola, E. *Wind Turbines in Icing Environment: Improvement of Tools for Siting, Certification and Operation—NEW ICE TOOLS*; Finnish Meteorological Institute: Helsinki, Finland, 2005.
11. Laakso, T.; Baring-Gould, I.; Durstewitz, M.; Horbaty, R.; Lacroix, A.; Peltola, E.; Ronsten, G.; Tallhaug, L.; Wallenius, T. *State-of-the-Art of Wind Energy in Cold Climates*; VTT: Esbourne, Finland, 2010.
12. Gagnon, R.E.; Groves, J.; Pearson, W. Remote ice detection equipment—RIDE. *Cold Reg. Sci. Technol.* **2012**, *72*, 7–16. [CrossRef]
13. Gupta, S.; Robinson, C.; Sanderson, D.; Morrison, A. Den Brook Wind Farm Risk Assessment. Available online: http://www.den-brook.co.uk/media/2417078/Den-Brook-Risk-Assessment-2013.pdf (accessed on 26 June 2019).
14. Kaposvari, M.; Weidl, T. Assessment of the ice throw and ice fall risks nearby wind energy installations. In Proceedings of the Winterwind, Piteå, Sweden, 2–4 February 2015.
15. Froidevaux, P.; Bourgeois, S. Forecasting Ice accretion on Rotor Blades: Models and Validation. In Proceedings of the Winterwind, Skellefteå, Sweden, 6–8 February 2017.
16. Wadham-Gagnon, M.; Bolduc, D.; Boucher, B.; Camion, A.; Petersen, J.; Friedrich, H. Ice Profile Classification Based on ISO 12494. In Proceedings of the WinterWind 2013, Stockholm, Sweden, 11–14 February 2013; p. 48.
17. Erlend Bredesen, R. Understanding and acknowledging the ice throw hazard. In Proceedings of the WindEurope 2017, Amsterdam, The Netherlands, 28–30 November 2017.
18. Tammelin, B.; Cavaliere, M.; Holttinen, H.; Morgan, C.; Seifert, H.; Säntti, K. *Wind Energy Production in Cold Climate (WECO)*; Finnish Meteorological Institute: Helsinki, Finland, 1998.
19. Aven, T.; Ben-Haim, Y.; Boje Andersen, H.; Cox, T.; Droguett, E.L.; Greenberg, M.; Guikema, S.; Kröger, W.; Renn, O.; Thompson, K.M.; et al. Society for Risk Analysis Glossary; Society for Risk Analysis, August 2018. Available online: https://sra.org/sites/default/files/pdf/SRA%20Glossary%20-%20FINAL (accessed on 26 June 2019).
20. *Introduction to the IRGC Risk Governance Framework*; EPFL International Risk Governance Center: Lausanne, Switzerland, 2017.
21. Zio, E. The future of risk assessment. *Reliab. Eng. Syst. Saf.* **2018**, *177*, 176–190. [CrossRef]
22. Risk Assessment in Engineering: Principles, System Representation & Risk Criteria. Available online: https://www.jcss.byg.dtu.dk/Publications/Risk_Assessment_in_Engineering (accessed on 26 June 2008).
23. Sørensen, J.D. *Notes in Structural Reliability Theory and Risk Analysis*; Aalborg University: Aalborg, Denmark, 2011.
24. LeBlanc, M. *Recommendations for Risk Assessments of Ice Throw and Rotor Blade Failure in Ontario*; Garrad Hassan Canada Inc.: Vancouver, BC, Canada, 2007.
25. Sørensen, J.D.; Sørensen, J.N.; Lemming, J.K. Risk assessment of wind turbines close to highways. In Proceedings of the European Wind Energy Conference and Exhibition European Wind Energy Association (EWEA), Copenhagen, Denmark, 16–19 April 2012; pp. 348–356.
26. Sorensen, J.N. On the Calculation of Trajectories for Blades Detached from Horizontal Axis Wind Turbines. *Wind Eng.* **1984**, *18*, 160–175.

27. Thöns, S. On knowledge and utility management. In Proceedings of the 10th International Forum on Engineering Decision Making (IFED), Lake Louise, AB, Canada, 6–9 May 2018.
28. Thöns, S.; Kapoor, M. Value of information and value of decisions. In Proceedings of the 13th International Conference on Applications of Statistics and Probability in Civil Engineering (ICASP13), Seoul, Korea, 26–30 May 2019.
29. Raiffa, H.; Schlaifer, R. Applied Statistical Decision Theory. *J. Chem. Inf. Model.* **2013**, *53*, 1689–1699.
30. Faber, M.H.; Thöns, S. On the Value of Structural Health Monitoring. In Proceedings of the ESREL 2013, Amsterdam, The Netherlands, 30 September–2 October 2013.
31. Straub, D. Value of information analysis with structural reliability methods. *Struct. Saf.* **2014**, *49*, 75–85. [CrossRef]
32. Memarzadeh, M.; Pozzi, M. Value of information in sequential decision making: Component inspection, permanent monitoring and system-level scheduling. *Reliab. Eng. Syst. Saf.* **2016**, *154*, 131–151. [CrossRef]
33. Thöns, S. On the Value of Monitoring Information for the Structural Integrity and Risk Management. *Comput. Civ. Infrastruct. Eng.* **2018**, *33*, 79–94. [CrossRef]
34. Fakorede, O.; Feger, Z.; Ibrahim, H.; Ilinca, A.; Perron, J.; Masson, C. Ice protection systems for wind turbines in cold climate: Characteristics, comparisons and analysis. *Renew. Sustain. Energy Rev.* **2016**, *65*, 662–675. [CrossRef]
35. Thöns, S.; Faber, M.H.; Val, D.V. On the value of structural health monitoring information for the operation of wind parks. In Proceedings of the Safety, Reliability, Risk, Resilience and Sustainability of Structures and Infrastructure, 12th International Conference on Structural Safety and Reliability, Wien Vienna, Austria, 6–10 August 2017; Bucher, C., Ellingwood, B.R., Frangopol, D.M., Eds.; TU Verlag: Vienna, Austria, 2017; pp. 3008–3017.
36. *ISO, I., 2394: 2015_ General Principles on Reliability of Structures*; International Organization for Standardiz: Geneva, Switzerland, 2015.

Paper 4:

Title:

Lifetime Estimation and Failure Risk Analysis in a Power Stage Used in Wind-Fuel Cell Hybrid Energy Systems

Authors:

Sima Rastayesh, Sajjad Bahrebar, Amir Sajjad Bahman, John Dalsgaard Sørensen and Frede Blaabjerg

Published in:

Electronics 2019, 8, 1412; doi:10.3390/electronics8121412

electronics

MDPI

Article

Lifetime Estimation and Failure Risk Analysis in a Power Stage Used in Wind-Fuel Cell Hybrid Energy Systems

Sima Rastayesh [1,*], Sajjad Bahrebar [2], Amir Sajjad Bahman [3], John Dalsgaard Sørensen [1] and Frede Blaabjerg [3]

1 Department of Civil Engineering, Aalborg University, 9220 Aalborg Ø, Denmark; jds@civil.aau.dk
2 Department of Mechanical Engineering, Technical University of Denmark, 2800 Kongens Lyngby, Denmark; sajbahr@mek.dtu.dk
3 Department of Energy Technology, Aalborg University, 9220 Aalborg, Denmark; amir@et.aau.dk (A.S.B.); fbl@et.aau.dk (F.B.)
* Correspondence: sir@civil.aau.dk; Tel.: +45-6054-6777

Received: 25 October 2019; Accepted: 23 November 2019; Published: 26 November 2019

Abstract: This paper presents a methodology based on the failure mode and effect analysis (FMEA) to analyze the failures in the power stage of wind-fuel cell hybrid energy systems. Besides, fault tree analysis (FTA) is applied to describe the probabilistic failures in the vital subcomponents. Finally, the reliability assessment of the system is carried out for a five-year operation that is guaranteed by the manufacturer. So, as the result, the reliability analysis proves that the metal oxide semiconductor field effect transistor (MOSFET) and electrolytic capacitor are the most critical components that introduce damages in the power circuit. Moreover, a comparative study on the reliability assessment by the exponential distribution and the Weibull distribution show that the B1 lifetime obtained by the Weibull distribution is closer to reality.

Keywords: failure mode and effect analysis; failure mechanism; power stage; reliability; wind-fuel cell hybrid energy systems

1. Introduction

Renewable energy systems are rapidly growing in the power sector industry, such as wind turbines, solar energy, and also fuel cells [1–4]. Renewable energy sources are proliferating even more than the expected estimations, although each has its pros and cons. For instance, wind turbines are dependent on wind means climate condition, while fuel cells demand hydrogen-rich fuel. Furthermore, one tricky issue is to keep power production stable; hybrid energy systems facilitate such disadvantages [5,6]. A hybrid wind-fuel cell system usually includes a wind turbine, proton exchange membrane fuel cells (PEMFC), ultracapacitor, an electrolyzer, and a power convertor. Wind turbine power output variations because of wind speed change could be reduced by a fuel cell stack. In this system, the wind turbine and the fuel cell supply the load simultaneously; in order to save extra energy produced by the wind turbine when wind is over speeding, it is converted to hydrogen utilizing an electrolyzer to be used in the fuel cell when needed. Minimizing voltage fluctuations in the system and generating AC voltage are, respectively, the ultracapacitors and the power converter functions [7,8]. PEMFC is a kind of fuel cell being developed by General Electric Corporation as a renewable energy system in many applications, such as transportation, stationary applications, and portable applications, as well as hybrid energy systems [9,10]. Generally, PEMFCs are divided into three main subsystems that contain: Power conditioner, stack, and balance

of plant (BoP) [11]. A power conditioner is one of the crucial subsystems, in which the DC/DC converter regulates the output from the PEMFC stack to a fixed DC voltage [12]. The power stage component is a critical part of the power conditioner subsystem in a PEMFC system which includes active and passive subcomponents. Active subcomponents consist of primary metal oxide semiconductor field effect transistors (MOSFETs) and secondary MOSFETs, which both could contain eight transistors, and their functions are to control the electrical current, voltage regulation, boost switching, and also rectification. Besides, there are passive subcomponents including: Input and output electrolyte capacitors, transformer, choke, varistor, shunt resistor, fuse, and heatsink. The functions of these components are filtering, transmission of current and voltage, and interconnection between different components. MOSFETs as active subcomponents and electrolytic capacitors as passive subcomponents are more significant due to their functions and applications. MOSFETs are used as a switch where the electrical current passes at a desired time interval. In addition, electrolyte capacitors work as a storage for the electrical energy and stabilization of the current voltage [13–15]. There are many studies of capacitors' reliability and failure analysis [16–18] and this paper focuses on the MOSFET as a critical active subcomponent in the power stage and carrying out a diverse failure mechanism analysis of it by failure mode and effect analysis (FMEA) technique.

Achieving a product that can meet customers' demands with the best design, construction, production, and operation costs is one of the main goals in all industries [19,20]. Reliability is a critical criterion of a product's performance, expressed in both deterministic and probabilistic approaches. In the deterministic expression, failure modes and mechanisms are often discussed based on observations, while in the probabilistic case, the failure issues are studied based on statistics [21]. Function investigations and analysis of each system require an individual function analysis of each component, its subsets, and their interaction. The advantages and disadvantages of a component entirely depend on the subsets it is used in. Evidently, the use of defective components with a short lifetime will reduce the efficiency and lifetime of the component and the main system. Therefore, prior to the reliability evaluation of a system, its related components, and failure modes, as well as failure mechanisms of its components and even critical subcomponents, should be adequately comprehended [22].

The literature review shows that the FMEA method is an essential step in conducting a failure mode and failure mechanisms evaluation [11,23]. The FMEA method has been used in multiple types of industry and it is based on discovering, arranging, and decreasing the failures or faults. The majority of the literature available on the PEMFC systems have performed a brief study about failure modes and failure mechanisms [24–26], also most studies were on system-level and non-electrical parts of the PEMFC system, such as electrochemical parts, BoP, and stack part [27–29]. Reliability, availability, and risk study of different parts of the PEMFC are important issues that should be assessed completely. For system recognition, there are main steps, which are significant for the identification of the systems and it is the basis for this study. FMEA focuses on prevention by facilitating process improvement and identifying and eliminating concerns as well as the development of a process or design [30].

Fault tree analysis (FTA) is used for reliability assessment of a system. The fault tree approach is a deductive process by means of which an undesirable event, called the top event, is postulated, and the possible ways for this event to occur are systematically deduced. The deduction process is performed so that the fault tree embodies all component failures (i.e., failure modes) that contribute to the occurrence of the top event. The fault tree itself is a graphical representation of the various combinations of failures that led to the occurrence of the top event [31]. The fault tree itself is a logical model, and thus represents the qualitative characterization of the system logic. There are, however, many quantitative algorithms to evaluate fault trees. For example, the concept of cut sets can also be applied to fault trees by using the Boolean algebra method. This methodology has been used in several applications as well as PEMFCs [32,33]. The focus of the FTA suggested in this paper is the failure of power stage as the top event by considering filters as input and output.

In this paper, the FMEA method is used for the power stage component as a central part of the power conditioner subsystem of a PEMFC system. FMEA as a technique in reliability analysis is used to rank the estimated risk priority with various potential failure modes for critical subcomponents and potential failure modes/mechanisms. According to the FTA of the power stage, it is demonstrated how the failure could happen. Furthermore, with the use of exponential and Weibull distributions by applying Monte Carlo simulation, the reliability is estimated and the reliability curve is presented within the 5-year guarantee period for the system analyzed.

2. Power Stage Components

In the wind-fuel cell system as a hybrid energy system application, the power conditioner subsystem of a PEMFC system carries out the primary power conversion from the input voltage to the output voltage. Usually, a power stage has three parts: Input filter, power amplifier, and output filter. MOSFETs are used as an active subcomponent and it are significant and important due to functions and applications. The power amplifier contained in this case is sixteen MOSFETs used as switches and rectifier where the electrical current is conducted at the desired time interval. Besides, two transformers are used to isolate the primary and secondary sides and to store transient energies during transients.

Furthermore, a voltage dependent resistor (VDR) or varistor is used as control/limit for excessive transient voltage. Both the input filter and the output filter contain the fuse, choke, shunt resistor, and an electrolytic capacitor. A shunt resistor functions as a type of current sensor used in the power stage [13,34]. The schematic of the PEMFC's different levels and all of the main elements of the power stage are depicted and identified in Figure 1 and Figure 2, respectively.

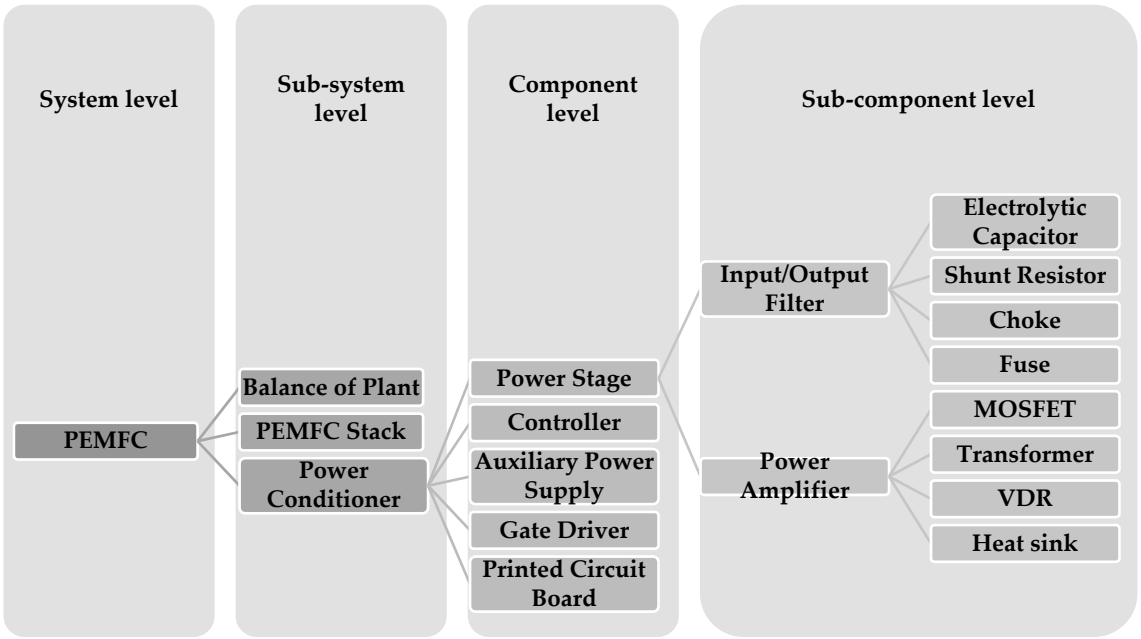

Figure 1. Simplified schematic of the proton exchange membrane fuel cell (PEMFC) categorized in different levels.

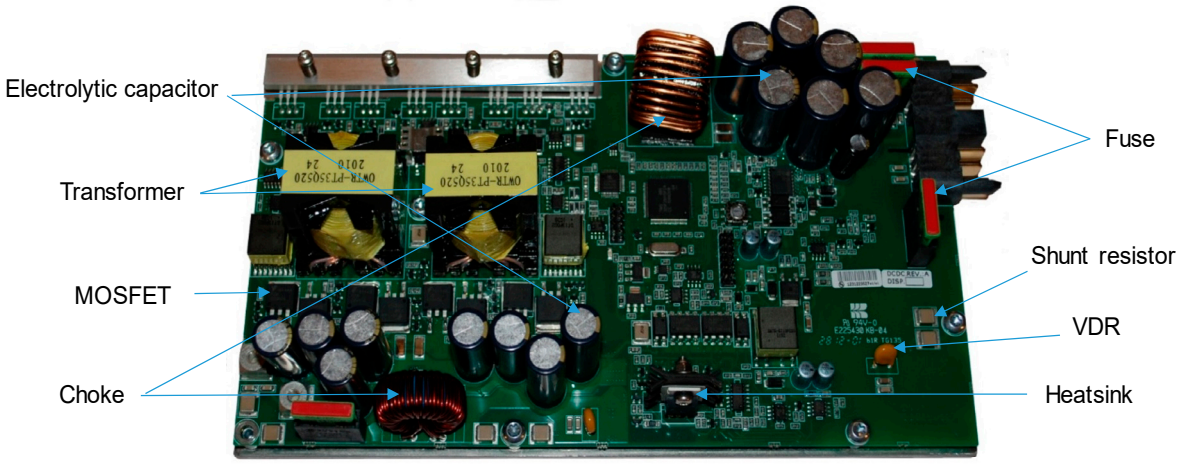

Figure 2. Critical power stage subcomponents in a power conditioner used in PEMFC.

3. Failure Mechanisms and Failure Modes Analysis

Each system has internal durability that may be varied due to particular internal or external circumstances. Failure occurs when exerted stress exceeds the capacity of a system [35]. Failure mechanisms are physical processes that cause failures or stress that, in turn, reduce the stability of the system [36]. These mechanisms are different for mechanical and electrical equipment [37]. Mechanical failure mechanisms can generally be divided into three categories: Tension creation, strength reduction, and stress increase. However, the failure mechanism in electrical equipment is more complicated than that of mechanical failure mechanism due to the complexity of electrical assemblies, which can be divided into three general categories of electrical stress (tension), inherent failure, and external failure. Each of these mechanisms will cause a functional problem and reduce the reliability [38].

First, electrical tension mechanism: Application of an exceeded voltage or current intensity to an electrical component leads to stress creation, reduced performance, or degradation. Additionally, extreme electrical currents increase the heat and local melting at sensitive points of the circuit, which often result in the catastrophic failure or hidden damages of the circuit [21,39], such as failure mechanism type of the MOSFETs and the electrolytic capacitors.

Second, inherent failure mechanism: This mechanism is related to the electronic component itself. These kinds of failure mechanisms are often related to semiconductor components/chips and the growth of active electrical layers on their surface. In general, the inherent failure mechanisms include ion contamination, gate oxide breakdown, surface charge spreading, and hot electrons [21,39]. These failures often occur due to weaknesses in the manufacturing process or incomplete print design techniques.

Third, external failure mechanism: This failure mechanism generally occurs because of external factors, such as mounting and packaging problems, and the way of connecting with other components in the unit or system environmental effects [39]. Today, due to the growth of knowledge and technology in the design and manufacturing of electronic components, external failures are more important than the inherent failure of the components. Die attachment failure, electron migration, corrosion, radiation, and internal connection failures are among common failure mechanisms of external failure in the electronic components.

Applying an exceeded voltage to the MOSFET as a top subcomponent of the power stage in a circuit is a partial and secondary fault. However, the existence of electrostatics because of high voltage discharge in this element is a partial and primary fault, leading to local melting and the oxide gate's breakdown. Both conditions, i.e., the electrostatic discharge (ESD) and the electrical over stress (EOS), are included in a subset of failures due to electrical stresses. Because of improper processing of the oxide gate or mentioned electrical stresses, differences appear in voltage and current characteristics

of the MOSFET. This defect, comprising an intrinsic failure mechanism and electrical stress, traps electrons at the common interface of the oxide gate, creating improper electrical fields and energizing electrons to enter the oxide, resulting in a threshold voltage shift and short circuit. This failure mechanism steps as an instance on the critical active subcomponent of the power stage as illustrated in Figure 3.

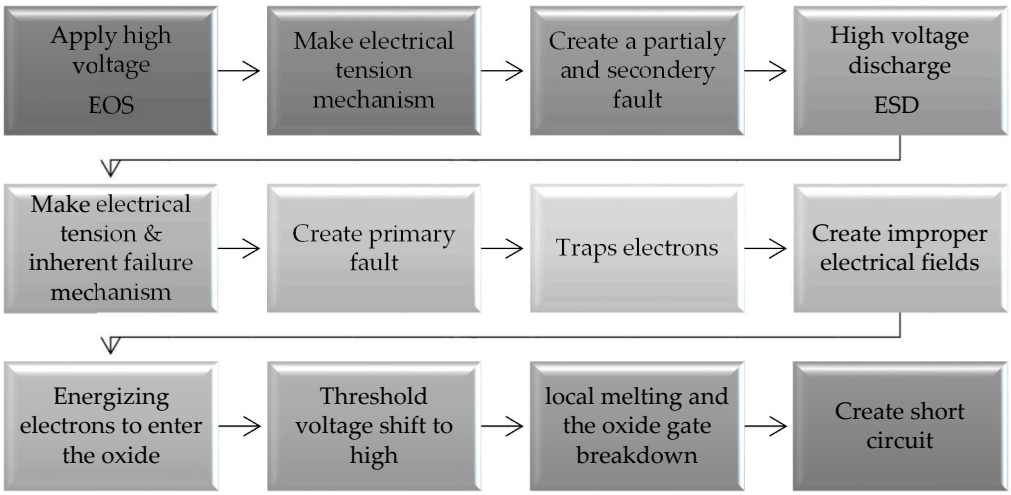

Figure 3. Failure mechanism analysis of the metal oxide semiconductor field effect transistor (MOSFET).

FMEA is an important step in the reliability assessment. The design is the primary objective of the FMEA. Another objective of the FMEA is to identify and classify the potential risk of components [40]. It can support the fault-tolerant plan, testability, security, logistic patronage, and pertaining functions for system FMEAs; the aim is to review the design and predict the damage to the system. Improvements of the test and verification of the plans are other targets of the FMEA [41]. Figure 4 shows the process of an FMEA for the power stage in the PEMFC. This methodology could be applied in the state-of-the-art of the PEMFC industry in order to overcome shortages in identifying the critical failure mechanism for each component. Occurrence (O), Detectability (D), and Severity (S) are used in the FMEA methods as three risk factors. Input parameters of three factors are scored by a four-point scale to classify different failures, depending on the case study [42]. Based on Tables 1–3, scale factors start from one to four shown in the ranking, specified for very low to high risk, respectively. Tables 1–3 show the O, D and S classification respectively [43,44]. Table 4 is the FMEA table with the top functions, failure modes, failure cause, failure mechanism, and mechanism type, as well as risk priority number (RPN) as an initial estimation of risk of subcomponents of the power stage in a PEMFC system [45,46].

By implementation of the FMEA and using the scales for severity (S), occurrence (O), and detection (D) factors and by multiplying these input factors [44], the highest risk priority percentage for each subcomponent of the power stage is recognized, which is demonstrated in the Pareto plot of RPN for each subcomponent for a power stage, as shown in Figure 5. As it can be seen, MOSFET and electrolyte capacitor are the most effective on reliability and lifetime of the power stage with around 50% risk. Furthermore, other subcomponents, like transformer and choke, are in the less priority level for risk analysis; that is why they are not considered in following sections.

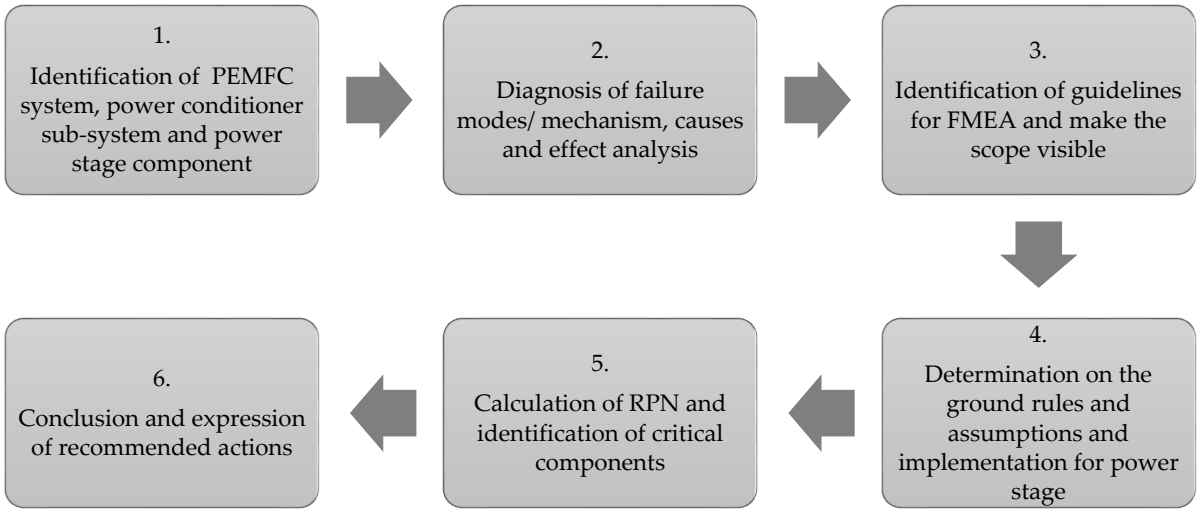

Figure 4. Failure mode and effect analysis (FMEA) process for the power stage in PEMFC.

Table 1. Occurrence (O) rating scale in FMEA analysis.

Ranking	Criteria	Description
1	Very low	Unlikely to occur at all
2	Low	Remote—once in 1 to 10 number
3	Medium	Rare—once in 10 to 100 number
4	High	Occasional—once in 100 to 1000 number

Table 2. Detection (D) rating scale.

Ranking	Criteria	Description
1	High	Detectable with a shutdown
2	Medium	Detectable according to the deviation
3	Low	Detectable by a sensor
4	Very low	Not physically detectable

Table 3. Severity (S) rating scale.

Ranking	Criteria	Description
1	Very low	Negligible changes like temperature
2	Low	Reduction in ability to work
3	Medium	Loss of ability to work
4	High	Major damage to work

Table 4. Failure modes, causes, and mechanisms of power stage components.

#	Sub-Components of Power Stage	Top Function	Top Failure Mode	Top Failure Cause	Top Failure Mechanism	Mechanism Type	S	O	D	RPN
1	**Fuse**	Protecting	Fail to protect	High voltage/ temperature	Over voltage	Electrical tension mechanism/ overstress	2	3	2	12
2	**Electrolytic capacitor**	Filtering and storing	Does not filter and store	High current/ temperature	Leakage and Short/open circuit	Electrical tension mechanism/ overstress	4	2	4	32
3	**Choke**	Smoothing and resist changing	Fail to smooth and resist changing	Manufacturing defect and high temperature	Short/open circuit	Inherent failure mechanism/ wear out	3	3	3	27
4	**Shunt resistor**	Measuring of currents	Fail to measure currents	Manufacturing defect and high temperature	Overvoltage	Inherent failure mechanism/ wear out	3	2	2	12
5	**MOSFET**	Protection and regulation	Fail to switch and regulation	High voltage/current/ temperature	Gate oxide short/breakdown, EOS, ESD	Electrical tension mechanism/ overstress	4	3	4	48
6	**VDR**	Compensating voltage	Does not compensate voltage	Manufacturing defect and high temperature	Overvoltage	Electrical tension mechanism/ overstress	2	2	2	8
7	**Transformer**	Inducting and reinforcing	Does not reinforce	Manufacturing defect and high temperature	Leakage and short/open circuit	Inherent failure mechanism/ wear out	3	3	3	27
8	**Heatsink**	Heat reducing	Does not heat reduce	Manufacturing defect	Thermal damage	External failure mechanism/ overstress	2	1	2	4

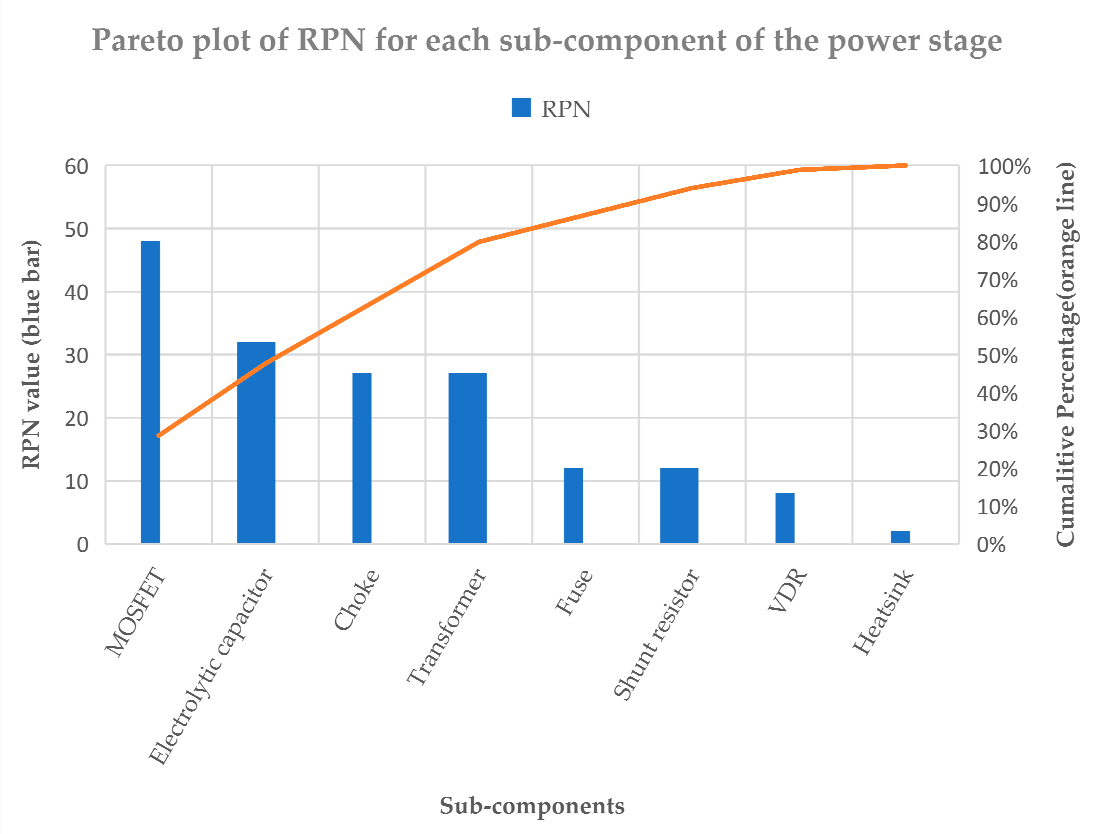

Figure 5. The Pareto plot of risk priority number (RPN) for each subcomponent of the power stage.

4. Fault Tree Analysis

This section is dedicated to introducing failures of the power stage, where the relationship among their subcomponents is delineated by means of the fault tree. The FTA is a deductive method based on the assumption of an unacceptable situation or an event contrary to the main purpose of the system. This unacceptable situation/event is called the "top event". In the analysis of the fault tree, it is required to distinguish a component fault from a system fault that results from more than one component [33,47]. Also, the classification of failures into primary and secondary categories will be advantageous in the estimation of the fault tree. That means primary failures include occurrence under normal/tolerable (designed) system conditions, while secondary failures occur in a component and in a state that the system is not designed, and they are usually caused by inappropriate external conditions [48]. The fault tree of the power stage is shown in Figure 6.

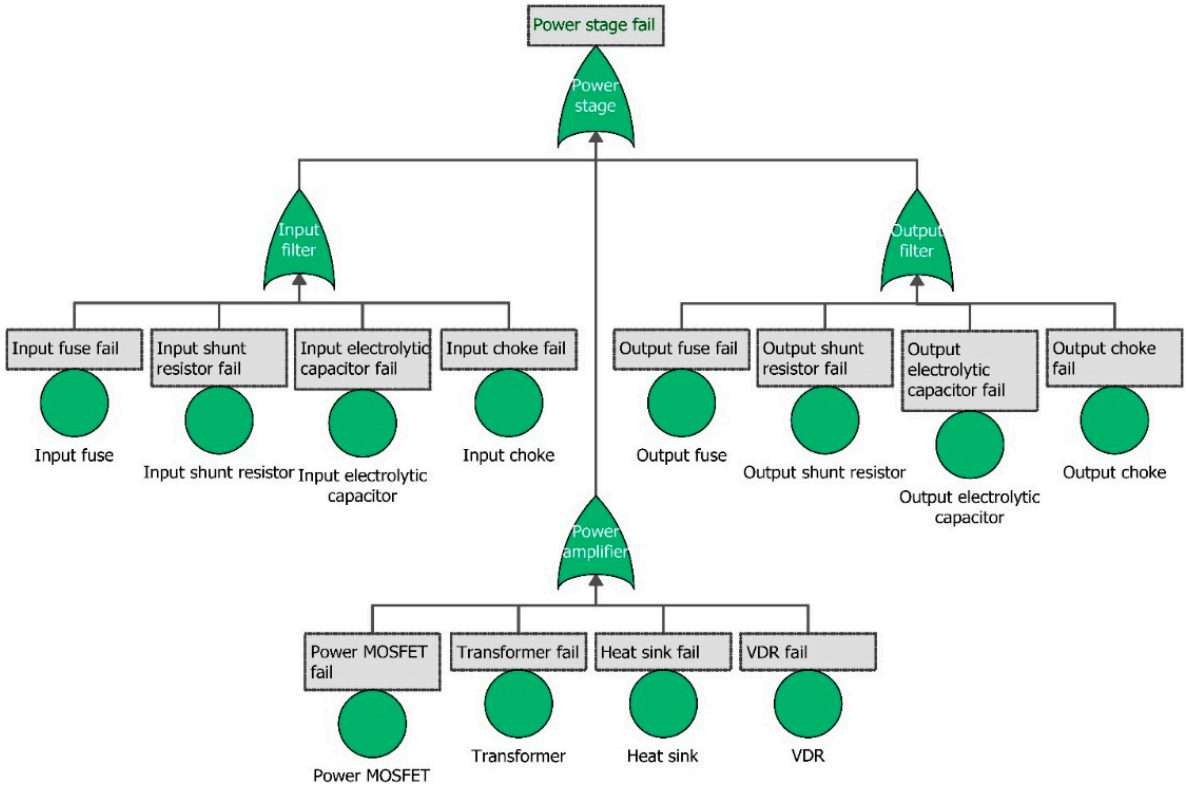

Figure 6. Fault tree of the power stage of PEMFC.

The investigation is performed through the whole reliability conditions and calculates the results for each component by using the probabilistic reliability generic data of the power stage [7,13]. Using MIL-HDBK-217F (Military Handbook: Reliability Prediction of Electronic Equipment), as well as some physics of failure-based and mission profile-based approaches [12], all data are collected for the FTA. Reliability of exponential distribution is given by Equation (1):

$$\mathrm{R(t)} = exp(-\lambda.\mathrm{t}) \tag{1}$$

where, $\mathrm{R(t)}$ is the reliability over time t, and λ is the failure rate. Moreover, reliability of Weibull distribution is given by Equation (2):

$$\mathrm{R(t)} = exp\left[-(\frac{t}{\eta})^{\beta}\right] \tag{2}$$

where, β is the shape parameter, and the scale parameter is η. The shape parameter is also known as the Weibull slope [49,50]. It should be mentioned that by considering β equals 1 in the Weibull distribution, it would be exactly an exponential distribution, which can show the useful life part of the bathtub curve throughout the product lifecycle failure rate, Equation (3).

$$\lambda = \frac{\beta}{\eta}.\left(\frac{t}{\eta}\right)^{\beta-1} \text{ if } \beta = 1 \Longrightarrow \eta = \frac{1}{\lambda} \quad (3)$$

Table 5 illustrates all critical subcomponents of the power stage with their failure rates and Weibull parameters, calculated based on Equation (3).

Table 5. Failure rate and Weibull parameters.

System	Components	Failure Rate (λ)	Weibull Parameters	
			Shape Parameter (β)	Scaling Parameter (η)
Power stage	Fuse	0.02×10^{-6}	1	5.00×10^{7}
	Electrolytic capacitor	0.11×10^{-6}	1	8.33×10^{6}
	Choke	0.16×10^{-9}	1	5.95×10^{9}
	Shunt resistor	0.43×10^{-9}	1	2.31×10^{9}
	MOSFET	0.58×10^{-6}	1	1.91×10^{6}
	VDR	0.43×10^{-9}	1	2.31×10^{9}
	Transformer	0.15×10^{-6}	1	6.51×10^{6}
	Heatsink	0.06×10^{-6}	1	1.66×10^{7}

5. Results and Discussion of Reliability Analysis

The reliability curve in Figure 7 shows the system reliability along with time when the reliability is the probability of the system not failed by time. The reliability is calculated by implementing Monte Carlo simulation with point results every 100 h with start time 1 h and end time five years for 1000 number of simulations of the system using the ReliaSoft BlockSim software package. The reliability curve of the power stage, along with the operating years, is illustrated in Figure 6. It is noted that the B1 lifetime is estimated at 21,300 h (887.5 days) in the case of a shape parameter one ($\beta = 1$) for all of components shown in Table 2, which is illustrated with the blue color. However, reliability curve with the red color shows B1 at 40,900 h (1704 days) because it has different shape parameters estimated just for MOSFET and electrolytic capacitor; their shape parameter values are taken from [7], 2.59 and 1.93, respectively. Hence, scaling parameters are estimated 1.61×10^6 for the MOSFET and 2.18×10^6 for the electrolytic capacitor. In fact, this figure clearly illustrates more realization in comparison with not considering Weibull distribution for reliability analysis. In other words, the obtained reliability curve of the system from the Weibull data is very close to the reality experienced in the system.

Consequently, failure analysis shows that two subcomponents of the power stage, which contains MOSFET as an active component and electrolytic capacitor as a passive component, have the most effect on the changes of the reliability as well as the critical failure and hidden damages to the circuit of the system as discussed and demonstrated before in the Pareto plot (Figure 5) from risk analysis of each subcomponent of the power stage based on the FMEA technique. By inserting the Weibull parameter (blue curve) for these two components in the reliability analysis, the results are more reasonable rather than exponential distribution (red one).

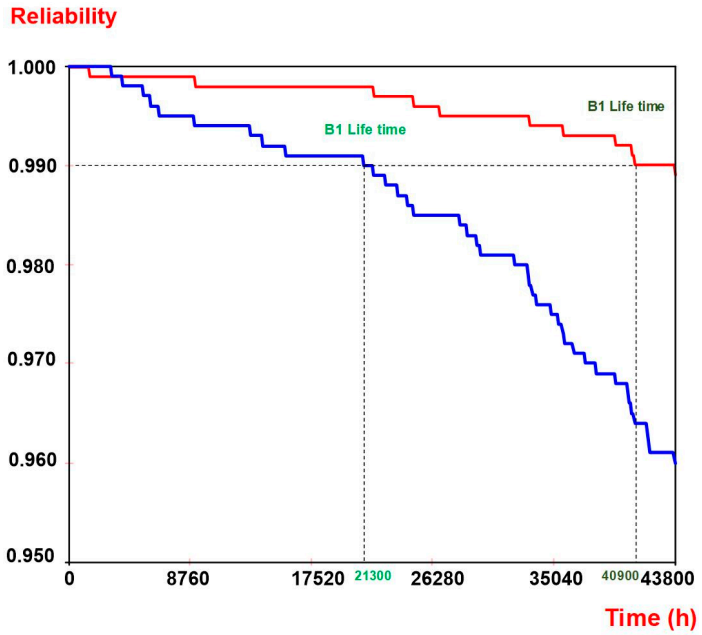

Figure 7. Reliability curve of power stage along with the operating hours (blue, Weibull distribution; red, exponential distribution).

The results of the proposed methodology are comparable and complementary with the results of other methodologies. For example, considering the critical power electronic components, the annual accumulated damage is estimated, due to the real mission profile of the fuel cell system. Then, the Monte Carlo analysis is applied to obtain the Weibull distribution of the power semiconductors lifetime. The presented reliability estimation and findings using FMEA and FTA by assuming Weibull distributions have their pros and cons. For instance, it is more detailed, focusing on subcomponents, components, and system; on the other hand it is more understandable, simple, easy, and faster.

6. Conclusions

This paper has presented a failure mechanism analysis of the power stage components in a hybrid wind-fuel cell system by using the FMEA and the FTA. The FMEA identified and analyzed the failure mechanism of power stage components for selected critical subcomponents, which their failures may have significant effects on the system reliability. Some of the failure modes of an active subcomponent such as MOSFET are switching losses, conduction losses, improper pieces selection, failure to operate as designed, voltage and current fluctuations, fractured, overloading, shock failure, and contact damage. Moreover, some of the failure modes of passive subcomponent like electrolyte capacitors are: Non-amplification, improper pieces selection, failure to function as intended for any piece, voltage, and current fluctuations, breakage, electric current, improper assembly, inadequate support (structural), fractured, loosened, open-circuited, overloading, oxidized, shock failure, short-circuited, contact damage, swells, thinning, distortion, and vibration. Furthermore, the FTA is constructed by considering the results of the FMEA with three significant parts: Input filter, power amplifier, and output filter. The reliability curve of the power stage can be estimated in five years, which is consistent with the defined guarantee period. It is concluded that the B1 lifetime of the power stage is 2.4 years for the same shape parameter (assumed exponential distribution) and 4.7 years for different shape parameters (assumed Weibull distribution), which is closer to real experience. It is recommended to use Weibull distribution for reliability analysis rather than exponential distribution as it leads to more realistic results. Since the Weibull parameters are not usually available for all components or difficult to obtain by reliability tests, FMEA is recommended to distinguish the high-risk components and consequently to find their Weibull parameters for reliability analysis.

Author Contributions: The main idea for the paper was proposed by S.R. S.R. wrote the first draft of the paper, except Section 2, which was drafted by S.B. S.R. and S.B. developed the methodology. S.R. and S.B. post-processed the results. A.S.B., J.D.S., and F.B., supervised the findings of this work and reviewed methodology. All authors contributed for articulating the research work in its current form as a full research manuscript.

Funding: The research leading to these results has been partly conducted under the INFRASTAR (infrastar.eu) project in the field of reliability approaches for decision making for wind turbines and bridges, which has received funding from the European Union's Horizon 2020 research and innovation program under the Marie Skłodowska-Curie grant agreement No 676139. The grant is gratefully acknowledged.

Conflicts of Interest: The authors declare no conflict of interest.

References

1. Khan, F.I.; Hawboldt, K.; Iqbal, M.T. Life Cycle Analysis of wind-fuel cell integrated system. *Renew. Energy* **2005**, *30*, 157–177. [CrossRef]
2. Eroglu, M.; Dursun, E.; Sevencan, S.; Song, J.; Yazici, S.; Kilic, O. A mobile renewable house using PV/wind/fuel cell hybrid power system. *Int. J. Hydrogen Energy* **2011**, *36*, 7985–7992. [CrossRef]
3. Cetin, E.; Yilanci, A.; Ozturk, H.K.; Colak, M.; Kasikci, I.; Iplikci, S. A micro-DC power distribution system for a residential application energized by photovoltaic-wind/fuel cell hybrid energy systems. *Energy Build.* **2010**, *42*, 1344–1352. [CrossRef]
4. Iqbal, M.T. Modeling and control of a wind fuel cell hybrid energy system. *Renew. Energy* **2003**, *28*, 223–237. [CrossRef]
5. Haddad, A.; Ramadan, M.; Khaled, M.; Ramadan, H.S.; Becherif, M. Triple hybrid system coupling fuel cell with wind turbine and thermal solar system. *Int. J. Hydrogen Energy* **2019**. [CrossRef]
6. Onar, O.C.; Uzunoglu, M.; Alam, M.S. Dynamic modeling, design and simulation of a wind/fuel cell/ultra-capacitor-based hybrid power generation system. *J. Power Sources* **2006**, *161*, 707–722. [CrossRef]
7. Khan, M.J.; Iqbal, M.T. Dynamic modeling and simulation of a small wind-fuel cell hybrid energy system. *Renew. Energy* **2005**, *30*, 421–439. [CrossRef]
8. Fathabadi, H. Novel standalone hybrid solar/wind/fuel cell/battery power generation system. *Energy* **2017**, *140*, 454–465. [CrossRef]
9. Beuscher, U.; Cleghorn, S.J.C.; Johnson, W.B. Challenges for PEM fuel cell membranes. *Int. J. Energy Res.* **2005**, *29*, 1103–1112. [CrossRef]
10. Zhang, J. *PEM Fuel Cell Electrocatalysts and Catalyst Layers: Fundamentals and Applications*; Springer Science & Business Media: Berlin/Heidelberg, Germany, 2008; ISBN 9781848009356.
11. Bahrebar, S.; Blaabjerg, F.; Wang, H.; Vafamand, N.; Khooban, M.-H.; Rastayesh, S.; Zhou, D. A Novel Type-2 Fuzzy Logic for Improved Risk Analysis of Proton Exchange Membrane Fuel Cells in Marine Power Systems Application. *Energies* **2018**, *11*, 721. [CrossRef]
12. Zhou, D.; Wang, H.; Blaabjerg, F. Mission Profile Based System-Level Reliability Analysis of DC/DC Converters for a Backup Power Application. *IEEE Trans. Power Electron.* **2018**, *33*, 8030–8039. [CrossRef]
13. Zhou, D.; Wang, H.; Blaabjerg, F.; Kor, S.K.; Blom-Hansen, D. System-level reliability assessment of power stage in fuel cell application. In Proceedings of the 2016 IEEE Energy Conversion Congress and Exposition (ECCE), Milwaukee, WI, USA, 18–22 September 2016; pp. 1–8.
14. Bahrebar, S.; Zhou, D.; Rastayesh, S.; Wang, H.; Blaabjerg, F. Reliability assessment of power conditioner considering maintenance in a PEM fuel cell system. *Microelectron. Reliab.* **2018**, *88–90*, 1177–1182. [CrossRef]
15. Bahrebar, S.; Blaabjerg, F.; Wang, H.; Zhou, D.; Rastayesh, S. System-level Risk Analysis of PEM Fuel Cell Using Failure Mode and Effect Analysis. In Proceedings of the IRSEC 2018, 5th International Reliability and Safety Engineering Conference, Shiraz, Iran, 9–10 May 2018.
16. Soliman, H.; Wang, H.; Blaabjerg, F. A Review of the Condition Monitoring of Capacitors in Power Electronic Converters. *IEEE Trans. Ind. Appl.* **2016**, *52*, 4976–4989. [CrossRef]
17. Wang, H.; Blaabjerg, F. Reliability of Capacitors for DC-Link Applications in Power Electronic Converters—An Overview. *IEEE Trans. Ind. Appl.* **2014**, *50*, 3569–3578. [CrossRef]
18. Huai, W.; Liserre, M.; Blaabjerg, F.; De Place Rimmen, P.; Jacobsen, J.B.; Kvisgaard, T.; Landkildehus, J. Transitioning to physics-of-failure as a reliability driver in power electronics. *IEEE J. Emerg. Sel. Top. Power Electron.* **2014**, *2*, 97–114.

19. Bahman, A.S.; Jensen, S.M.; Iannuzzo, F. Failure mechanism analysis of fuses subjected to manufacturing and operational thermal stresses. *Microelectron. Reliab.* **2018**, *88–90*, 304–308. [CrossRef]
20. Rahimi, T.; Jahan, H.; Blaabjerg, F.; Bahman, A.; Hosseini, S. Fuzzy-Logic-Based Mean Time to Failure (MTTF) Analysis of Interleaved Dc-Dc Converters Equipped with Redundant-Switch Configuration. *Appl. Sci.* **2018**, *9*, 88. [CrossRef]
21. Modarres, M.; Kaminskiy, M.; Krivtsov, V. *Reliability Engineering and Risk Analysis: A Practical Guide*, 3rd ed.; CRC Press: Boca Raton, FL, USA, 2010.
22. Pang, H.; Yu, T.; Song, B. Failure mechanism analysis and reliability assessment of an aircraft slat. *Eng. Fail. Anal.* **2016**, *60*, 261–279. [CrossRef]
23. Pandey, A.; Singh, M.; Sonawane, A.U.; Rawat, P.S. FMEA Based Risk Assessment of Component Failure Modes in Industrial Radiography. *Int. J. Eng. Trends Technol.* **2016**, *39*, 216–225. [CrossRef]
24. Krishnan, K.J.; Kalam, A.; Zayegh, A. Experimental investigation of H2 generator and PEM fuel cell as a remote area back-up power. In *Proceedings of the Procedia Engineering*; Elsevier Ltd.: Amsterdam, The Netherlands, 2012; Volume 49, pp. 66–73.
25. Wang, Y.; Liu, H.; Lu, C.; Zhou, B. PEM fuel cell health state assessment using a geometrical approach and mahalanobis distance. In Proceedings of the Proceedings of the World Congress on Intelligent Control and Automation (WCICA), Guilin, China, 12–15 June 2016; pp. 1312–1316.
26. Lee, S.; Zhou, D.; Wang, H. Reliablity assessment of fuel cell system—A framework for quantitative approach. In Proceedings of the ECCE 2016—IEEE Energy Conversion Congress and Exposition, Milwaukee, WI, USA, 18–22 September 2016.
27. Rabbani, A.; Rokni, M. Dynamic characteristics of an automotive fuel cell system for transitory load changes. *Sustain. Energy Technol. Assess.* **2013**, *1*, 34–43. [CrossRef]
28. Javed, K.; Gouriveau, R.; Zerhouni, N.; Hissel, D. Improving accuracy of long-term prognostics of PEMFC stack to estimate remaining useful life. In Proceedings of the IEEE International Conference on Industrial Technology, Seville, Spain, 17–19 March 2015; pp. 1047–1052.
29. Whiteley, M.; Fly, A.; Leigh, J.; Dunnett, S.; Jackson, L. Advanced reliability analysis of Polymer Electrolyte Membrane Fuel Cells using Petri-Net analysis and fuel cell modelling techniques. *Int. J. Hydrogen Energy* **2015**, *40*, 11550–11558. [CrossRef]
30. Arabian-Hoseynabadi, H.; Oraee, H.; Tavner, P.J. Failure Modes and Effects Analysis (FMEA) for wind turbines. *Int. J. Electr. Power Energy Syst.* **2010**, *32*, 817–824. [CrossRef]
31. Vesely, W.E.; Goldberg, F.F. *Fault Tree Handbook*, 16th ed.; U.S. Government Printing Office: Washington, DC, USA, 1981.
32. Whiteley, M.; Dunnett, S.; Jackson, L. Failure Mode and Effect Analysis, and Fault Tree Analysis of Polymer Electrolyte Membrane Fuel Cells. *Int. J. Hydrogen Energy* **2016**, *41*, 1187–1202. [CrossRef]
33. Collong, S.; Kouta, R. Fault tree analysis of proton exchange membrane fuel cell system safety. *Int. J. Hydrogen Energy* **2015**, *40*, 8248–8260. [CrossRef]
34. Pourramazan, A.; Saffari, S.; Barghandan, A. Study of Failure Mode and Effect Analysis (FMEA) on Capacitor Bank Used in Distribution Power Systems. *Ijireeice* **2017**, *5*, 113–118.
35. Larrucea, X.; Belmonte, F.; Welc, A.; Xie, T. Reliability Engineering. *IEEE Softw.* **2017**, *34*, 26–29. [CrossRef]
36. Mathew, S.; Alam, M.; Pecht, M. Identification of failure mechanisms to enhance prognostic outcomes. *J. Fail. Anal. Prev.* **2012**, *12*, 66–73. [CrossRef]
37. Young, A.L.; Hilmas, G.E.; Zhang, S.C.; Schwartz, R.W. Mechanical vs. electrical failure mechanisms in high voltage, high energy density multilayer ceramic capacitors. *J. Mater. Sci.* **2007**, *42*, 5613–5619. [CrossRef]
38. Toh, S.L.; Tan, P.K.; Goh, Y.W.; Hendarto, E.; Cai, J.L.; Tan, H.; Wang, Q.F.; Deng, Q.; Lam, J.; Hsia, L.C.; et al. In-Depth Electrical Analysis to Reveal the Failure Mechanisms With Nanoprobing. *IEEE Trans. Device Mater. Reliab.* **2008**, *8*, 387–393. [CrossRef]
39. Modarres, M. *Risk Analysis in Engineering: Techniques, Tools, and Trends*; CRC Press: Boca Raton, FL, USA, 2006.
40. Feili, H.R.; Akar, N.; Lotfizadeh, H.; Bairampour, M.; Nasiri, S. Risk analysis of geothermal power plants using Failure Modes and Effects Analysis (FMEA) technique. *Energy Convers. Manag.* **2013**, *72*, 69–76. [CrossRef]
41. Jensen, F.; Morris, A.S.; Levin, M.A.; Kalal, T.T.; Pascoe, N.; Carlson, C. *Effective FMEAs*; Wiely: Hoboken, NJ, USA, 2012.

42. Berg, F.; Logistics, I.; Komenského, P. FMEA (failure mode and effects analysis) and proposal of risk minimizing in storage processes for automotive. *Acta Logist.* **2016**, *3*, 15–18.
43. Rafie, M.; Namin, F.S. Prediction of subsidence risk by FMEA using artificial neural network and fuzzy inference system. *Int. J. Min. Sci. Technol.* **2015**, *25*, 655–663. [CrossRef]
44. van Leeuwen, J.F.; Nauta, M.J.; de Kaste, D.; Odekerken-Rombouts, Y.M.C.F.; Oldenhof, M.T.; Vredenbregt, M.J.; Barends, D.M. Risk analysis by FMEA as an element of analytical validation. *J. Pharm. Biomed. Anal.* **2009**, *50*, 1085–1087. [CrossRef] [PubMed]
45. Wu, R.; Blaabjerg, F.; Wang, H.; Liserre, M. Overview of catastrophic failures of freewheeling diodes in power electronic circuits. *Microelectron. Reliab.* **2013**, *53*, 1788–1792. [CrossRef]
46. Shafiee, M.; Dinmohammadi, F. An FMEA-based risk assessment approach for wind turbine systems: A comparative study of onshore and offshore. *Energies* **2014**, *7*, 619–642. [CrossRef]
47. Placca, L.; Kouta, R. Fault tree analysis for PEM fuel cell degradation process modelling. *Int. J. Hydrogen Energy* **2011**, *36*, 12393–12405. [CrossRef]
48. Rastayesh, S.; Bahrebar, S. Importance Analysis of a Typical Diesel Generator Using Dynamic Fault Tree. *Int. J. Curr. Life Sci.* **2014**, *4*, 697–700.
49. Rastayesh, S.; Bahrebar, S.; Sepanloo, K. Time Dependent Reliability Of Emrgency Diesel Generator Station. *Indian J. Sci. Res.* **2014**, *1*, 453–460.
50. Bahrebar, S.; Rastayesh, S.; Sepanloo, K. Dynamic Availability Assessment on Tehran Research Reactor Water Cooling System. *Indian J. Sci.Res.* **2014**, *1*, 471–474.

Paper 5:

Title:

A System Engineering Approach Using FMEA and Bayesian Network for Risk Analysis—A Case Study

Authors:

Sima Rastayesh, Sajjad Bahrebar, Frede Blaabjerg, Dao Zhou, Huai Wang and John Dalsgaard Sørensen

Published in:

Sustainability 2020, 12, 77; doi:10.3390/su12010077

sustainability

MDPI

Article

A System Engineering Approach Using FMEA and Bayesian Network for Risk Analysis—A Case Study

Sima Rastayesh [1,*], Sajjad Bahrebar [2], Frede Blaabjerg [3], Dao Zhou [3], Huai Wang [3] and John Dalsgaard Sørensen [1]

1 Department of Civil Engineering, Aalborg University, 9000 Aalborg, Denmark; jds@civil.aau.dk
2 Department of Mechanical Engineering, Technical University of Denmark, 2800 Kongens Lyngby, Denmark; sajbahr@mek.dtu.dk
3 Department of Energy Technology, Aalborg University, 9000 Aalborg, Denmark; fbl@et.aau.dk (F.B.); zda@et.aau.dk (D.Z.); hwa@et.aau.dk (H.W.)
* Correspondence: sir@civil.aau.dk

Received: 24 November 2019; Accepted: 17 December 2019; Published: 20 December 2019

Abstract: This paper uses a system engineering approach based on the Failure Mode and Effect Analysis (FMEA) methodology to do risk analysis of the power conditioner of a Proton Exchange Membrane Fuel Cell (PEMFC). Critical components with high risk, common cause failures and effects are identified for the power conditioner system as one of the crucial parts of the PEMFCs used for backup power applications in the telecommunication industry. The results of this paper indicate that the highest risk corresponds to three failure modes including high leakage current due to the substrate interface of the metal oxide semiconductor field effect transistor (MOSFET), current and electrolytic evaporation of capacitor, and thereby short circuit, loss of gate control, and increased leakage current due to gate oxide of the MOSFET. The MOSFETs, capacitors, chokes, and transformers are critical components of the power stage, which should be carefully considered in the development of the design production and implementation stage. Finally, Bayesian networks (BNs) are used to identify the most critical failure causes in the MOSFET and capacitor as they are classified from the FMEA as key items based on their Risk Priority Numbers (RPNs). As a result of BNs analyses, high temperature and overvoltage are distinguished as the most crucial failure causes. Consequently, it is recommended for designers to pay more attention to the design of MOSFETs' failure due to high leakage current owing to substrate interface, which is caused by high temperature. The results are emphasizing design improvement in the material in order to be more resistant from high temperature.

Keywords: bayesian network; failure mode and effect analysis; proton exchange membrane fuel cell; power conditioner; risk analysis

1. Introduction

Global climate changes caused by conventional energy resources such as fossil fuels are one of the dominant motivations that engineers are trying to employ renewable energies. Also, fossil fuel resources are limited, and they will eventually be depleted with the rapid growth of energy consumption. The environmental damages in the world caused by non-renewable energies ends up to be approximately five trillion dollars per year [1]. Renewable energies, such as wind turbines, solar cells and fuel cell systems are proposed as solutions to solve these global problems. A fuel cell works as a source generating energy along with unique properties, which are being developed rapidly. In the global sustainable development perspective, fuel cells are suitable as they provide high energy conversion efficiency, various usages being a compact and environmental friendliness system. These are the foremost reason that fuel cell systems are used in energy systems; that is why they are

considered as one of the main sources of energy. The first fuel cell was demonstrated by a Welsh scientist and barrister William Grove in 1839. One type of fuel cells was improved by General Electric in the beginning of 1960s [2] which was the Proton-Exchange Membrane Fuel Cells (PEMFC) which are a kind of fuel cells, which are being developed mainly for transportation and portable applications and even in hybrid energy systems such as wind-fuel cell systems. High energy efficiency, less pollution, and high reliability are significant properties of the PEMFC systems [3]. The telecommunication industry has applied fuel cell systems for backup power [4]. Under this circumstance, availability and reliability, as well as risk, are important issues, which should be assessed carefully for them. PEMFC technology has been developed to overcome the instability and environmental concerns compared with conventional energy sources since the 1990s. Fuel cells are relatively expensive, having a higher cost, one ought to identify the high risk components to spend more money on their design to minimize the cost of failures. Failure Mode and Effect Analysis (FMEA), an organized technique for failure analysis, is applied to identify critical failure modes, failure causes, and effects of the items of interest, which can be applied for power electronics.

The risk is a measure of the potential expected loss occurring due to natural or non-natural activities [5]. Risk analysis has two facets: Quantitative and qualitative. In order to assess probabilities to make decisions, the quantitative risk analysis endeavor to estimate the risk in the form of probability (frequency) of a loss. Quantitative risk analysis is frequently a preferred approach when adequate field data, test data, and other evidence are available to estimate the likelihood and magnitude of the losses [6–9]. Qualitative risk analysis is the most widely used since it is quick and straightforward to perform. For this type, the potential loss is qualitatively estimated using linguistic scales such as low, medium, and high. Since this type of analysis barely needs to rely on actual data and its probabilistic treatment, the analysis is much simpler and easier to use and understand; however, it may be rather subjective [10].

FMEA is a structured and logical methodology for identifying, analyzing and ranking estimated risk having various potential failure modes. Furthermore, it is suggested to improve the methodology; for instance, changes in the design or control tests, which can assist engineers to prevent the failure or reduce its effects [11]. FMEA is a vital reliability tool to identify critical failure modes, failure causes, and failure mechanisms that can be used to diagnose probable failure and dissatisfactions of functions for any items in a system before they occur, aiming to reduce their risks [12].

The FMEA method is based on discovering, arranging, and decreasing the failures or faults; moreover, it has been used in multiple kinds of industry [13]. For instance, FMEA can be used for energy production systems such as wind turbines consisting of a complex system of electrical, mechanical and structural components [14]. Three risk factors, including Occurrence (O), Detectability (D), and Severity (S) are used in the FMEA. O designates the rate of the risks, D point to the likelihood of risks prediction earlier than their occurrence, and S is the significance of the risk to the system. The yield factor indicated as the Risk Priority Number (RPN) is the creation of the three input parameters grade the failure state which are scored by a 10-point scale. As a matter of fact, RPN is a quantitative and qualitative risk analysis in the form of numerical ranking of risk of each potential failure mode. It is constitued of the product of the three qualitative factors, S of the effect, likelihood of O of the cause, and likelihood of D of the cause in the robustness method [15]. Many standards are used to classify different faults, which occur in the PEMFC. In this paper, scales are extracted from the Automotive Industry Action Group (AIAG). Afterwards, by multiplying these input factors, their corresponding RPNs are recognized [16].

The reliability and availability of the PEMFC system, especially power conditioner, are vital in the condition of power grid outage used in the telecommunication stations backup power. Owing to that factor, risk assessment and failure effect analysis of the critical components are mandatory. There are several research studies available, which perform the FMEA for fuel cell systems with the emphasis on the fuel cell stack [17]. However, the means to implement the FMEA is not given or provided; thus, it is not given how this procedure is implemented by using either brain-storming or a system engineering

approach. In this paper, two aspects are combined to fulfill the gap in the existing literature. First, instead of focusing on the fuel cell stack, the power conditioner is comprehensively investigated, which are studied in terms of the critical power electronics components. Second, the FMEA is implemented based on system engineering approach having the given detailed implementation procedure.

Furthermore, Bayesian Network (BN) is utilized to analyze the most critical failure causes among more important items identified from FMEA. BN is a graphical model that containing nodes, symbolizing variables, and directed links between them standing for casual relationships. The relationships between variables are as if X causes Y, X is a parent of Y, and Y is a child of X. The probabilities are given as conditional probability distributions for each node, depending on the parents. When evidence is received for a node, the joint distribution can be updated using Bayes rule, and posterior marginal distributions can be found [18]. This will help designers to pay more attention on the development of the design for instance, material properties to avoid failures from obtained results by this method. For example, anion-deficient perovskites, as materials with high ionic conductivity and a wide range of temperature stability, are very suitable for fuel cell membranes [19]. Moreover, magneto dielectrics such as hexaferrites: are the materials that are promising for the production of capacitors, which are very necessary for their stable operation [20]. For the stable and steady operation of modern power plants and uninterruptible power systems, it is necessary to provide for their protection against unwanted external electromagnetic radiation. Such an electromagnetic effect can easily cause the collapse of the entire modern energy system. To prevent this, electromagnetic shields must be used [21,22].

To sum up, by using the FMEA for the PEMFC system, potential failure modes and risk of components are identified, and critical components are also classified. Furthermore, the potential of the risk priority number is assigned to any failure. The FMEA results offer which component is critical to have high RPNs. Moreover, some recommended solutions are suggested to create better conditions to reduce their risk. Therefore, damage to the entire system due to failure modes and causes is decreased. Finally, by implementing BN the impact of each failure cause is studied, to find which failure causes have the most effects among other failure causes in the MOSFET.

2. Description of PEMFC and Power Conditioner

2.1. PEMFC System

A PEMFC is an electrochemical system, which changes the chemical energy through the reaction of hydrogen and oxygen to electrical power. There are a variety of PEMFC applications such as mobile power generation systems and stations, automotive, aerospace and marine industries [23].

A typical configuration of the PEMFC system is shown in Figure 1, which consists of the Balance of Plant (BoP), the PEMFC stack, and the power conditioner. [7,8]. The BoP is a monitoring system having auxiliary parts, which serve to regulate the supply and balance hydrogen, air, water and thermal condition for the PEMFC stack. The PEMFC stack is an assembly of several single cells (output less than 1 V), bipolar plates, cooling plates, end plates, bolts, and gaskets, which converts the chemical energy into the electricity [23]. A power conditioner is composed of active and passive electrical components, enabling to regulate the fixed output from the PEMFC stack [24].

2.2. Power Conditioner Sub-System

This section presents the detailed configuration of the power conditioner sub-system for a PEMFC system in a backup power application. The block diagram of the power conditioner sub-system having 1 kW output power is shown in Figure 2, where five parts, are included which are the power stage, auxiliary power supply, gate driver, controller, and PCB, which can be further sub-divided [25]. The power stage consists of an isolated DC/DC converter. This part contains plenty of components (such as MOSFETs, capacitors, inductors, transformer, and other related components). The input voltage range is 30–65 V, while the output voltage is 48 V. As a result, a power converter that can work both in step-up

and step-down modes is preferred. Moreover, the isolation from primary-side and secondary-side is required according to the industry standard. Some of the functions of the subsystems are switching the electrical current at the desired time interval, rectifying current in the desired time interval and control, regulating and rectifying the electrical current and voltage level change.

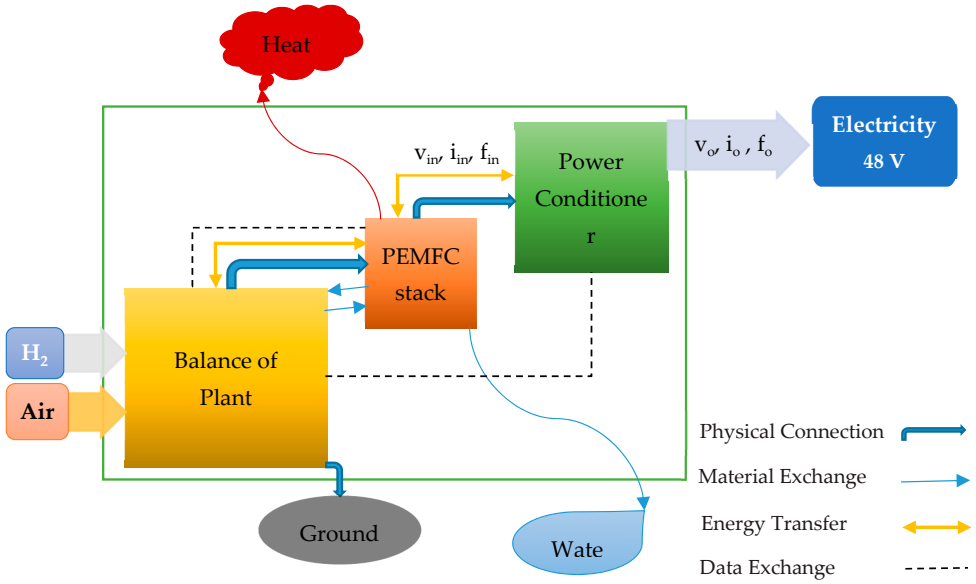

Figure 1. Block diagram of a typical PEMFC system used in a backup power application.

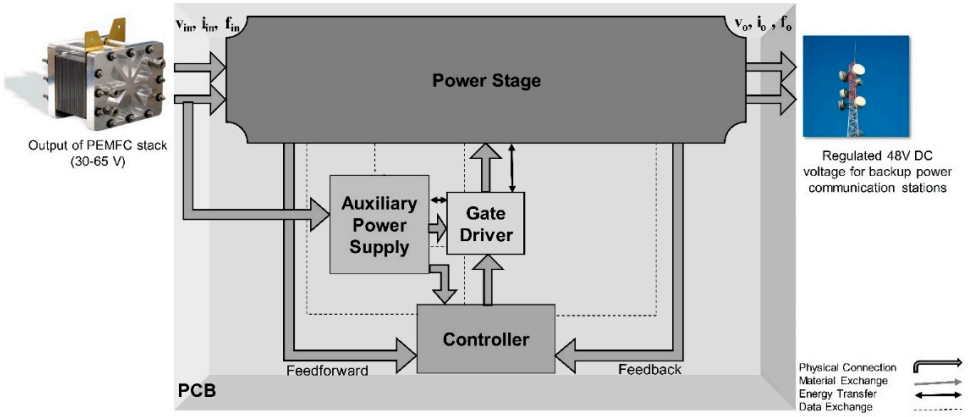

Figure 2. Block diagram of power conditioner (DC/DC converter).

In the power stage, eight primary and eight secondary MOSFETs are used as active switches having the function to control the electrical current in the system. Also, eight primaries and eight secondary diodes are applied in the converter. Moreover, two transformers are used to provide isolation between primary and secondary side. Besides, here are eight electrolytic capacitors having a capacity of 680 µF and 63 V in the primary and six electrolytic capacitors having the capacity of 390 µF and 100 V in the secondary side as a storage for the electrical energy and stabilization of the dc voltage. The overall objective of the power conditioner is that in the case of a step-up mode, the primary-side inductor is charged by the activation of all transistors; while it is discharged by the parallel connection of the two transformers. Alternatively, in the case of the step-down mode, the primary-side inductor is charged by the parallel connection of the transformers, while it is discharged by the series connection of the transformers [26]. The structure of the power converter used in this study is presented in Figure 3. Due to the variable output voltage of the fuel cell stack, a dc/dc power converter is required to match the voltage in telecom applications. A topology using galvanic isolation is shown in Figure 3, where

the rated power of the converter is 1 kW, and six 1 kW converters are connected in parallel for a 5 kW power stage to obtain the redundancy. Moreover, a synchronous rectification is adopted to achieve low conduction losses in the situation of low-voltage and high-current at the secondary-side of the transformer [26]. All the components in the power conditioner can be categorized of four levels of the PEMFC system as it is demonstrated in Figure 4.

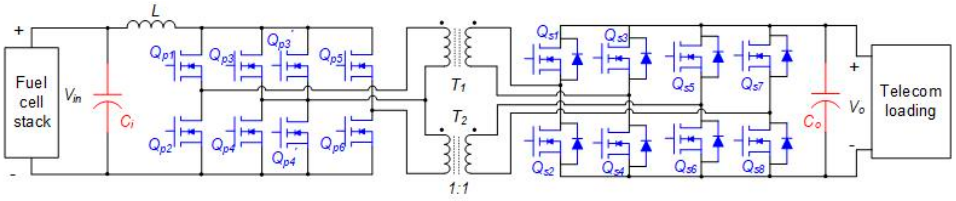

Figure 3. Structure of the power converter [26].

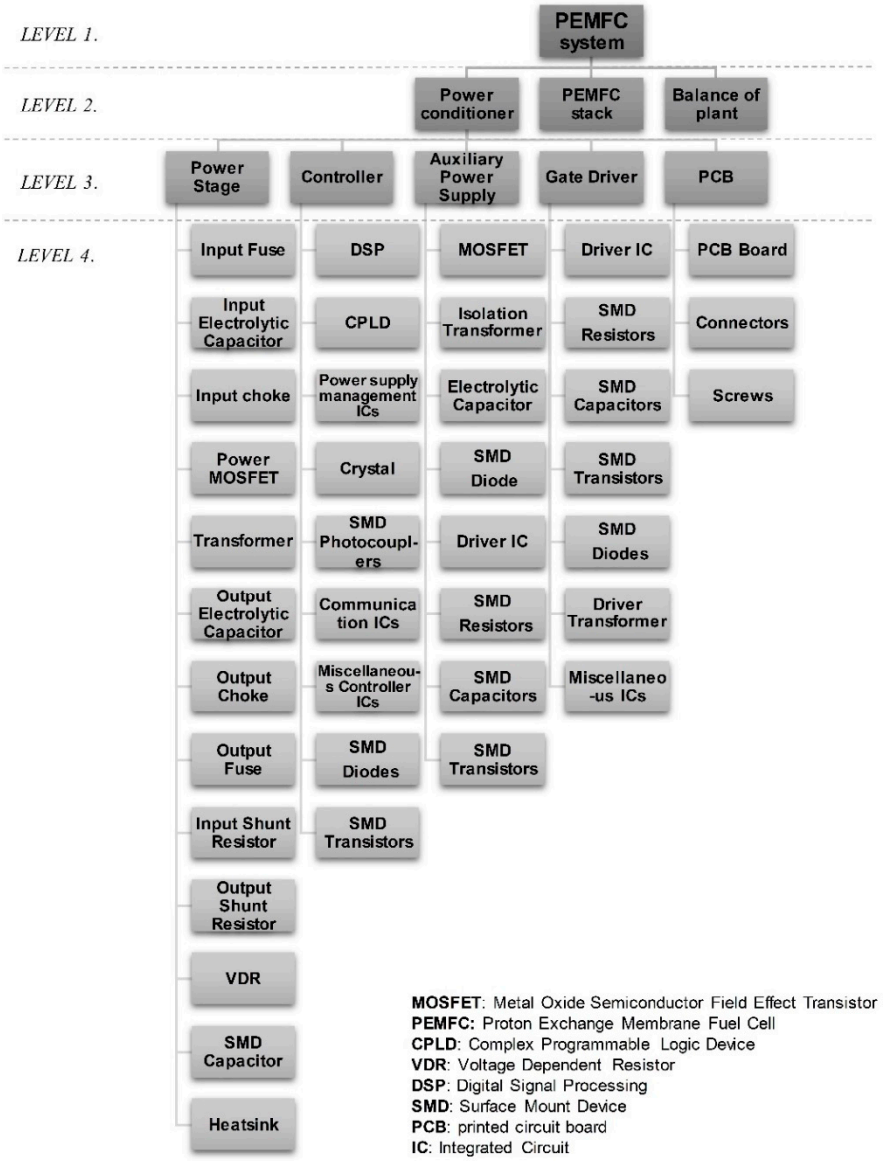

Figure 4. Four levels of PEMFC system along with all the main components and sub-components in the power conditioner.

3. System Engineering Approach Based FMEA of Power Conditioner

3.1. Boundary Diagram and FMEA Interface Matrix

In order to make a visible scope of the FMEA analysis, an FMEA block diagram (FMEA boundary diagram) is used to visualize the interfaces between the various sub-systems and components. The boundary diagram shows the physical and logical relationships among the main sub-systems of the PEMFC system, such as physical connection, material exchange, energy transfer, and data exchange. Besides, their inputs and outputs are also identified [3] (Figures 1 and 2 illustrate an overview of boundary diagram for the PEMFC system and the power conditioner sub-system). Moreover, the FMEA interface matrix is a chart on the vertical and horizontal axes interfaces, which ought to be considered in the examination of this kind of interface. As aforementioned, the physical connection, material exchange, energy transfer, and data exchange are four primary types of interfaces. Up to 50% or more of the total failures are normally seem in the interfaces. As a result, it is important that any FMEA considerately study the interfaces between the sub-systems and components besides their content. On top of the FMEA boundary diagram, as a complementary to it, the FMEA interface matrix is presented. The FMEA interface matrix for the PEMFC system is listed in Table 1 in connection with Figure 1; and the FMEA interface matrix for the power conditioner is listed in Table 2 and is related to Figure 2.

Table 1. FMEA interface matrix for three main systems of PEMFC.

PEMFC	Balance of Plant	PEMFC Stack	Power Conditioner
Balance of plant		PMED1	
PEMFC stack	PMED1		PE1
Power conditioner		PE1	

Interface Type: Physical (P), Material Exchange (M), Energy Transfer (E), Data Exchange (D); **Functional Necessity:** Must be present (1), Must not be present (2).

Table 2. FMEA interface matrix for the power conditioner.

Power Conditioner	Auxiliary Power Supply	Power Stage	Controller	Gate Driver	PCB
Auxiliary Power Supply		PED1	PD1	PED1	P1
Power Stage	PED1			PED1	P1
Controller	PD1			PD1	P1
Gate Driver	PED1	PED1	PD1		P1
PCB	P1	P1	P1	P1	

3.2. Function Block Diagram and Parameter Diagram

Another visual tool to describe the operation, interrelationships and interdependencies of the system functions is Function Block Diagram (FBD). Moreover, the Parameter diagram (P-diagram) is a functional tool to document input signals, noise factors, control factors, error states, and ideal response. It is more practical once the item under analysis is a complicated system where it is a time-consuming analysis; however, it can provide significant value in comprehending and controlling the system and recognizing the input to the FMEA techniques. Any of these tools are used for better detection of the FMEA of the four levels of classifications of the PEMFC system [27]. FBD of the PEMFC system is shown in Figure 5. Furthermore, the P–Diagram (PD) of the PEMFC is illustrated in Figure 6, which takes the inputs from a system and link those inputs to the desired outputs. In addition, it considers non-controllable influences from outside.

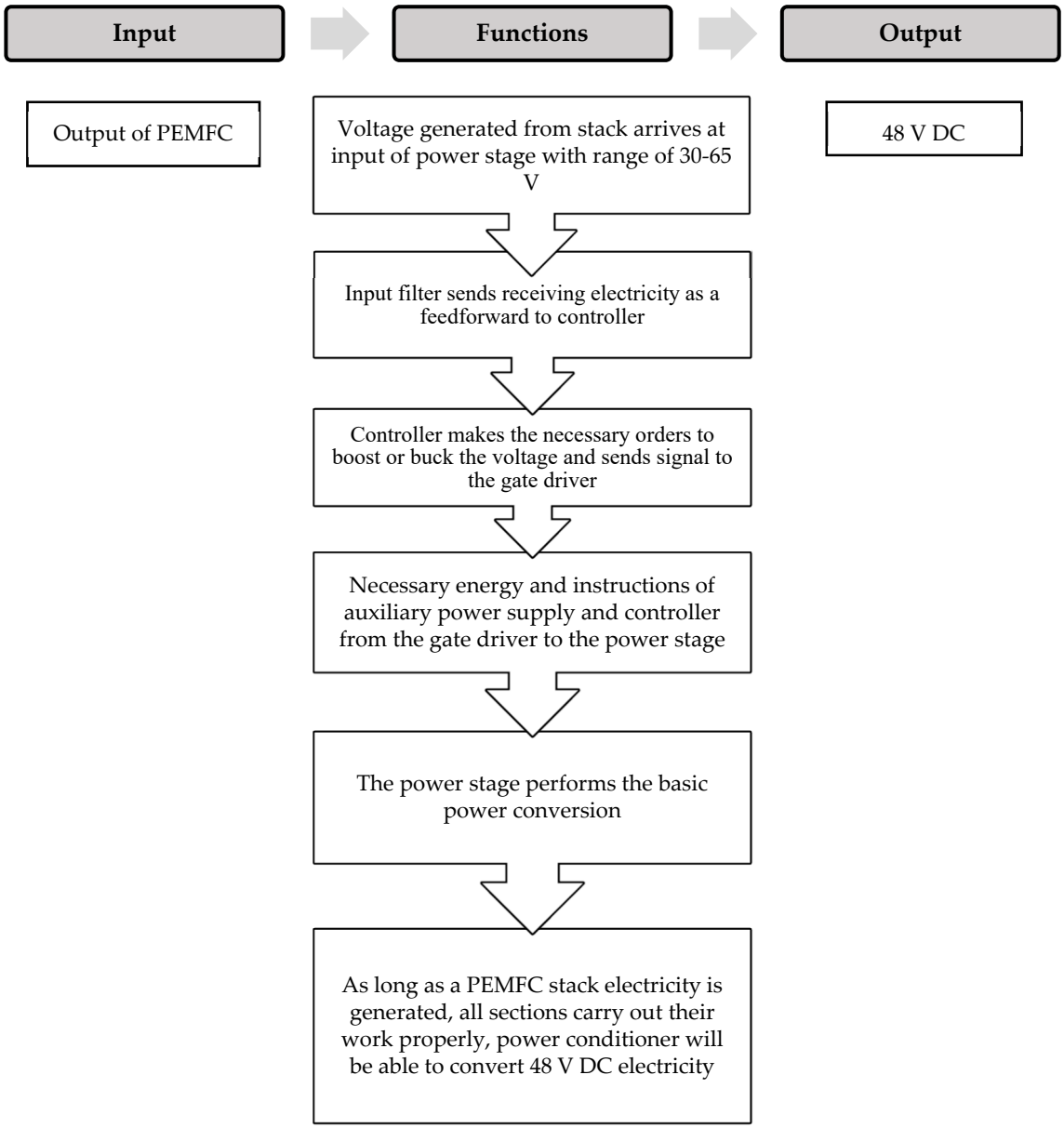

Figure 5. Function block diagram of the power conditioner.

3.3. Relationship of Functions and Failure Modes

As mentioned before, it is important that a FMEA precisely investigates the connective links among the sub-systems and components as well as their content. As shown in Figure 7, four levels of the PEMFC system are used to describe the power stage, which contains four critical components: MOSFETs, electrolytic capacitors, transformers and inductors (chokes). Generally, any failure mode is a failure cause for the power stage (Level 3). Similarly, failure modes of the power stage (Level 3) are failure causes of the power conditioner (Level 4). Figure 7 demonstrates the hierarchical impact of the failure of the PEMFC and interfaces among system, sub-system, and principal components. Two primary functions (F) and failure modes (FM) of the power conditioner and their relations with three levels are shown in Figures 8 and 9.

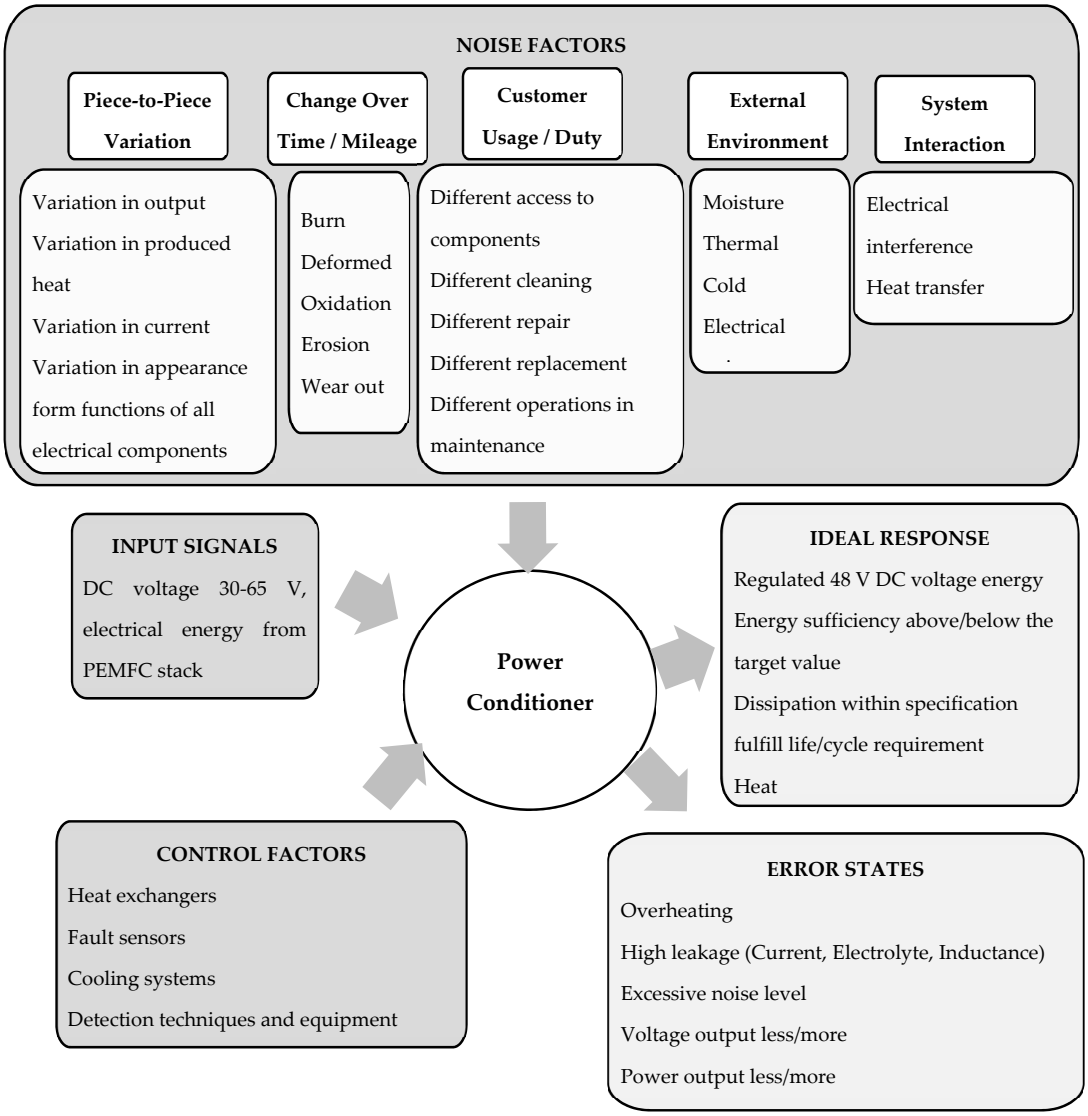

Figure 6. Parameter diagram of the power conditioner.

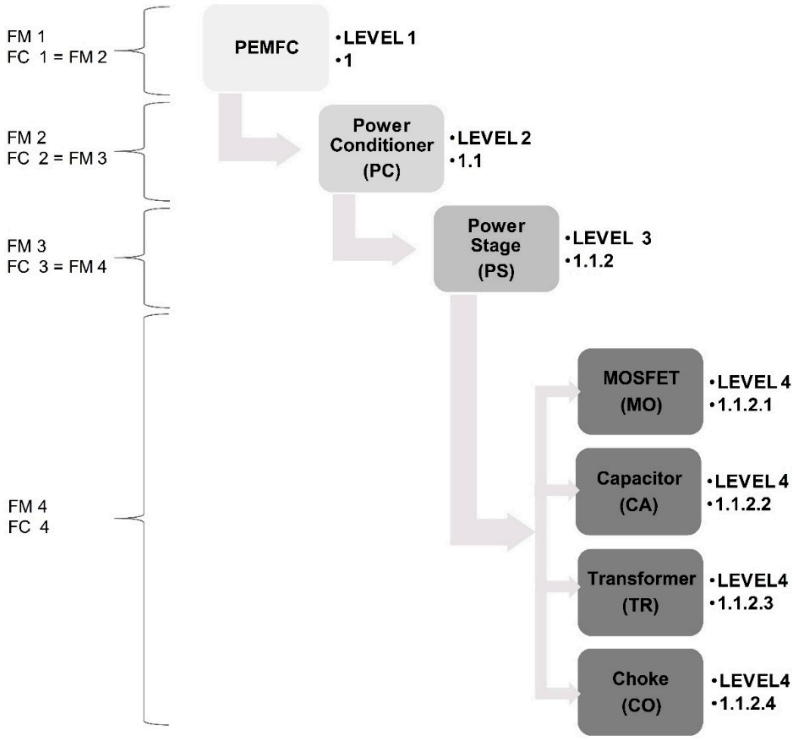

Figure 7. Interfaces between main parts of PEMFC with four levels.

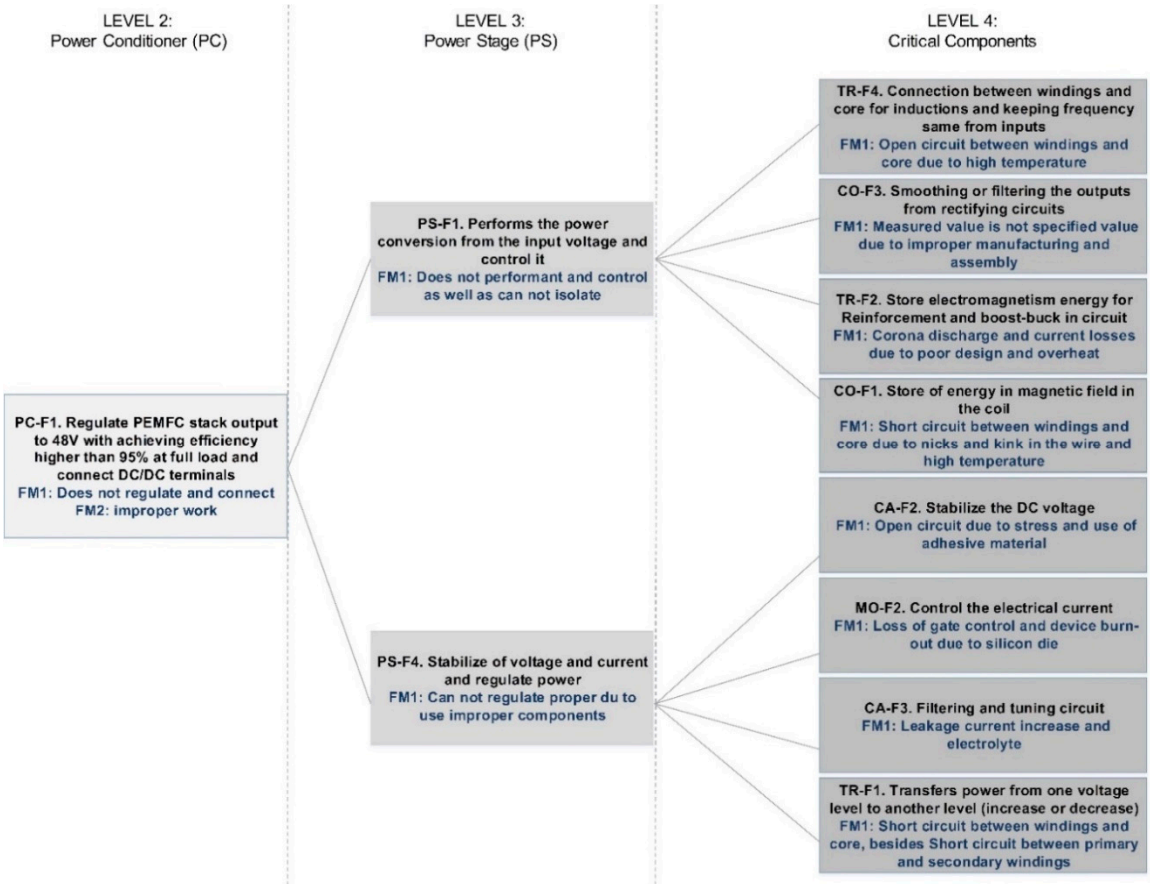

Figure 8. Relationship of functions and failure modes of the system to component levels of the power conditioner (1).

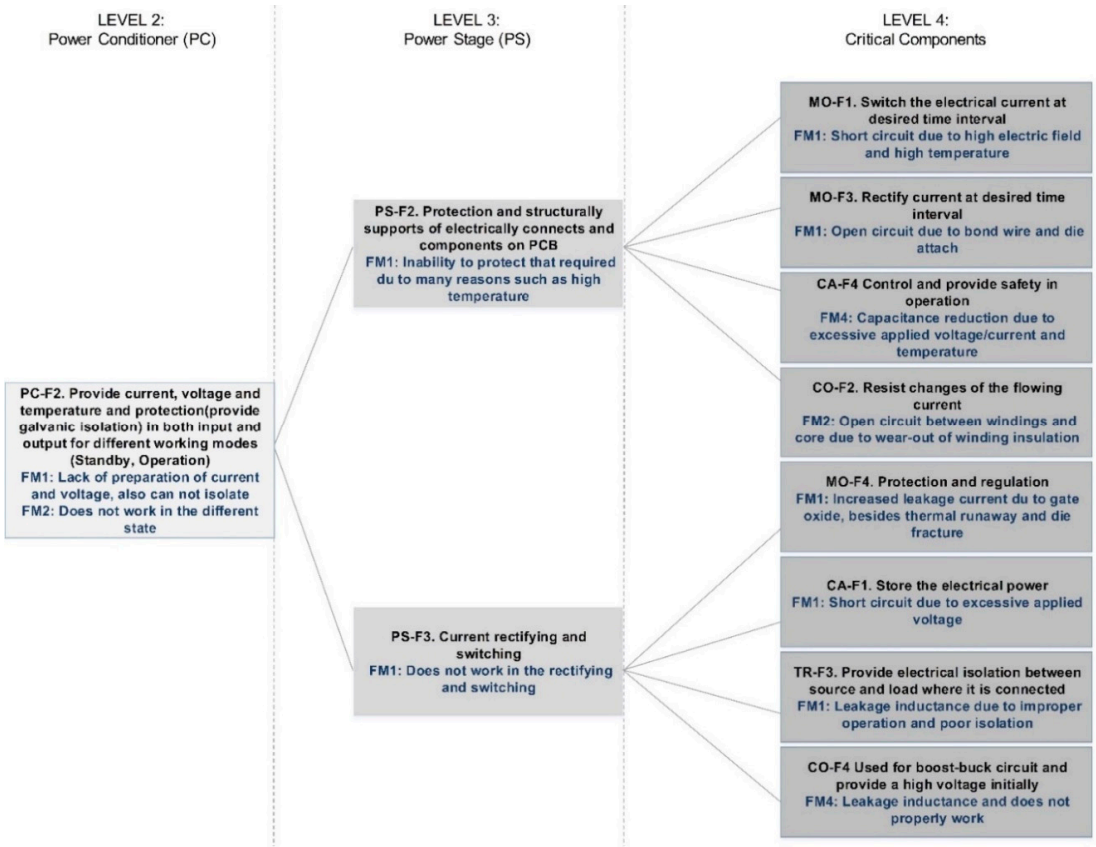

Figure 9. Relationship of functions and failure modes of system till component levels of the power conditioner (2).

3.4. FMEA Results

In this paper, a new estimation of the PEMFC system using FMEA is presented by focusing on power electronics components in the power conditioner. The analysis investigates numerous potential failure modes according to the API 580 (American Petroleum Institute), JEDEC (Joint Electron Device Engineering Council), NDI (Non-Destructive Inspection), and normal cause and failure for the industry affections. Specifically, parts of each level may have some failure modes and many failure causes. The failure modes of each level, in fact, are failure causes of the higher level. In the power conditioner, the power stage is identified as the most critical subsystem, and four critical components have the highest risk of failure and damage. Furthermore, the highest RPN is for the MOSFETs and capacitors are respectively having a result of 448, 392 with the failure mode of 'high leakage current due to substrate interface' and 'electrolyte evaporation'. High leakage current failure mode having two main causes, 'high current density' and 'over-voltage' has the highest risk number for the MOSFETs. Moreover, electrolytic evaporation by the deterioration of sealant material leads to insufficient sealing for the capacitors having the highest risk number in passive components. The FMEA of all the components and calculated RPNs for the power stage are illustrated in Table 3.

Table 3. FMEA table for critical sub-components of the power stage.

ID	Item	Function	Failure Mode	Failure Causes	Failure Effects	S	O	D	RPN
1.1.2.1	**MOSFET**	Switch electrical current at desired time interval	Short circuit, loss of gate control, and increased leakage current due to gate oxide	High temperature High electric field Over-voltage	Time dependent dielectric breakdown	9	7	5	**315**
		Control electrical current	High power dissipation, loss of gate control and device burn-out due to silicon die	High electric field Over-voltage Ionizing radiation	Latch-up, Increased forward voltage	8	7	5	**280**
		Rectify current at desired time interval	High leakage current due to substrate interface	High temperature High current Over-voltage High current density	Hot electrons	8	7	8	**448**
		Protection and regulation	Open circuit due to bond wire and die attach	High temperature High current density	Bond-wire cracking, lift-off; delamination of die attach	7	4	6	**168**
1.1.2.2	**Capacitor**	Store the electrical power	Short circuit between electrodes	Excessive applied voltage	Unable to store	9	4	6	**216**
		Stabilize the DC voltage	Open circuit	Mechanical stress Use of adhesive/coating material	Breakdown of terminal leads and corrosion	8	4	8	**256**
		Filtering and tuning circuit	Current and electrolyte evaporation	Deterioration of sealant material	Insufficient sealing	7	7	8	**392**
		Control and provide safety in operation	Capacitance reduction	Excessive ripple current High temperature Excessive applied voltage Reverse voltage applied	Electrolyte reduction, anode foil capacitance reduction, cathode foil capacitance reduction and deterioration of oxide film	7	7	6	**294**

Table 3. *Cont.*

ID	Item	Function	Failure Mode	Failure Causes	Failure Effects	S	O	D	RPN
1.1.2.3	**Transformer**	Increase or decrease power from one voltage level to another level	Short circuit between windings and core, besides short circuit between primary and secondary windings	High temperature	Impaired/improper operation	9	4	6	**216**
				Electrical overstress					
				Poor isolation	Impaired/improper operation				
				Low dielectric withstanding voltage					
		Connection between windings and core for induction and keeping frequency the same	Open circuit between windings and core	High Temperature	Does not connect	8	4	6	**192**
		Provide electrical isolation between source and load where it is connected	Leakage inductance	Faulty design and manufacturing techniques	Impaired/improper operation	5	3	7	**105**
		Store electromagnetism energy for reinforcement and boost-buck in circuit	Corona discharge and current losses	Poor design	High heat dissipation	4	4	7	**112**
1.1.2.4	**Choke**	Store of energy in magnetic field in the coil	Short circuit between windings and core	Nicks and kink in the wire	Does not connect	9	3	7	**189**
				High temperature					
		Resist changes of the flowing current	Open circuit between windings and core	Thermal overstress	Limited or not operation	8	4	6	**192**
				Wear-out of winding insulation					
		Smoothing or filtering the outputs from the rectifying circuits	Measured value is not the specified value	Manufacturing defect	Improper operation	7	3	7	**147**
				Improper assembly/soldering					
				Faulty layout and mounting of components					
		Use boost-buck circuit and provide a high initial voltage	Inductance leakage and does not properly work	Overload and overstress	Does not function properly	6	4	7	**168**

According to Table 3, the highest RPNs are seen and depicted clearly in Figure 10. Furthermore, by analyzing the output of the FMEA, the top failure modes are distinguished depending on the severity, concurrency, and detection rate. It is valuable to point out that the uppermost of risk priorities of failure modes requiring the severity parameter as well as occurrence rate refers to the short circuit in each of the four main components having an overstressed mechanism. Moreover, all leakages in the components such as leakage current in MOSFETs, electrolyte evaporation in capacitors and leakage inductance in inductors as well as transformers have the highest risk priorities of failure modes. This issue should be considered in order to reduce the risk by improving the design.

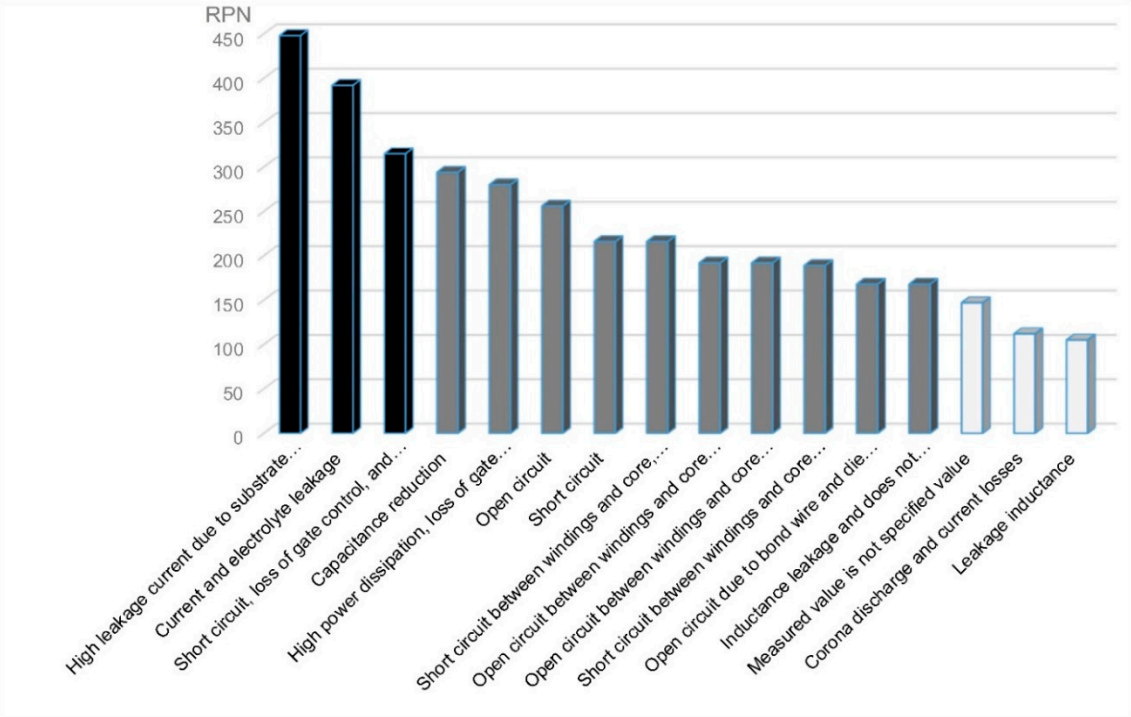

Figure 10. Pareto plot of RPNs for each failure mode analyzed in Table 3.

4. Risk Analysis

Risk analysis is one of the most rational methods to identify failure modes in fuel cell systems. The risk analysis using FMEA is an approach to prioritize the potential risk according to the failure causes [28]. In this risk analysis, the MOSFET having four main failure modes, and at least two causes for each one and average RPN = 303 in the power stage have the highest risk. Additionally, the capacitor item having four main failure modes and more than ten causes and average RPN = 274 is more critical compared to the inductor item having four main failure modes and six different causes and average RPN = 176. Finally, the transformer having four main failure modes, and six main causes has an average of RPN = 163.

Figure 10 illustrates three areas of critically failure modes for the crucial components of the power stage. The black color is considered for above 300 RPNs, and below 150 RPNs are colored with white. Most failure modes are in the medium range of risk, and they are shown with gray color. Extensive simulation studies, preventive control, use of diagnostic methods, predictive deployment technologies, employing visual management techniques, using sensors to distinguish failures, using preventive maintenance and developing inspection methods to identify hidden failures in the redundant items are among the recommended implementations for any of the components in the PEMFC system.

5. Bayesian Network

In a Bayesian analysis, the probability $P(A)$ of the event A is formulated as a degree of belief that A will occur [29].

Bayesian network (BN) refers to Bayes rule, given the event 'B', the probability of event 'A' is [$P(A|B)$]

$$P(A|B) = \frac{1}{P(B)} P(B|A)P(A), \quad (1)$$

where $P(A)$ is a prior estimate, $P(B|A)$ is a likelihood of A given B, and $P(B)$ is the marginal probability of B [30].

In order to build a BN based on the available FMEA, following BN is suggested:

In Figure 11, it is shown in an illustrative way how BN is built from the FMEA (Table 3) [31]. Finally, by merging common nodes, the BN for MOSFET is created as shown in Figure 12. The reason to choose the MOSFET is because of the results obtained from RPN. As shown in Figure 10, the first failure mode has the most significant influence on the system. The aim is to find, which failure cause has the most impact. Hugin as a tool is used for building the BN. It is considered that each node has two states, true and false.

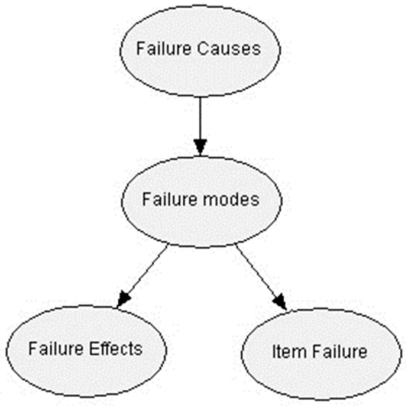

Figure 11. From FMEA to BN.

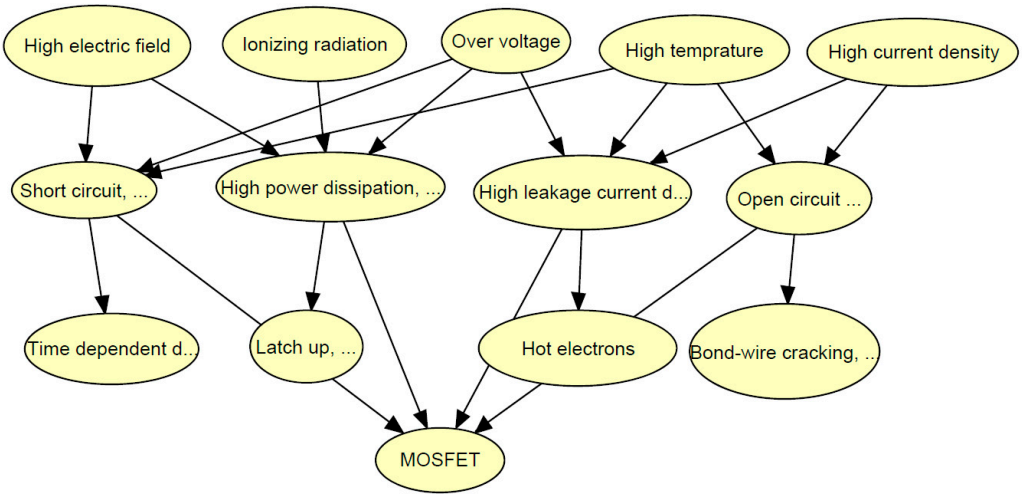

Figure 12. BN for the MOSFET.

The aim is to find the most significant failure cause in the failure of MOSFET by BN. From FMEA and Figure 10, high leakage current due to substrate interface is identified having the highest RPN which is one of the failure modes of MOSFET. Hence, MOSFET is analyzed to recognize the most important failure cause.

The process of making the BN is as follows:

1. BN is built based on Figure 11. from the FMEA in Table 3;
2. Joint failure modes and causes are merged;
3. For all failure causes two states are defined with equal probability of failure for their states: false and true;
4. Conditional probability tables (CPTs) are built. The maximum entropy theory is used to specify each probability of failure. Figure 13 shows two examples of conditional probability tables (CPTs).

High leakage current due to substrate interface

Over voltage	false				true			
High temprature	false		true		false		true	
High current density	false	true	false	true	false	true	false	true
false	1	0.66	0.66	0.34	0.66	0.34	0.34	0
true	0	0.34	0.34	0.66	0.34	0.66	0.66	1

Open circuit due to bond wire

High current density	false		true	
High temprature	false	true	false	true
false	1	0.5	0.5	0
true	0	0.5	0.5	1

Figure 13. Two examples of conditional probability tables (CPTs).

The importance analysis is carried out by assigning each failure cause as false or fail to find the probability of failure of the MOSFET. Figure 14 shows high temperature as an example of one of the failure causes.

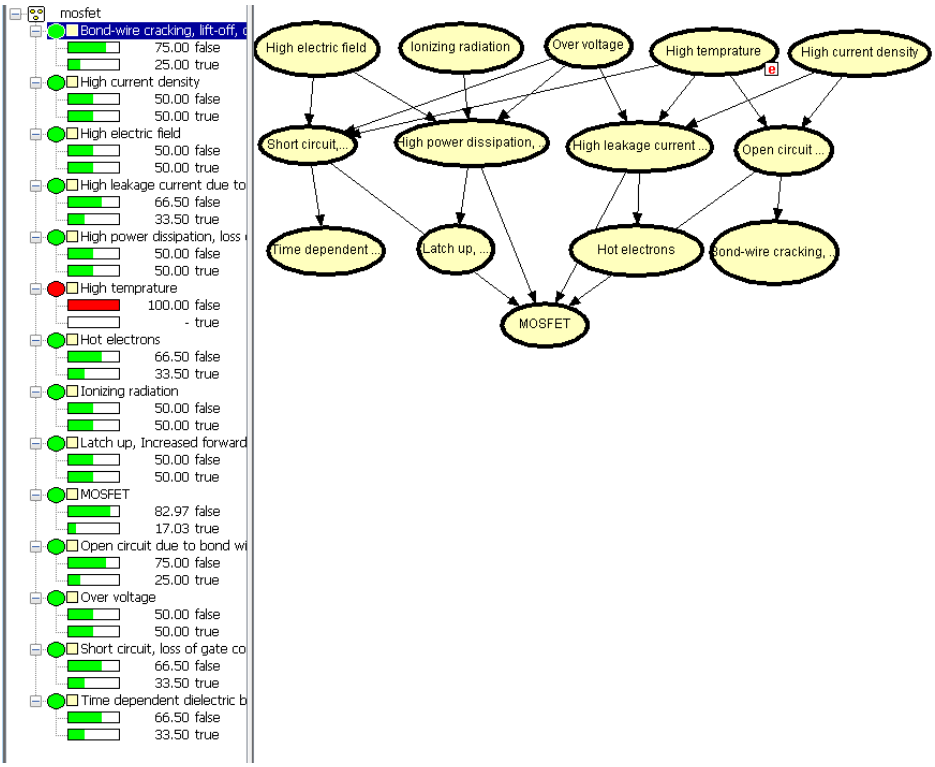

Figure 14. High temperature effect failure on the MOSFET.

Effect of each failure cause to MOSFET is calculated by the proposed BN. Table 4 compares failure causes in the MOSFET.

Table 4. Comparison of failure causes in the MOSFET.

Failure Cause	MOSFET Probability of Failure (%)
High Temperature	82.97
Over Voltage	79.78
High Current Density	77.00
High Electric Field	73.93
Ionizing Radiation	68.67

Comparing all failure causes effects on MOSFET failure shows that high temperature and overvoltage are the most important failure causes in MOSFET.

6. Conclusions

This study proposes a system engineering approach using FMEA for the risk analysis of the power conditioner in a PEMFC system. The highest RPNs correspond to the failure modes in three components, including high leakage current due to the substrate interface of the MOSFET, current and electrolytic evaporation of capacitor, and thereby short circuit, loss of gate control, and increased leakage current due to gate oxide of the MOSFET. Electronic components have a wide range of failure modes. The MOSFETs, capacitors, chokes, and transformers are the critical components of the power stage, which should be carefully considered in the development and implementation stage. In general, short circuit, open circuit, and leakage current are considered as the most important failure modes in the power supply system. Consequently, using a comprehensive FMEA analysis especially by using an extensive P-diagram, failure analysis, and its effects is studied in order to have a better understanding of the system in comparison with the available literature. Finally, BN is used to analyze the most critical failure causes among more important items identified from the FMEA, MOSFET and capacitor. The reason to use BN is that it was difficult to find RPNs of each failure cause, so the BN is implemented by two states of true and false or in other words failure and success to find the most critical failure cause. High temperature and overvoltage are ascertained utilizing BN. Knowing this fact will help designers to pay more attention on material properties to avoid failure causing by high temperature and overvoltage.

Author Contributions: The main idea for the paper was proposed by S.R. and S.B. wrote the first draft of the paper. S.R. and S.B. developed the methodology. S.R. and S.B. post-processed the results. D.Z., H.W., F.B. and J.D.S. supervised the findings of this work and reviewed methodology and results. All authors contributed for articulate the research work in its current form as full research manuscript. All authors have read and agreed to the published version of the manuscript.

Funding: The paper presents research results from the Marie Skłodowska-Curie Innovative Training Network INFRASTAR in the field of reliability approaches for decision-making for wind turbines and bridges. The project INFRASTAR (infrastar.eu) has received funding from the European Union's Horizon 2020 research and innovation program under the Marie Skłodowska-Curie grant agreement No. 676139. The grant is gratefully acknowledged.

Conflicts of Interest: The authors declare no conflict of interest.

References

1. Barbir, F. Front Matter. In *PEM Fuel Cells*; Elsevier: Amsterdam, The Netherladns, 2013; p. iii. ISBN 9780123877109.
2. Zawodzinski, T.A. PEM fuel cells: How things work. *ACS Div. Fuel Chem. Prepr.* **2004**, *49*, 470.
3. Wu, J.; Yuan, X.Z.; Martin, J.J.; Wang, H.; Zhang, J.; Shen, J.; Wu, S.; Merida, W. A review of PEM fuel cell durability: Degradation mechanisms and mitigation strategies. *J. Power Sources* **2008**, *184*, 104–119. [CrossRef]

4. Krishnan, K.J.; Kalam, A.; Zayegh, A. Experimental investigation of H2 generator and PEM fuel cell as a remote area back-up power. *Procedia Eng.* **2012**, *49*, 66–73. [CrossRef]
5. Modarres, M. *Risk Analysis in Engineering: Techniques, Tools, and Trends*; CRC Press: Boca Raton, FL, USA, 2006.
6. Rastayesh, S.; Bahrebar, S.; Sepanloo, K. Time Dependent Reliability of Emergency Diesel Generator Station. *Indian J. Sci. Res.* **2014**, *1*, 453–460.
7. Bahrebar, S.; Rastayesh, S.; Sepanloo, K. Dynamic Availability Assessment on Tehran Research Reactor Water Cooling System. *Indian J. Sci. Res.* **2014**, *1*, 471–474.
8. Rastayesh, S.; Bahrebar, S. Importance Analysis of a Typical Diesel Generator Using Dynamic Fault Tree. *Int. J. Curr. Life Sci.* **2014**, *4*, 697–700.
9. Rastayesh, S.; Long, L.; Sørensen, J.D.; Thöns, S. Risk Assessment and Value of Action Analysis for Icing Conditions of Wind Turbines Close to Highways. *Energies* **2019**, *12*, 2653. [CrossRef]
10. Modarres, M.; Kaminskiy, M.; Krivtsov, V. *Reliability Engineering and Risk Analysis: A Practical Guide*, 3rd ed.; CRC Press: Boca Raton, FL, USA, 2010.
11. Barends, D.M.; Oldenhof, M.T.; Vredenbregt, M.J.; Nauta, M.J. Risk analysis of analytical validations by probabilistic modification of FMEA. *J. Pharm. Biomed. Anal.* **2012**, *64–65*, 82–86. [CrossRef]
12. Narayanagounder, S.; Gurusami, K. A New Approach for Prioritization of Failure Modes in Design FMEA using ANOVA. *World Acad. Sci. Eng. Technol.* **2009**, *3*, 524–531.
13. Rhee, S.J.; Ishii, K. Using cost based FMEA to enhance reliability and serviceability. *Adv. Eng. Inform.* **2003**, *17*, 179–188. [CrossRef]
14. Arabian-Hoseynabadi, H.; Oraee, H.; Tavner, P.J. Failure Modes and Effects Analysis (FMEA) for wind turbines. *Int. J. Electr. Power Energy Syst.* **2010**, *32*, 817–824. [CrossRef]
15. Kim, K.O.; Zuo, M.J. General model for the risk priority number in failure mode and effects analysis. *Reliab. Eng. Syst. Saf.* **2018**, *169*, 321–329. [CrossRef]
16. Whiteley, M.; Dunnett, S.; Jackson, L. Failure Mode and Effect Analysis, and Fault Tree Analysis of Polymer Electrolyte Membrane Fuel Cells. *Int. J. Hydrogen Energy* **2016**, *41*, 1187–1202. [CrossRef]
17. Benmouna, A.; Becherif, M.; Depernet, D.; Gustin, F.; Ramadan, H.S.; Fukuhara, S. Fault diagnosis methods for Proton Exchange Membrane Fuel Cell system. *Int. J. Hydrogen Energy* **2017**, *42*, 1534–1543. [CrossRef]
18. Nielsen, J.J.; Sørensen, J.D. Bayesian Networks as a Decision Tool for O&M of Offshore Wind Turbines. In *ASRANet, Proceedings of the Integrating Stuctural Analysis, Risk & Reliability: 5th International ASRANet Conference, Edinburgh, UK, 14–16 June 2010*; ASRANet Ltd.: Glasgow, UK, 2010.
19. Trukhanov, S.V.; Troyanchuk, I.O.; Trukhanov, A.V.; Fita, I.M.; Vasil'ev, A.N.; Maignan, A.; Szymczak, H. Magnetic properties of La0.70Sr0.30MnO2.85 anion-deficient manganite under hydrostatic pressure. *JETP Lett.* **2006**, *83*, 33–36. [CrossRef]
20. Trukhanov, S.V.; Trukhanov, A.V.; Turchenko, V.A.; Trukhanov, A.V.; Tishkevich, D.I.; Trukhanova, E.L.; Zubar, T.I.; Karpinsky, D.V.; Kostishyn, V.G.; Panina, L.V.; et al. Magnetic and dipole moments in indium doped barium hexaferrites. *J. Magn. Magn. Mater.* **2018**, *457*, 83–96. [CrossRef]
21. Trukhanov, A.V.; Grabchikov, S.S.; Solobai, A.A.; Tishkevich, D.I.; Trukhanov, S.V.; Trukhanova, E.L. AC and DC-shielding properties for the Ni80Fe20/Cu film structures. *J. Magn. Magn. Mater.* **2017**, *443*, 142–148. [CrossRef]
22. Arpaia, P.; Buzio, M.; Capatina, O.; Eiler, K.; Langeslag, S.A.E.; Parrella, A.; Templeton, N.J. Effects of temperature and mechanical strain on Ni-Fe alloy CRYOPHY for magnetic shields. *J. Magn. Magn. Mater.* **2019**, *475*, 514–523. [CrossRef]
23. Zhang, J. *PEM Fuel Cell Electrocatalysts and Catalyst Layers: Fundamentals and Applications*; Springer Science & Business Media: Berlin/Heidelberg, Germany, 2008; ISBN 9781848009356.
24. Zhou, D.; Wang, H.; Blaabjerg, F.; Kor, S.K.; Blom-Hansen, D. System-level reliability assessment of power stage in fuel cell application. In Proceedings of the 2016 IEEE Energy Conversion Congress and Exposition (ECCE), Milwaukee, WI, USA, 18–22 September 2016; pp. 1–8.
25. Bahrebar, S.; Zhou, D.; Rastayesh, S.; Wang, H.; Blaabjerg, F. Reliability assessment of power conditioner considering maintenance in a PEM fuel cell system. *Microelectron. Reliab.* **2018**, *88–90*, 1177–1182. [CrossRef]
26. Zhou, D.; Wang, H.; Blaabjerg, F. Mission Profile Based System-Level Reliability Analysis of DC/DC Converters for a Backup Power Application. *IEEE Trans. Power Electron.* **2018**, *33*, 8030–8039. [CrossRef]

27. Jensen, F.; Morris, A.S.; Levin, M.A.; Kalal, T.T.; Pascoe, N.; Carlson, C. *Effective FMEAs*; Wiely: Hoboken, NJ, USA, 2012.
28. Rastayesh, S.; Bahrebar, S.; Bahman, A.S.; Sørensen, J.D.; Blaabjerg, F. Lifetime Estimation and Failure Risk Analysis in a Power Stage Used in Wind-Fuel Cell Hybrid Energy Systems. *Electronics* **2019**, *8*, 1412. [CrossRef]
29. Faber, M.H. *Statistics and Probability Theory*; Topics in Safety, Risk, Reliability and Quality; Springer: Dordrecht, The Netherlands, 2012; Volume 18, ISBN 978-94-007-4055-6.
30. Kjaerulff, U.B.; Madsen, A.L. *Bayesian Networks and Influence Diagrams: A Guide to Construction and Analysis*; Springer: New York, NY, USA, 2008; ISBN 9780387741017.
31. Hamza, Z.; Abdallah, T. Mapping Fault Tree into Bayesian Network in safety analysis of process system. In Proceedings of the 2015 4th International Conference on Electrical Engineering (ICEE), Bounerdes, Algeria, 13–15 December 2015; pp. 1–5.

Paper 6:

Title:

Reliability assessment of power conditioner considering maintenance in a PEM fuel cell system

Authors:

Sajjad Bahrebar, Dao Zhou, Sima Rastayesh, Huai Wang and Frede Blaabjerg

Published in:

Microelectronics Reliability 2018, 88-90, 1177-1182; doi: 10.1016/j.microrel.2018.07.085

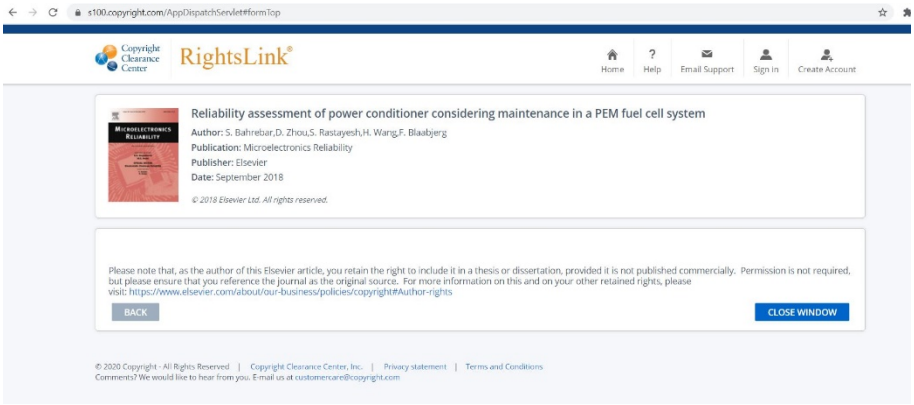

Microelectronics Reliability 88–90 (2018) 1177–1182

Contents lists available at ScienceDirect

Microelectronics Reliability

journal homepage: www.elsevier.com/locate/microrel

Reliability assessment of power conditioner considering maintenance in a PEM fuel cell system

S. Bahrebar[a], D. Zhou[a,*], S. Rastayesh[b], H. Wang[a], F. Blaabjerg[a]

[a] Department of Energy Technology, Aalborg University, Aalborg, Denmark
[b] Department of Civil Engineering, Aalborg University, Aalborg, Denmark

ARTICLE INFO

Keywords:
Reliability assessment
Fault-tree analysis
Weibull distribution
Maintenance

ABSTRACT

Proton exchange membrane fuel cell recently emerges in the telecom backup power, where its reliability and availability issues are with high priority. In this paper, as one of the fragile sub-systems, the reliable performance of the power conditioner, including the power stage, the controller, the gate driver, the auxiliary the power supply and the printed circuit board, is the key focus. According to the configuration and main functions of the aforementioned key components, the fault tree structure of power conditioner can be established. With the help of the Weibull distribution, the random failure mode and wear-out failure mode impacts on the reliability can be estimated. Moreover, the reliability and availability curves can be studied by considering the maintenance scheme. In this case study, it can be seen that the wear-out issue is more worthy to be taken care compared to the random failure. Moreover, the regular maintenance with the key components significantly increases the reliability and availability performance of the power conditioner.

1. Introduction

Recently, renewable energy generation is rapidly growing in the power sector. One of them is the fuel cells, which are becoming more promising for various kinds of applications [1]. The first fuel cell was prototyped by a British scientist in 1839 [2]; in the 1990s, proof-of-concept fuel cells followed, and sub-scale and full-scale prototype systems were developed to demonstrate the technology [3]. Proton Exchange Membrane Fuel Cells (PEMFCs) are one of the promising types, as they can be used in multiple applications. The PEMFCs transform the chemical energy into electrical power via the electrochemical reaction [4]. From the sustainable development perspective, the PEMFCs are more suitable and competitive in comparison with other renewable energy systems, as the fuel cell contributes on high energy conversion efficiency, a more compact design and environmentally friendly [5]. In addition, as budgets in any project are limited in both the design and operational stages, it is reasonable to invest in critical components in order to increase the reliability of the system. Since fuel cell systems are used for reliability or safety critical occasions such as backup power for the emergency, their reliable operation is vital. For the aforementioned reason, it is required to pay more attention to their reliability and availability.

Reliability assessment is frequently a crucial and mandatory step in designing and analyzing systems [6]. An important characteristic of engineering systems is that they behave dynamically, i.e., their response to an initial perturbation evolves as system components interact with one another as well as with the environment [7]. In addition, different maintenance strategies could have different impacts on reliability and availability; while maximal reliability and availability or minimal costs in a system could be achieved when these strategies are optimized [8].

In this paper, the Fault Tree Analysis (FTA), as a conventional method for reliability assessment [9, 10] is designed to illustrate the relations between basic event logical variables and significant components. One of the principal aspects that could affect system reliability is aging. Considering aging effects in the calculations by choosing an appropriate reliability distribution is an important issue. At last, by applying Monte Carlo simulation and considering maintenance and inspection policy, the availability is calculated for five years of the system operation.

2. System configuration and reliability assessment method

2.1. Critical components of power conditioner

The power conditioner is one of the main sub-systems in the PEMFC system, which consists of five components: the power stage, the auxiliary power supply, the gate driver, the controller and the Printed

* Corresponding author.
E-mail address: zda@et.aau.dk (D. Zhou).

https://doi.org/10.1016/j.microrel.2018.07.085
Received 9 June 2018; Received in revised form 28 June 2018; Accepted 8 July 2018
Available online 30 September 2018

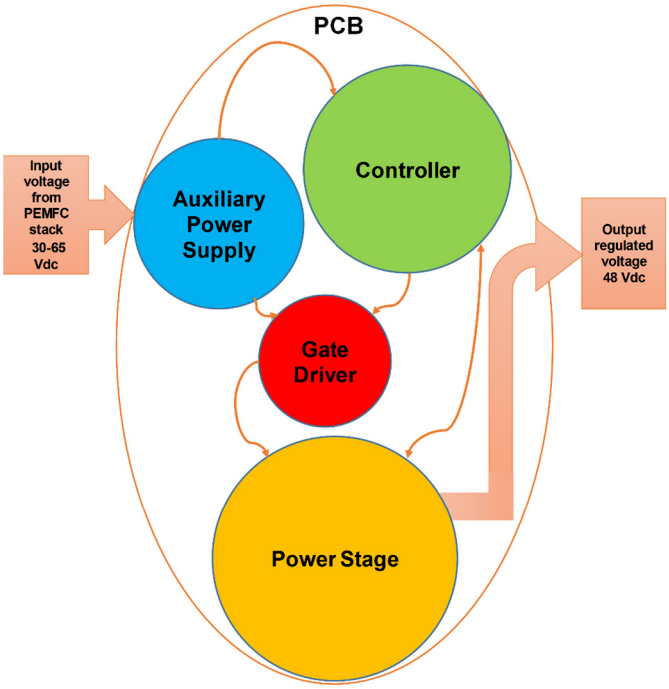

Fig. 1. The configuration of the power conditioner.

Circuit Board (PCB) [11]. Fig. 1 illustrates the configuration of the power conditioner.

All components of the power conditioner and their key sub-components are shown in Fig. 2. Concisely, the main functions of components in the power conditioner are listed as follows [12]:

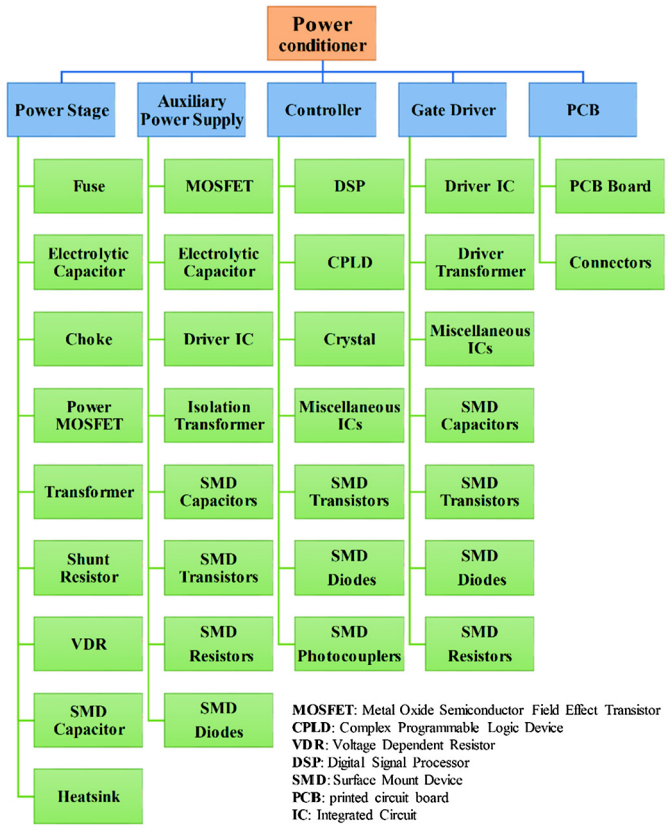

Fig. 2. All components and sub-components of the power conditioner.

1. The power stage mainly consists of the isolated DC/DC converter, which performs the basic power conversion from wide range of the input voltage (+30–65 V_{dc}) to fixed output voltage (+48 V_{dc}).
2. The controller makes it possible to operate the converter in either boost mode or buck mode, depending on the fuel cell output voltage. In addition, the output of the controller is the drive signal of the power devices, which is further sent to the gate driver.
3. The gate driver aims to amplify the drive signals from the microprocessor in order to actively control the power switches on and off.
4. The function of the auxiliary power supply is to power on all of the Integrated Circuits (ICs) used in the controller and gate driver.
5. As shown in Fig. 1, all of the key sub-components are accommodated in the PCB. In addition, the connectors are used to link the input power and output load.

2.2. Fault tree analysis

The fault tree approach is a deductive process by means of which an undesirable event (top event) is postulated, and the possible ways for this event to occur are systematically deduced [6]. The deduction process is performed so that the fault tree embodies all component failures (i.e., failure modes) that contribute to the occurrence of the top event. The fault tree itself is a graphical representation of the various combinations of failures that lead to the occurrence of the top event [13].

The postulated fault events that appear on the fault tree may not be exhaustive. Only those events considered important can be included. However, it should be noted that the decision for inclusion in failure events is not arbitrary. Besides, it is affected by the fault tree construction procedure, system design and operation, operating history, available failure data, and experience of the analyst. At each intermediate point, the postulated events represent the immediate, necessary, and sufficient causes for the occurrence of the intermediate (or top) events [6]. Based on the key sub-components as shown in Fig. 2 and the operation principle of the power conditioner, the fault tree structure of this case study can be developed and established. As shown in Fig. 3, the relationship between the sub-system of the power conditioner and the five components, as well as the corresponding component and its sub-components are described in detail.

3. Random and wear-out failure modes

3.1. Basic concepts

The bathtub curve describes a general form of the failure rate through the life cycle of the product, which basically includes three regions as shown in Fig. 4 [14, 15]:

1. Decreasing failure rate, known as early failures.
2. Constant failure rate, known as random failures.
3. Increasing failure rate, known as wear-out failures.

In region one, the initial failure rate is high but decreases rapidly as defective components are identified and discarded. In region two, the failure rate is generally low and constant, which can be expressed by the exponential distribution. The exponential distribution is the probability distribution referring to a process, in which events occur continuously and independently at a constant mean rate. In region three, the failure rate increases due to [the] aging and wear out effects, which can be analyzed in reliability engineering by using the Weibull distribution.

The Weibull distribution is a probability distribution, which can generally be determined by the shape parameter β and the scale parameter η. The shape parameter is also known as the Weibull slope [6]. If β is equal or less than one, it approximately becomes exponential distribution, and η expresses the mean value [6]. If β is more than one, the

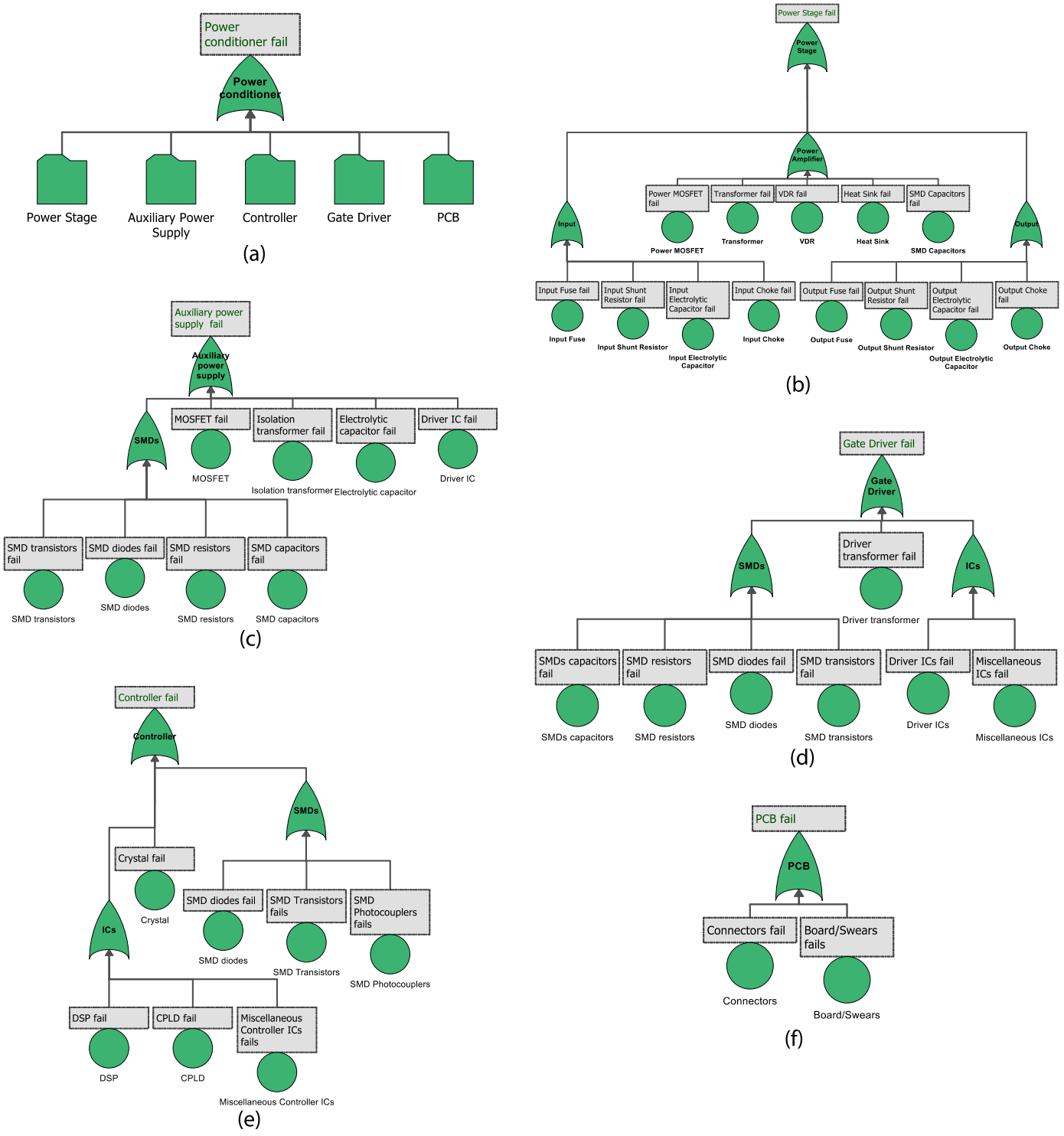

Fig. 3. Fault tree simulations of the power conditioner. (a) Sub-system of the power conditioner. (b) Components of the power stage. (c) Components of the auxiliary power supply. (d) Components of the gate driver. (e) Components of the controller. (f) Components of the printed circuit board.

probability density function generally has a maximum value. This shape factor is used to represent the aging effect on components by increasing failure rates. Table 1 summarizes the relationship between the shape parameter and the corresponding failure rate [16]. It is worth mentioning that the exponential distribution is a particular case of the Weibull distribution.

Due to the lack of a reliability model at the stage of the early failures, only the constant failure and wear-out failure stages are considered in the following. With respect to the random failure stage, the failure rate can be obtained from MIL-HDBK-217F. In addition, if $\beta = 1$, the relationship between the scale parameter and failure rate λ can be found,

$$\lambda = \frac{f(t)}{R(t)} = \frac{\beta}{\eta}\left(\frac{t}{\eta}\right)^{\beta-1} \Rightarrow \eta = \frac{1}{\lambda} \quad (1)$$

with respect to the wear-out failure stage, assuming that the shape parameter equals two, the scale factor can be calculated by using the goodness of fit testing method. With the information of the scale factor

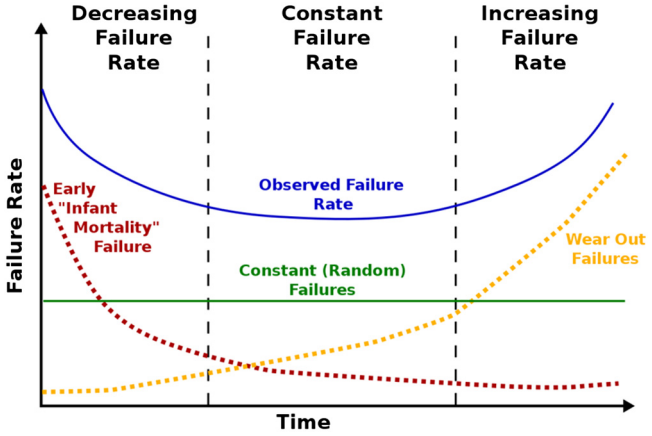

Fig. 4. Bathtub curve failure rate at three important regions.

Table 1
Shape parameter in Weibull distribution.

$\beta = 1$	Exponential distribution
$\beta < 1$	Decreasing Failure Rate (DFR)
$\beta > 1$	Increasing Failure Rate (IFR)
$\beta = 3.5$	Normal Distribution

and the shape factor. Reliability curve can be deduced as follow:

$$R(t) = e^{-\left(\frac{t}{\eta}\right)^{\beta}} \quad (2)$$

Considering both the random failure ad wear-out failure, Table 2 lists 5 main components and 33 sub-components with the failure rate and Weibull parameters in the entire power conditioner.

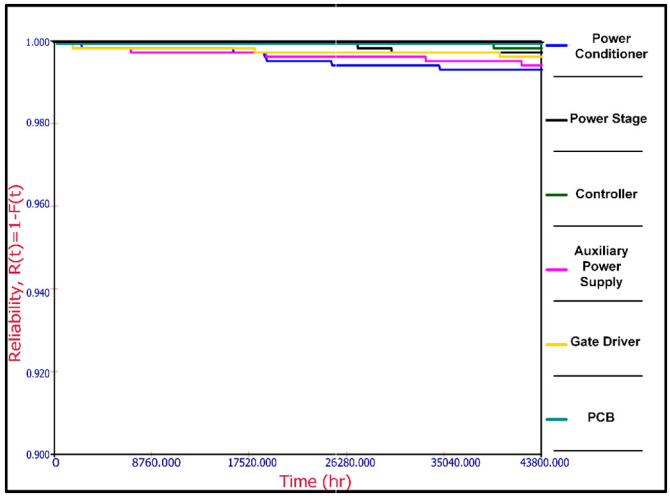

Fig. 5. Reliability comparison of five main components in the case of the random failure.

3.2. Reliability comparison between random and wear-out failure

After performing the FTA and assigning parameters of Weibull distribution to the power conditioner, the reliability curve of 5 main components can be calculated within 43,800 h (5 years), where 1000 times of Monte Carlo simulation is used. As shown in Figs. 5 and 6, it is noted that the random failure mode and the wear-out failure mode are represented by the exponential distribution ($\beta = 1$) and Weibull

Table 2
Weibull parameters for all the sub-components in the cases of random failure and wear-out failure.

Sub-system of PEMFC	Components	Sub-components	Failure rate (λ)	Weibull parameters	
				Scaling parameter (η) with $\beta = 1$	Scaling parameter (η) with $\beta = 2$
Power conditioner	Power stage	Fuse	0.02E-6	5E7	5.64E7
		Electrolytic capacitor	0.12E-6	8.33E6	9.4E6
		Transformer	0.15E-8	6.66E8	7.52E8
		Choke	0.16E-9	6.25E9	7.05E9
		Power MOSFET	0.52E-6	1.92E6	2.17E6
		Shunt resistor	0.43E-9	2.32E9	2.62E9
		VDR	0.43E-9	2.32E9	2.62E9
		SMD capacitor	0.69E-9	1.45E9	1.63E9
		Heatsink	0.06E-6	1.66E7	1.88E7
	Auxiliary power supply	MOSFET	0.52E-6	1.92E6	2.17E6
		Electrolytic capacitor	0.12E-6	8.33E6	9.4E6
		Driver IC	0.38E-8	2.63E8	2.97E8
		Isolation transformer	0.15E-6	6.66E6	7.52E6
		SMD capacitor	0.69E-9	1.45E9	1.63E9
		SMD transistors	0.44E-5	2.27E5	2.56E5
		SMD diodes	0.02E-6	5E7	5.64E7
		SMD resistors	0.39E-9	2.56E9	2.89E9
	Controller	DSP	0.12E-6	8.33E6	9.41E6
		CPLD	0.32E-8	3.12E8	3.53E8
		Crystal	0.11E-6	9.09E6	1.03E7
		Miscellaneous ICs	0.38E-8	2.63E8	2.97E8
		SMD transistors	0.44E-5	2.27E5	2.57E5
		SMD diodes	0.02E-6	5E7	5.64E7
		SMD photo-couplers	0.16E-6	6.25E6	7.05E6
	Gate driver	Driver IC	0.38E-8	2.63E8	2.97E8
		Driver transformer	0.15E-6	6.66E6	7.05E6
		Miscellaneous ICs	0.38E-8	2.63E8	2.97E8
		SMD capacitors	0.69E-9	1.45E9	1.63E9
		SMD transistors	0.44E-5	2.27E5	2.56E5
		SMD diodes	0.02E-6	5E7	5.64E7
		SMD resistors	0.39E-9	2.56E9	2.89E9
	PCB	PCB board	0.18E-5	5.55E5	6.27E5
		Connectors	0.38E-6	2.63E6	2.97E6

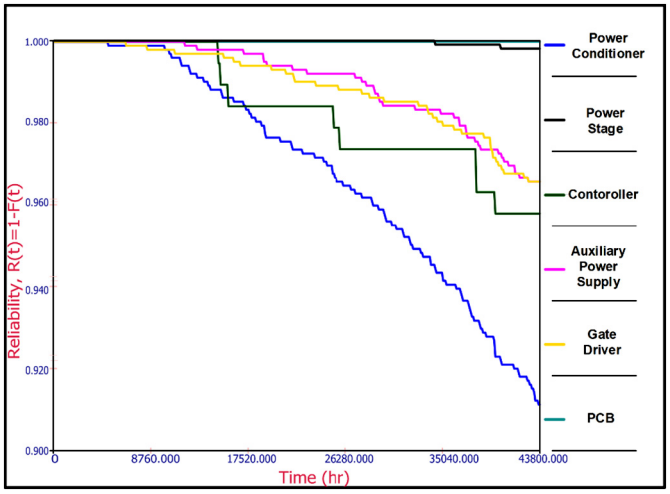

Fig. 6. Reliability comparison of five main components in the case of the wear-out failure.

distribution (β = 2), respectively.

In fact, these figures are the comparison between the random and wear-out behavior of the power conditioner sub-system. The top three reliability-critical components are the gate driver, the auxiliary power supply, and the controller, respectively. Moreover, it is evident that the wear-out failure mode is more significant than the random failure. The designed 5-year operation causes the damage < 1% for the random failure, while it leads to the damage much > 10% in the case of wear-out failure. In other words, proper maintenance needs to be applied in order to guarantee the lifetime demand.

4. Reliability, maintainability, and availability

4.1. Concept of maintenance

Maintenance is the ability to maintain or restore a system in functioning state, which contains inspections and repairs. In this paper, it involves the repair and inspection conditions in 9 critical sub-components among 33 basic sub-components of all system. These components, including transistors, capacitors, transformers, diodes, DSP, CPLD, crystal, and PCB, are identified through the sensitivity analysis. Maintenance can affect the maintainability directly by shortening the time spent on the repair (Mean Time To Repair MTTR). With the decreasing MTTR and increasing the average time interval between repairs (Mean Time Between Failure MTBF) at the optimum point, the availability can be increased using its definition:

$$Availability = \frac{\text{Uptime}}{\text{Uptime} + \text{Downtime}} = \frac{\text{MTBF}}{\text{MTBF} + \text{MTTR}} \quad (3)$$

Since the repair or inspection time can be changed according to different conditions, a normal distribution with standard deviation 10% is modeled with the mean of 720 h and standard deviation of 72 h. Fig. 7 demonstrates the comparison of the reliability curve in the power conditioner without repair and with inspection and repair every 720 h in five years. By assuming a Weibull distribution and the wear-out of the system, it is noted 1% increase in reliability within the 5-year operation.

4.2. Availability curve

Reliability curve calculated the probability that the system is in an available state, without ever having entered an unavailable state, at a certain point in time. Availability curve is the probability that a system (or component) is operational at any random time. This is very similar

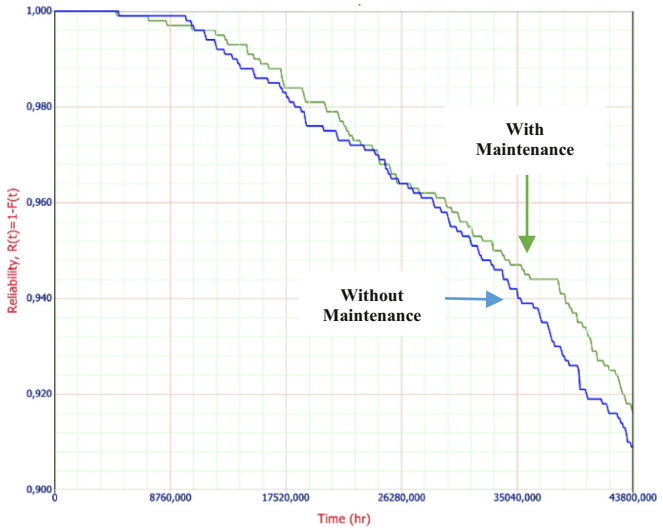

Fig. 7. Reliability of power conditioner without repair and inspection (blue) and with repair and inspection (green) considering Weibull distribution. (For interpretation of the references to colour in this figure legend, the reader is referred to the web version of this article.)

to the reliability function, which gives a probability that a system can function at the given time. Unlike the reliability, the instantaneous availability measure incorporates maintainability information. At any given time, the system is operational with the following conditions:

1. It functions properly during time with probability *R(t)*, or,
2. It functions properly since the last repair at time *u*, 0 < u < t, with probability:

$$\int_0^t R(t-u)m(u)du \quad (4)$$

With *m(u)* being the renewal density function of the system. The point of availability is the summation of these two probabilities, or:

$$A(t) = R(t) + \int_0^t R(t-u)m(u)du \quad (5)$$

Fig. 8 shows availability curve of power conditioner, which considering effects of maintenance on the availability of the system for a 5-

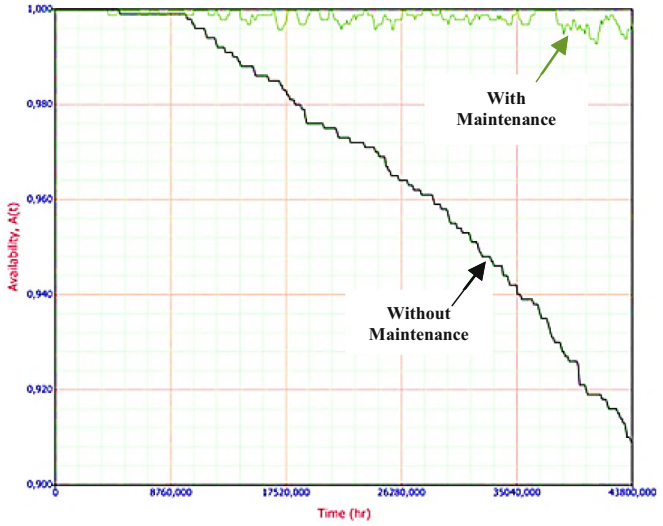

Fig. 8. Availability of power conditioner without maintenance (black) and with maintenance (green). (For interpretation of the references to colour in this figure legend, the reader is referred to the web version of this article.)

year period. It can be seen that the availability of the system significantly increases by using maintenance scheme.

5. Conclusion

In this paper, the reliability and availability issues of power conditioner system in the PEM fuel cell is studied according to the relationship among all key components. With the help of fault tree analysis, the reliability of the power conditioner is calculated within 5 years. Random failure and wear-out failure are compared in order to have a better understanding of the real behavior of the system, where the wear-out issue is more significant compared to the random failure. Considering maintenance intervals, the availability of the system increases in accordance with planned maintenance. Taking into account the inspection intervals, another solution for decision makers to optimize maintenance interval is to look at the inspection or monitoring systems. The repair actions for critical components could make a huge difference in the availability of the system. On the other hand, the optimum maintenance intervals could be further investigated.

References

[1] S. Bahrebar, et al., A novel type-2 fuzzy logic for improved risk analysis of proton exchange membrane fuel cells in marine power systems application, Energies 11 (4) (Mar. 2018) 721.
[2] J. Zhang, PEM Fuel Cell Electrocatalysts and Catalyst Layers: Fundamentals and Applications, (2008).
[3] X.Z. Yuan, H. Li, S. Zhang, J. Martin, H. Wang, A review of polymer electrolyte membrane fuel cell durability test protocols, J. Power Sources 196 (22) (2011) 9107–9116.
[4] J. Wu, et al., A review of PEM fuel cell durability: degradation mechanisms and mitigation strategies, J. Power Sources 184 (1) (2008) 104–119.
[5] J. Zhang, H. Zhang, J. Wu, J. Zhang, Pem Fuel Cell Testing and Diagnosis, (2013).
[6] M. Modarres, M. Kaminskiy, Vasiliy Krivtsov, Reliability Engineering and Risk Analysis: A practical guide, Third edition, CRC Press, 2010.
[7] S. Bahrebar, S. Rastayesh, K. Sepanloo, Dynamic availability assessment on Tehran research reactor water brief description of TRR cooling, Indian J. Sci. Res. 1 (2) (2014) 471–474.
[8] J. Endrenyi, S. Aboresheid, R.N. Allan, The present status of maintenance strategies and the impact of maintenance on reliability, IEEE Trans. Power Syst. 16 (4) (2001).
[9] L. Placca, R. Kouta, Fault tree analysis for PEM fuel cell degradation process modelling, Int. J. Hydrog. Energy 36 (19) (Sep. 2011) 12393–12405.
[10] M. Whiteley, S. Dunnett, L. Jackson, Failure mode and effect analysis, and fault tree analysis of polymer electrolyte membrane fuel cells, Int. J. Hydrog. Energy 41 (2) (2016) 1187–1202.
[11] D. Zhou, H. Wang, and F. Blaabjerg, "Mission profile based system-level reliability analysis of DC/DC converters for a backup power application," IEEE Trans. Power Electron., (IEEE early access).
[12] S. Lee, D. Zhou, H. Wang, Reliablity assessment of fuel cell system - a framework for quantitative approach, Proc. of ECCE 2016 (Energy Convers. Congr. Expo.), 2016.
[13] S. Collong, R. Kouta, Fault tree analysis of proton exchange membrane fuel cell system safety, Int. J. Hydrog. Energy 40 (25) (Jul. 2015) 8248–8260.
[14] L.E. Bechtold, D. Redman, B. Tawfellos, Semiconductor reliability using random and wearout failure models, Proc. of Annu. Reliab. Maintainab. Symp. 2014.
[15] S. Rastayesh, S. Bahrebar, K. Sepanloo, Time dependent reliability of rmergency diesel generator station, Indian J. Sci. Res. 1 (2) (2014) 453–460.
[16] M. Modarres, Risk Analysis in Engineering: Techniques, Tools, and Trends, (2006).

ISSN (online): 2446-1636
ISBN (online): 978-87-7210-867-4 AALBORG UNIVERSITY PRESS